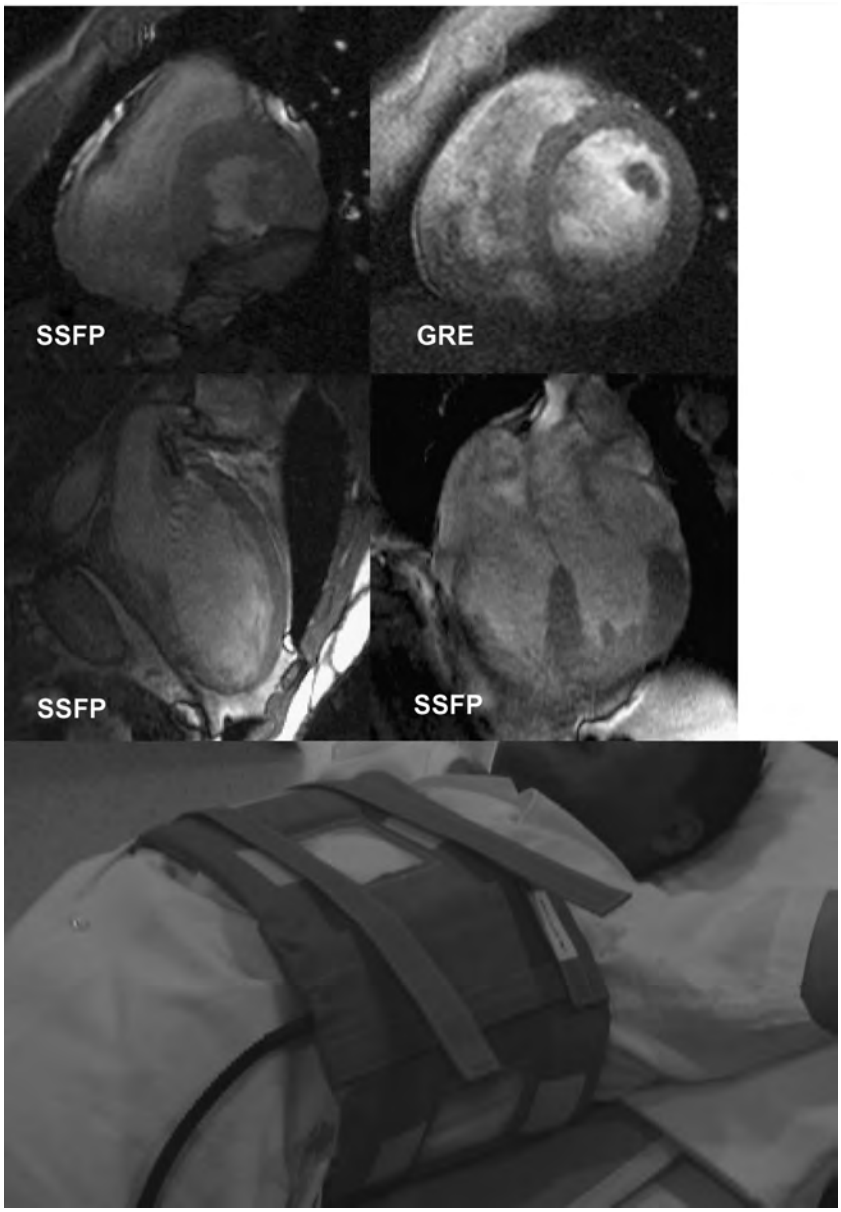

LV and its function were excellent (see images). Complete coverage of the LV was achieved using an imaging FOV from 18–20 cm. This approach combined with higher field systems may provide close to optimal imaging of the left ventricle.

Conclusions: The flexible surface coil provided sufficient RF penetration for CMR imaging at 3 Tesla. An unaliased FOV of 18–20 cm was easily acquired in three moderate sized subjects. Further studies are needed to establish FOV, penetration, and SNR tradeoffs compared with other available coils.

408. MRI-Documented Neo-Intimal Dissection and Co-Localization of Novel Apoptotic Markers: Apolipoprotein C-1, Ceramide and Caspase-3 in Watanabe Heritable Hyperlipidemic Rabbit Sub-Renal Aorta

Henning Steen,[1] Antonia Kolmakova, PhD,[2] Matthias Stuber, PhD,[3] Subroto Chatterjee, PhD,[2] Joao A. C. Lima, MD.[4]
[1]*Cardiology, Universität Heidelberg, Heidelberg, Germany,* [2]*Pediatrics, Johns HOpkins, Baltimore, MD, USA,* [3]*Radiology, Johns HOpkins, Baltimore, MD, USA,* [4]*Cardiology, Johns HOpkins, Baltimore, MD, USA.*

Introduction: Apoptotic aortic vascular smooth muscle cell (VSMC) death is known to contribute to plaque vulnerability and-rupture/neo-intimal dissection. Human plasma apolipoprotein C-I (apoC-I) has been implicated in apoptotic VSMC death via recruiting a neutral sphingo-myelinase (N-SMase)-ceramide(Cer)-caspase-3(Cas-3)-pathway in vitro. MRI is a promising non-invasive to visualize atherosclerotic disease in the arterial wall.

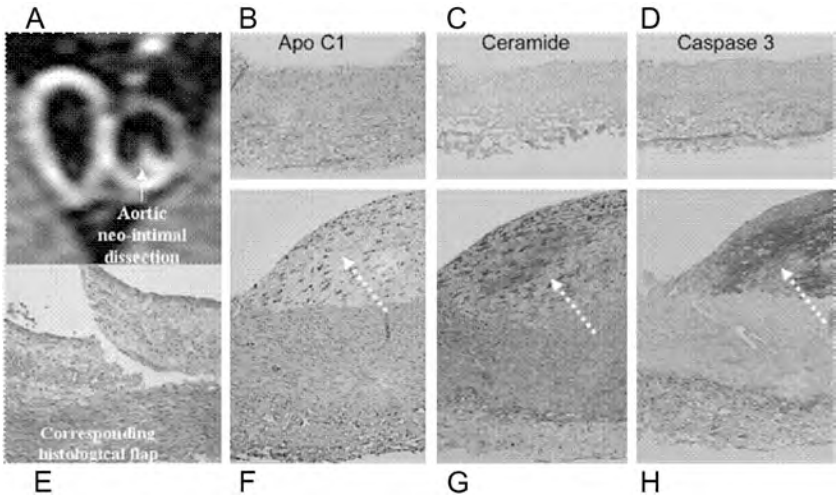

Figure 1.

Purpose: We visualized neo-intimal dissection non-invasively in vivo by MRI and hypothesized that enhanced immuno-histochemical evidence of aforementioned apoptotic molecules could be detected and quantified in areas of visualized plaque rupture.

Methods: We imaged 9 Watanabe hereditable hyperlipidemic rabbits (WHHL; I:3WHHL, II:6WHHL fed with high cholesterol diet for 3 months) before and after Russel's viper venom induced aortic plaque rupture using 3D black blood fast spin-echo vessel wall images on a 1.5 T MR system (Philips). After sacrifice, MRI detected aortic plaque ruptures were analyzed qualitatively via immuno-histochemistry (IH) and quantitatively via Western Blots.

Results: Three animals of group II had MRI-visualized neo-intimal dissection (Fig. 1A) verified by histology (Fig. 1E). There, IH showed marked increases in apoC-1, Cer and Cas-3 (Fig. 1F–H, dashed arrows) compared to I(Fig. 1B–D). Western blots revealed increased (2.5fold ± 05) active N-SMase and Cas-3 when compared to I.

Conclusions: In-vivo MRI visualized neo-intimal dissection was accompanied by IH localization of apoC-I, Cer and Cas-3 previously implicated in aortic smooth muscle cell apoptosis in-vitro and further incriminates these molecules in apoptosis induced atherosclerotic neo-intimal dissection/plaque rupture.

409. Quantification of the Severity of Congenital Aortic Stenosis Using CMR and Echocardiography

Javier Ganame,[1] Steven Dymarkowski, MD, PhD,[2] Andrew M. Taylor, MD, MRCP, FRCR,[2] Marc Gewillig, MD, PhD,[1] Luc Mertens, MD, PhD,[1] Jan Bogaert, MD, PhD.[2]
[1]*Pediatric Cardiology, University Hospitals Leuven, Leuven, Belgium,* [2]*Radiology, University Hospitals Leuven, Leuven, Belgium.*

Introduction: In the last two decades Echocardiography-Doppler (Echo) has become the standard technique to evaluate patients with aortic stenosis (AS). However, Echo has some limitations, first, a good image quality is not always feasible; secondly the peak velocity may be underestimated due to the angle dependency of the Doppler technique; third, the valve area measured by planimetry mostly requires a transesophageal approach. The use of CMR may, therefore, be of interest for clinical evaluation to overcome these difficulties.

Purpose: To assess the accuracy of CMR compared to Echo when measuring the aortic valve area and peak gradient in patients with congenital AS.

Methods: Fifteen patients with moderate to severe congenital AS (mean age: 12.8 ± 2.8 years) were included in this study. All CMR studies were performed on a 1.5 T Philips Intera CV MR unit. After correct localisation of the aortic valve using cine MRI, flow measurements parallel to the aortic valve plane were acquired using a velocity-encoded breath-hold TFE-sequence with retrospective ECG gating. The temporal resolution was 30 msec/frame. The peak aortic gradient was calculated using the simplified Bernoulli equation ($4 \times V_2^2$). The aortic valve area was measured using the continuity equation (Area = LVOT area × {VTI LVOT/VTI Ao}). A linear regression analysis was performed to describe the correlation between the two techniques.

Results: For the aortic valve area a strong correlation was found ($r = 0.81$, $p < 0.001$; mean Echo 1.0 ± 0.4 cm^2 vs. mean CMR: 1.1 ± 0.3 cm^2) (Fig. 1). Moreover, in only 1 pt a difference greater than 0.3 cm^2 was noted. Also a strong correlation was noted for the peak gradient ($r = 0.8$, $p < 0.001$ (Fig. 1); however, CMR tended to overestimate the peak velocity beyond the aortic valve (mean peak velocity Echo: 56.6 ± 15.5 mmHg vs. CMR: 87.8 ± 50.2 mmHg).

Conclusions: In a congenital AS population the aortic valve area measurements with CMR correlate well with the

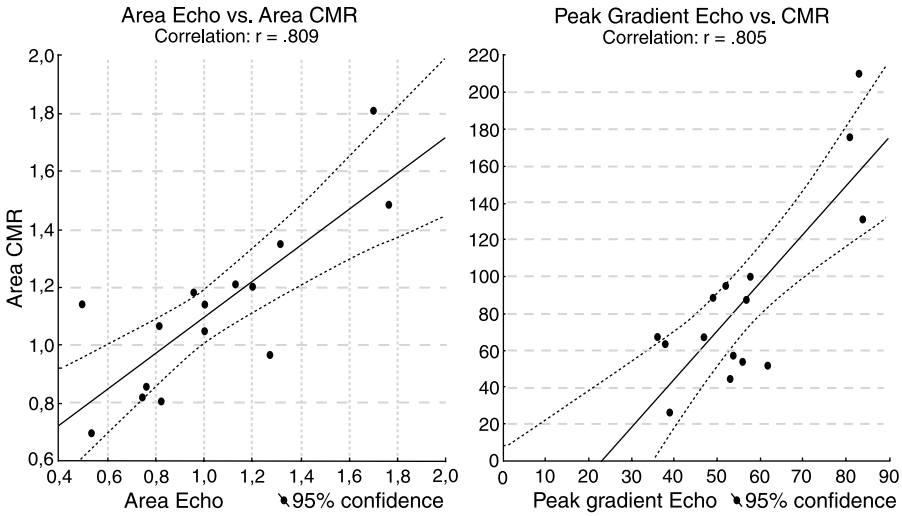

Figure 1.

Echo ones when using the continuity equation formula. These data suggest that CMR could be used as a reliable alternative to Echo for the evaluation of patients with congenital AS.

410. In Vivo Detection of Area-at-Risk by $MnCl_2$ Enhancement in Mouse Models of Reperfused and Non-Reperfused Myocardial Infarction

Brent A. French, PhD,[1] Zequan Yang, MD/PhD,[1] Stuart S. Berr, PhD,[2] Yaqin Xu, MD/PhD,[1] R. Jack Roy, RT,[2] Frederick H. Epstein, PhD.[2] [1]*Biomedical Engineering, University of Virginia, Charlottesville, VA, USA,* [2]*Radiology, University of Virginia, Charlottesville, VA, USA.*

Introduction: Upon injection, manganese ions gain access to cardiomyocytes via calcium channels and enhance perfused regions of myocardium by virtue of their T1-shortening effect. Recent studies have demonstrated that $MnCl_2$ infusion during acute ischemia delineates myocardial area-at-risk up to two hours after reperfusion in a canine model (Aletras et al., 2004). However, this application of $MnCl_2$ has yet to be reported in a mouse model of coronary occlusion (Yang et al., 2004).

Purpose: This study sought to confirm that $MnCl_2$ can be used in mice to delineate the ischemic area-at-risk during coronary occlusion for subsequent detection by MRI. Furthermore, we sought to demonstrate that $MnCl_2$ can be used to delineate ischemic regions in the setting of permanent coronary occlusion, and that Mn-enhanced imaging could be combined with Gd-enhanced infarct imaging.

Methods: Six male C57Bl/6 mice were studied. Four mice were subject to permanent coronary ligation. Two mice were subject to a 45 min coronary occlusion followed by reperfusion. In the mice undergoing permanent ligation, imaging was performed 1–2 days following occlusion with $MnCl_2$ (30 μmol/kg) administered by IP injection 20 min prior to imaging. In mice undergoing transient coronary occlusion, $MnCl_2$ (30 μmol/kg) was administered by IP injection 5 min after the beginning of coronary occlusion and imaging was performed 1–2 hours after reperfusion. After Mn-enhanced imaging, 0.2–0.4 mmol/kg of Gd-DTPA was infused through an indwelling IP line to perform infarct imaging. Images were acquired using an ECG-gated inversion/recovery (IR) gradient echo sequence on a 4.7 T Varian scanner. Imaging parameters were TR = 3 s, TI = 480 ms, TE = 3.6 ms, and flip angle = 90°. After sequentially acquiring images enhanced by $MnCl_2$ and by both contrast agents (Gd-DTPA and $MnCl_2$), subtraction analysis was performed to indicate Mn-enhanced regions in blue and Gd-enhanced regions in red. After imaging, the mouse hearts were removed and assessed histologically for perfused myocardium (stained blue by Phthalo blue) and for necrotic tissue (left white after TTC stained viable tissue red).

Results: The 30 μmol/kg IP bolus of $MnCl_2$ was well tolerated in all animals. Attempts to elevate the dose to 60 μmol/kg led to decreases in heart rate and respiratory function. In all six mice, the location of perfused regions could be defined by Mn-enhancement. Figures 1A and 1B show results from MR imaging and histologic analysis of post-mortem tissue (respectively) for one of the transiently occluded mice. Mn-enhanced, perfused regions of the heart shaded blue by subtraction analysis (A) correspond well with the perfused regions of heart in the gross tissue section dyed blue with Phthalo Blue (B). Similarly, Gd-enhanced, infarcted regions of the heart shaded red by subtraction analysis (A) correspond well with infarcted regions of the heart which remain white after TTC staining (B). Note, however, that residual Gd-DTPA is evident in the LV chamber, and that enhancment due to Gd-DTPA located just beyond the epicardial surface might easily be misinterpreted as infarcted tissue.

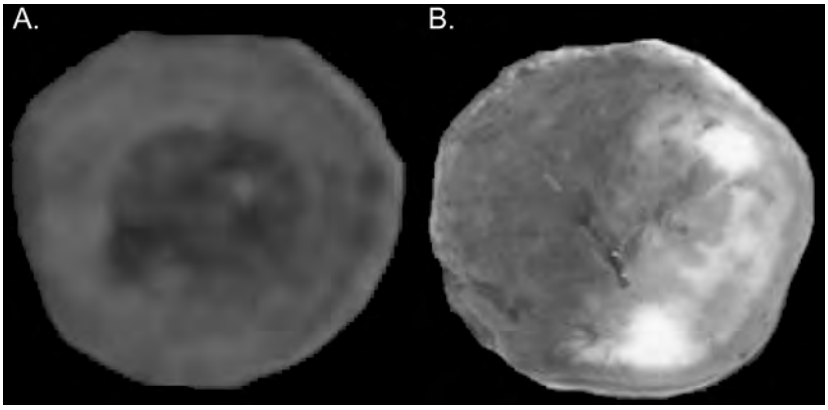

Figure 1.

Conclusions: Mn-enhanced imaging detects perfused regions of myocardium in mice subjected to permanent coronary occlusion. Perfused regions of myocardium can also be labeled with $MnCl_2$ during ischemia, then non-invasively imaged subsequent to reperfusion in mice, as previously described in canines (Aletras et al., 2004). Finally, Gd-DTPA can be administered subsequent to Mn-enhanced imaging to detect infarcted tissue. While toxicity is a concern, the concept of using one contrast agent (e.g., $MnCl_2$) to identify perfused myocardium and a second contrast agent (e.g., Gd-DTPA) to identify infarcted myocardium should prove useful for the non-invasive determination of infarct size as a percent of area-at-risk: an endpoint of critical importance in clinically evaluating the efficacy of infarct-limiting therapies.

REFERENCES

Aletras, A. H., et al. (2004). *Proc. Int. Soc. Mag. Reson. Med.* 11:1841.
Yang, Z., et al. (2004). *Circulation* 109:1161–1167.

411. Improving Navigator Gating in ssfp coronary mra

Thanh D. Nguyen, PhD, Pascal Spincemaille, PhD, Yi Wang, PhD. *Radiology, Weill Medical College of Cornell University, New York, NY, USA.*

Introduction: Effective motion suppression in cornary MRA requires accurate motion information. this implies that the time delay between the motion detection by navigator echo and MRA data acquisition has to be minimal (<20 msec). for navigator gated coronary MRA using the steady state free procession (SSFP) sequence, the preparation dummy RF pulses for steady state is quite long (∼80 msec). the standard use of navigator before the dummy RFs may not be adequate.

Purpose: This work is to investigate a new magnetization preparation scheme for navigator SSFP 3D coronary MRA that executes the navigator and fat saturation pulses in steady state after the dummy RFs in order to minimize the delay between the magnetization preparation and the image echoes.

Methods: Magnetization behavior were simulated using the Bloch equation. the pulse sequence was implemented and

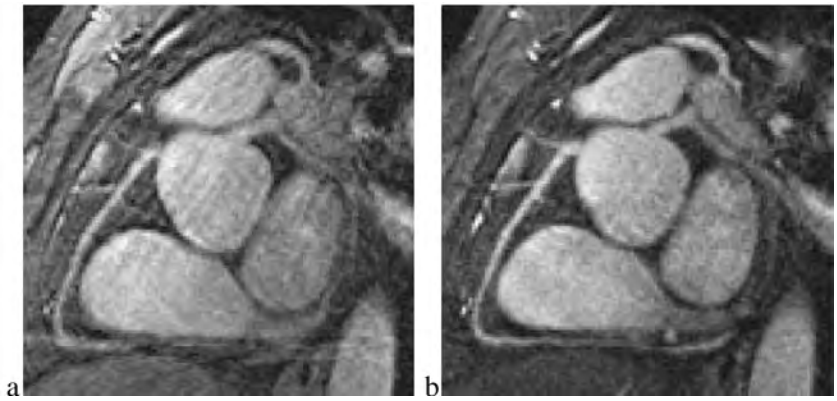

Figure 1. MIP images of RCA acquired with a) the previous and b) the new scheme. Reduced motion artifacts, improved vessel delineation at distal portions, and more effective fat and myocardium suppression are depicted in b.

evaluated on a 1.5 T whole body MRI system. a real time navigator gating system was implemented using BIT3 board and a SUN workstation (latency time < 15 msec). the phase-reordered automatic window selection (PAWS) algorithm was implemented utilized for gating. the real time navigator SSFP 3D coronary MRA with navigator before and after dummy RFs were performed on human subjects ($n = 7$).

Results: Compared to the previous preparation scheme that executes the navigator and fat saturation pulses before the dummy RFs, the new scheme was found to provide more effective motion suppression, significantly improved blood-to-myocardium contrast-to-noise ratio (46%, $p < 0.001$) at slightly but insignificantly decreased blood signal-to-noise ratio (2%, $p = 0.73$), significantly reduced fat signal-to-noise ratio (32%, $p < 0.001$), and better overall image quality ($p = 0.05$; Wilcoxon paired sample signed ranked test).

Conclusions: A new magnetization preparation scheme for steady-state free procession navigator 3D coronary MRA that executes the navigator echo and the fat saturation immediately before the image echoes allows more effective motion & fat suppression and improved CNR for coronary MRA.

412. ECG-Triggered Dynamic Time-Resolved Magnetic-Resonance Angiography of the Thoracic Aorta

David N. Sandman, MD,[1] Timothy J. Carroll, PhD,[1] Orlando P. Simonetti, PhD,[2] Kelly O'Hara, BS,[1] John Salanitri, MD,[1] Ty Cashen, BS,[1] F. Scott Pereles, MD,[1] Edwin Wu, MD,[3] James C. Carr, MD.[1] [1]*Feinberg School of Medicine, Department of Radiology, Northwestern University, Chicago, IL, USA,* [2]*Siemens Medical Solutions, Chicago, IL, USA,* [3]*Feinberg School of Medicine, Department of Medicine, Division of Cardiology, Northwestern University, Chicago, IL, USA.*

Introduction: Time-resolved subsecond contrast-enhanced magnetic resonance angiography (SS-MRA) (Finn et al., 2002), which utilizes acquisition times of 700–800 msec per 3D data set, has been shown to be particularly useful for assessing high-flow abnormalities in the thoracic aorta, such as shunts and dissections. Because of the close proximity to the heart, cardiac motion artifact can frequently obscure subtle findings in the ascending aorta. Acceleration techniques for contrast-enhanced MRA using TREAT (time-resolved, echo-sharing, angiographic technique) and iPAT (intelligent parallel acquisition technique) have recently been developed. When these are used in combination with conventional SS-MRA, it is possible to reduce the acquisition time to less than 300 msec. With frame durations this short, it is possible to use ECG-triggering to gate the acquisition period to diastole, thereby eliminating any cardiac motion artifact. The purpose of this study was to compare conventional SS-MRA to ECG-gated contrast-enhanced MRA using TREAT and iPAT, for the assessment of thoracic aortic disease.

Methods: 58 patients with suspected disease of the thoracic aorta underwent time-resolved contrast-enhanced MRA on Siemens 1.5 T Sonata and Avanto scanners. All patients had correlative imaging with echocardiography, CT or conventional axial MRI. 31 patients were imaged using a conventional subsecond 3D FLASH sequence (SS-MRA) with short TR (TR/TE: 1.6/0.7; flip angle 20°; 256 readout; 6 partitions; 2.6 × 1.4 × 15 mm voxels). 27 patients were imaged with a newer pulse sequence, which combines SS-MRA with TREAT and iPAT. The TREAT sequence, which is based on the original TRICKS (time-resolved imaging of contrast kinetics) (Korosec et al., 1996) concept, uses a novel k space echo-sharing approach with elliptical centric reordering (Fig. 1). When combined with iPAT, the acquisition time was 300 msec per 3D set. ECG-triggering was used to gate the acquisition period to diastole. Scanning parameters were similar to the conventional SS-MRA technique. For both techniques, imaging was carried out in an oblique sagittal orientation and 6 cc of Gadolinium were injected at 6 cc/sec.

A quantitative analysis of vessel sharpness was performed for both techniques in five different anatomic locations (aortic root, ascending aorta, aortic arch, upper thoracic aorta, lower thoracic aorta). Two different methods were used. The first method involved generating a point-spread function across the vessel wall and calculating the upslope of the resultant curve. The second measure involved calculating the profile and distribution of signal intensities across the vessel lumen. Statistical comparisons were performed using a Students t-test, with significance determined at the 5% level.

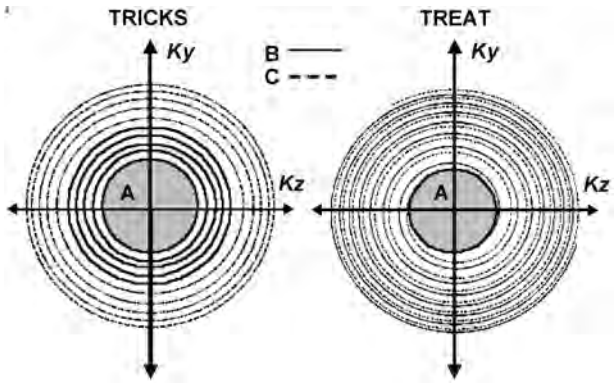

Figure 1. A comparison of the k-space segmentation schemes of hypothetical 3-region (A, B and C regions) TRICKS and TREAT pulse sequences. (a) An elliptically centric encoded TRICKS acquisition acquires A, B, and C regions concentrically with the A region covering the central 1/3 of k-space (solid gray region), the second 1/3 is the B-region (solid lines) and peripheral 1/3 the C-region (dashed lines). (b) The TREAT sequence defines the A-region the same as TRICKS, but interleaves the B-(solid lines) and C-regions (dashed lines).

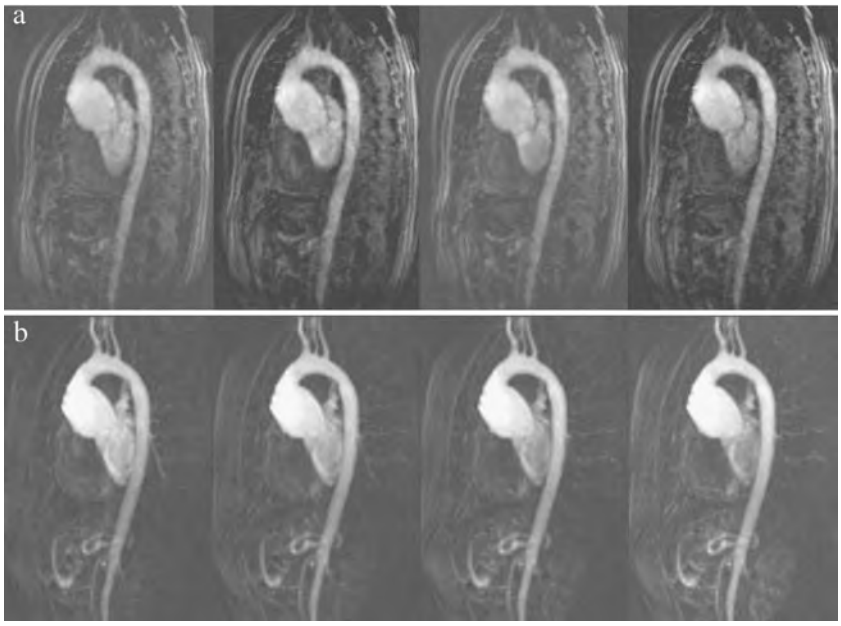

Sequential peak intensity frames of SS-MRA (a) and TREAT (b) sequences in patient with proximal thoracic aneurysm. Note changes in heart dynamics and decreased sharpness of vessel edges in (a).

A qualitative analysis was also performed by two independent observers. Image quality and sharpness were scored on a scale of 1–5. Image artifact was graded on a 3 point scale. The results were compared using a student's t-test.

The presence of pathology in the thoracic aorta was also noted for both techniques.

Results: Quantitative measurements of image sharpness were higher for the ECG-gated technique compared to the conventional SS-MRA (Table 1). This was statistically significant in the aortic root ($p < 0.05$). Qualitative values of image sharpness and quality were higher for the ECG-gated technique ($p < 0.001$). There were fewer artifacts

Table 1.

a)	"Slope"			"Profile error"		
$n = 20$	SS-MRA ($n = 10$)	TREAT ($n = 10$)	p-value	SS-MRA ($n = 10$)	TREAT ($n = 10$)	p-value
Root	0.157(0.065)	0.205(0.094)	<0.05	0.236(0.057)	0.192(0.047)	<0.05
Ascend	0.173(0.047)	0.197(0.081)	n.s.	0.252(0.046)	0.243(0.053)	n.s.
Arch	0.214(0.059)	0.205(0.049)	n.s.	0.288(0.046)	0.260(0.056)	n.s.
Upper Thor	0.214(0.066)	0.197(0.064)	n.s.	0.257(0.044)	0.256(0.034)	n.s.
Lower Thor	0.220(0.065)	0.216(0.095)	n.s.	0.281(0.040)	0.270(0.064)	n.s.

b)	Artifact		Image quality		Sharpness	
n = 58	SS-MRA (n = 31)	TREAT (n = 27)	SS-MRA	TREAT	SS-MRA	TREAT
Root	1.48(0.70)	4.25(0.57)	2.25(0.74)	3.69(0.81)	2.26(0.75)	3.70(0.81)
Ascend	0.98(0.78)	0.28(0.47)	2.89(0.98)	3.91(0.76)	290(0.99)	3.93(0.77)
Arch	0.44(0.57)	0.130(0.33)	3.15(0.38)	4.17(0.60)	3.54(0.84)	4.19(0.61)
Upper Thor	0.35(0.45)	1.11(0.29)	3.66(0.64)	4.20(0.56)	380(0.64)	4.22(0.56)
Lower Thor	0.34(0.43)	0.11(0.29)	3.68(0.61)	4.20(0.56)	3.70(0.61)	4.22(0.56)
Pulm aa	0.35(0.43)	0.150(0.33)	3.65(0.63)	4.150(0.65)	3.66(0.64)	4.17(0.65)
p-value	<0.05		<0.05		<0.05	

a) Results of quantitative image analysis of vessel sharpness, based on the two describes measures. Statistically significant differences were found in both analyses at the aortic root. b) Results of qualitative image analysis of presence of artifact, overall image quality, and vessel sharpness. All values are reported as mean score (standard deviation) from pooling the scores of the independent readers. All differences were significant at the 5% level.

visible on the ECG-gated technique ($p < 0.001$) compared to the conventional SS-MRA. Both techniques were equally accurate at detecting aortic pathology (100% sensitivity).

Conclusion: ECG-triggered, time-resolved CE-MRA produced sharper and higher quality images compared to conventional SS-MRA, particularly in the ascending aorta. ECG-triggered, time-resolved CE-MRA with TREAT and iPAT is a superior technique for evaluating the thoracic aorta and may be particularly useful for better demonstrating disease in the ascending portion.

REFERENCES

Finn, et al. (2002). *Radiology* 224:896–904.
Korosec, F. R., et al. (1996). *Magn. Reson. Med.* 36:345–351.

413. Contrast-Enhanced MR Coronary Artery Wall Imaging: Comparison with Multidetector CT and X-ray Angiography

Susan B. Yeon, MD, JD,[1] Adeel Sabir, MD,[2] Melvin Clouse, MD,[2] David Maintz, MD,[3] Warren J. Manning, MD,[4] René M. Botnar, PhD.[1] [1]*Cardiovascular Division, Beth Israel Deaconess Medical Center, Boston, MA, USA,* [2]*Department of Radiology, Beth Israel Deaconess Medical Center, Boston, MA, USA,* [3]*Department of Clinical Radiology, University of Muenster, Muenster, Germany,* [4]*Cardiovascular Division and Department of Radiology, Beth Israel Deaconess Medical Center, Boston, MA, USA.*

Introduction: Plaque characteristics underlie the pathophysiologic processes that produce the clinical sequelae of atherosclerotic disease. Assessment of plaque by conventional luminographic techniques fails to adequately reveal the nature and quality of plaque burden and associated potential risk. Contrast enhanced MR techniques have been found to be useful for characterization of carotid artery and aortic plaque. Preliminary work has explored the potential utility of contrast enhancement for assessment of coronary artery plaque (Maintz D et al. RSNA 2004 abstract) but the significance of such contrast enhancement has not been defined.

Purpose: We sought to determine the relationship between coronary artery wall contrast enhancement by MR, plaque assessment by multidetector computed tomography (MDCT) coronary angiography, and lumen stenosis by conventional x-ray angiography (CATH) in a series of patients referred for coronary angiography.

Methods: MR scans were performed on a 1.5-T Gyroscan ACS-NT scanner (Philips Medical Systems) with 5-element cardiac synergy coil. Coronary artery imaging of the right and left systems was performed using an ECG triggered, free-breathing navigator gated targeted 3D SSFP coronary MRI sequence. Imaging parameters included $1.0 \times 1.0 \times 3.0$ mm voxel size, TR/TE = 5.7/2.8 ms, flip angle = 110°, and slice number = 20. Contrast-enhanced vessel wall imaging was performed using a T1-weighted black blood 3D IR-TFE sequence in the same imaging plane and with the same voxel size with TR/TE = 6.1/1.9 ms, flip angle = 30°, inversion time ~300 ms. The inversion time was calculated based on the dose of and timing after contrast injection. Gadolinium-DTPA (gadopentetate dimeglumine, Magnevist®) 0.2 mmol/kg was administered ~60 minutes prior to the start of imaging. Imaging time was ~12 minutes/each sequence for each coronary artery system. MDCT (16 detector, Toshiba Aquilion CFX) was performed following administration of 120 ml nonionic contrast agent (Isovue 300®). Scan parameters included slice thickness = 0.5 mm, pixel size = 0.23×0.23 mm, gantry rotation time = 0.4 s, total scan time = 25–30 s. Image analyses were performed for the proximal and mid segments of the RCA, LAD, and LCX coronary arteries. The presence of contrast enhancement by MR in each segment was assessed. The presence of noncalcified and calcified plaque by MDCT in each segment was independently evaluated. These results were compared to the distribution of clinically reported ≥30% coronary artery stenoses by CATH.

Results: 45 coronary artery segments in 8 patients were evaluated (1 segment not evaluated due to vessel size, 2 segments due to stents). MR coronary artery wall contrast enhancement was observed in segments with and without calcified and noncalcified plaque by MDCT. MR contrast

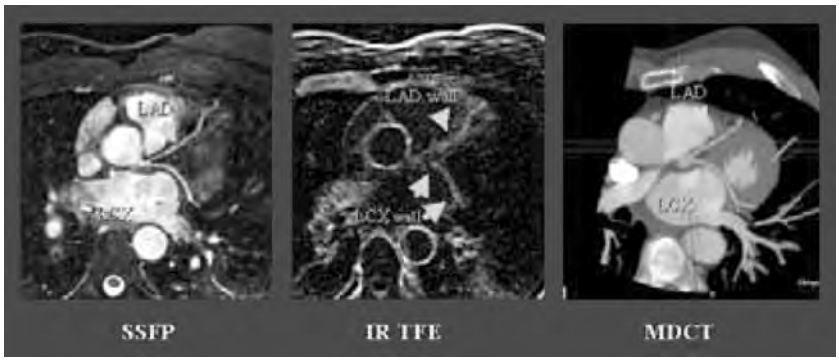

enhancement was observed in 7 (35%) of 20 segments with no plaque by MDCT, 1 (33%) of 3 segments with noncalcified plaque, 3 (38%) of 8 segments with mildly to moderately calcified plaque and in 7 (50%) of 14 with moderately to severely calcified plaque by MDCT. Calcified plaque was observed in 5 (100%) of 5 segments with clinically reported coronary artery stenosis. Diffuse coronary artery wall contrast enhancement was observed in the segments of 4 (80%) of 5 clinically reported coronary artery lesions but also in 14 segments without angiographically apparent coronary disease.

Conclusions: These preliminary findings demonstrate a complex relationship between coronary artery wall contrast enhancement, plaque calcium and lumen stenosis. Future work will be directed toward further defining plaque characteristics and clinical factors associated with coronary wall contrast enhancement.

REFERENCES

Huber, M. E., et al. (2003). Performance of a new gadolinium-based intravascular contrast agent in free-breathing inversion-recovery 3D coronary MRA. *Magn. Reson. Med.* 49(1):115–121.

Kramer, C. M., et al. (2004). Magnetic resonance imaging identifies the fibrous cap in atherosclerotic abdominal aortic aneurysm. *Circulation* 109(8):1016–1021.

Yuan, C., et al. (2002). Contrast-enhanced high resolution MRI for atherosclerotic carotid artery tissue characterization. *J. Magn. Reson. Imaging* 15(1):62–67.

414. Single Breath-Hold Whole-Heart MRCA with Variable-Density Spirals at 3 T

Juan M. Santos,[1] Charles H. Cunningham,[1] Brian A. Hargreaves,[1] Jin H. Lee,[1] Bob S. Hu,[2] Dwight G. Nishimura,[1] John M. Pauly.[1] [1]*Electrical Engineering, Stanford University, Stanford, CA, USA,* [2]*Cardiovascular Medicine, Palo Alto Medical Foundation, Palo Alto, CA, USA.*

Introduction: Breath held and navigator-gated coronary sequences at 1.5 T have demonstrated encouraging results. However, long scan times and incomplete coverage continue to be major limitations of coronary MRCA. Ideally the increased signal-to-noise ratio of 3 T whole-body imaging systems could be used to improve image quality, increase resolution, and reduce scan time. The higher resonance frequency at 3 T could also improve the performance of chemically-selective contrast preparation. However, increased susceptibility artifacts and increased T1 at the higher field strength have resulted in mixed reports at 3 T. In this work we describe a new thin-slice, high-resolution, multi-slice spiral sequence to cover the entire heart in a single breath hold. This improves SNR, reduces slice-to-slice misregistration and reduces susceptibility artifacts at 3 T.

Purpose: Design and test a breath-held whole-heart coronary acquisition system for 3 T.

Methods: The improved spectral resolution and higher available signal at 3 T allowed us to redesign both the spectral-spatial excitation, and the spiral readout gradients. The wider spectral separation of water and fat at 3 T permitted a much shorter spectral-spatial excitation, while improving the spatial slice profile. The higher signal level allowed shorter readouts to be designed, with improved volumetric coverage, and reduced off-resonance artifacts.

RF Excitation: We have designed a spectral-spatial RF pulse that excites very thin (1.6 mm to 2 mm) slices. This was achieved using a 1-3-3-1 sublobe envelope with 40 mT/m gradient amplitude and 4.8 ms total duration. By oscillating in polarity the RF sublobes, the unwanted bipolar excitation at −440 Hz was suppressed. This enables the use of 1.2 ms sublobe duration (the same as used at 1.5 T), giving thinner slices than would be possible otherwise. *Readout:* To improve temporal and spatial resolution, a spiral-based variable-density sampling scheme was utilized. Sampling density was linearly reduced from 20 cm FOV for low frequencies to 3 cm FOV for high frequencies. As the energy content of high spatial frequencies is relatively low, there is no significant aliasing introduced by reducing the FOV. To obtain an in-plane resolution of 0.7 mm, each slice is acquired with 17 spirals of 5.8 ms. Such a short readout reduces the off-resonance artifacts. Virtually no heart displacement occurs between slices during the 14 ms repetition time. 40 slices were required for 8 cm coverage in the through-plane direction. The sequence was implemented on a GE Signa 3.0 T VH/i system, with 40 mT/m maximum gradient amplitude and 150 T/m/s slew rate. A body coil was used for transmission and a 5-inch surface coil was used for reception.

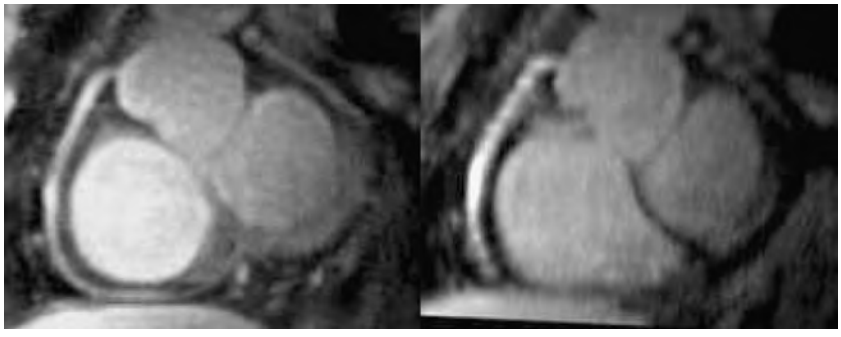

Results: The left image shows the RCA for the whole-heart acquisition where the RCA is visualized in a single slice. The right image shows the same artery but acquired with the slices in the axial direction and reformatted to give the same view. The thin slices and reduced TR allow for virtually artifact free images of the vessel.

Conclusions: Coronary imaging remains difficult due to the need for higher temporal and spatial resolution, thinner slices, and volumetric coverage. Current noninvasive imaging methods all suffer from some drawback. The current sequence exploits the improved spectral separation and increased SNR to cover the entire heart in a single breathhold at high resolutions. The scan time is comparable to current Multi-detector CT angiography but with better temporal resolution. Given this basic sequence, internal or external contrast mechanisms can be incorporated.

415. Optically Coupled Op-Amp Transmit Amplifier and RF Coils For Use In Cardiovascular Intervention

William Overall, PhD,[1] Greig Scott, PhD,[1] Michael McConnell, MD, MSEE,[2] John Pauly, PhD.[1] [1]*Electrical Engineering, Stanford University, Stanford, CA, USA,* [2]*Cardiovascular Medicine, Stanford University, Stanford, CA, USA.*

Introduction: RF safety remains a significant concern for the clinical utility of MRI in cardiovascular interventions. We have developed a system for local RF excitation using an optically coupled RF transmit coil. The relatively small excitation region and low volumetric power deposition inherent to such a technique renders heating of nearby wires insignificant when this coil alone is used for RF transmission. In addition, optical coupling between the RF coil and scan hardware reduces the number of potentially hazardous wires in the scan room. Here, we demonstrate the imaging capabilities of transmit-mode micro-coils using both twin-lead and solenoid configurations.

Methods: To provide power to the micro-coil, the RF amplifier of a GE Signa 1.5 T research scanner was bypassed and replaced with optical fibers providing RF and gating signals to an op-hyphen;based RF amplifier located in the magnet bore (see Figure 1). This miniature battery-powered amplifier can continuously provide 29 mW to a tuned coil at 64 MHz. Because of the small excited volume, SAR deposition is below all limits and available RF power is limited only by the supply and slew rate capabilities of the OPA847 op amp that drives the coil. Both a twin-lead transmitter and a nine-turn solenoid were tested. Each coil was designed to measure less than 7 French in diameter. For imaging, hard-pulse and adiabatic excitations of varying lengths were combined with a 2DFT gradient-echo pulse sequence. Imaging time depended on the duration of the excitation pulse used, but was less than 6 seconds per image in all cases.

Results: Images acquired using this apparatus (see Figure 1) demonstrate good SNR in the region of the coil. For the twin-lead coil, spin saturation near the coil occurred with a 3.6-ms hard RF pulse. As the hard-pulse duration increased further, the extent of excitation increased while spins closest to the coil lost signal due to over-tipping. A 20-ms secant/tangent adiabatic half passage excitation improved signal uniformity, resulting in a maximum SNR around 60 in the region near the coil. For a given pulse sequence, images exhibit similar peak SNR regardless of solenoid or twin-lead configuration.

Conclusions: High-quality images can be acquired with intravascular micro-coil excitation. This concept may be

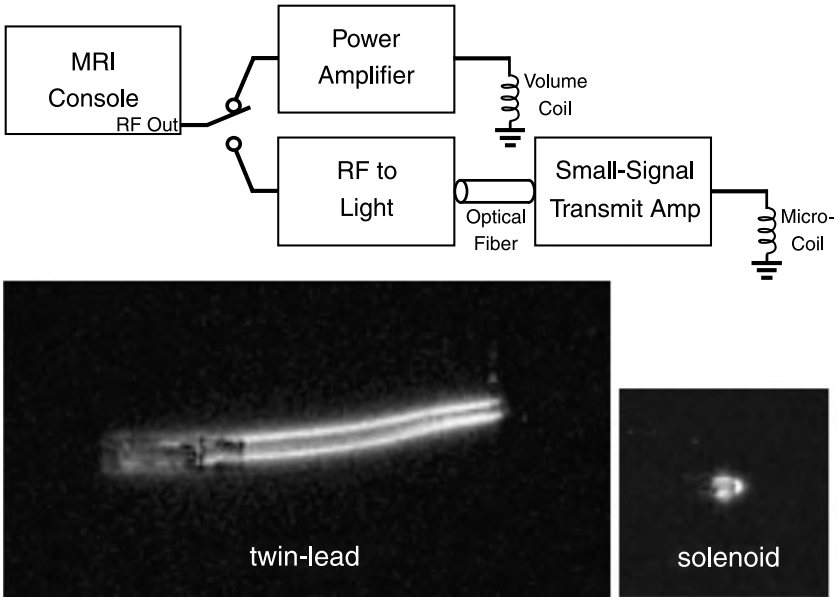

Figure 1.

applied to intravascular imaging and navigation with virtually no risk of catheter heating. Because image SNR is primarily dictated by the receiver hardware, image quality is relatively unaffected by the configuration of the intravascular coil and RF amplifier as long as adequate tipping is achieved. Adiabatic excitation pulses show promise for providing large, uniform signal over an extended region near the coil. Further optimization of the amplifier hardware should allow faster excitations and incorporation of innovative excitation pulses. When used in conjunction with a second RF transmitter for excitation over a larger volume, inversion tagging and selective saturation imaging is possible.

416. Magnetic Resonance Coronary Angiography with An Intravascular Contrast Agent: Initial Experiences in 24 Volunteers

Kai Nassenstein, Kai Uwe Waltering, Sandra Massing, Thomas Schlosser, Peter Hunold, Joerg Barkhausen. *Department of Diagnostic and Interventional Radiology, University Hospital Essen, Essen, Germany.*

Introduction: Within the last 5 years, hard-and software developments have made magnetic resonance angiography of the coronary arteries (MRCA) feasible, but the specificity of current approaches remains insufficient for broad clinical use. However, recent developments have launched different intravascular contrast agents into preclinical studies, which may help to overcome some of the limitations of MRCA. Either iron particles or gadolinium chelates without and with albumin binding have so far been evaluated. All blood pool MR contrast agents have been reported to improve signal-to-noise ratio (SNR) as well as contrast-to-noise ratio (CNR) of blood vessels and surrounding tissues, but they differ in plasma half-life time. Due to fast renal excretion of some macromolecular compounds, SNR and CNR values significantly decrease as soon as 10 minutes after injection.

Purpose: The aim of our study was to assess MS-325, a protein binding intravascular contrast agent with long plasma half-life time, for MRCA.

Methods: 24 healthy volunteers (10 female, 14 male, mean age 29.8 ± 6.1 years) were included in this study. All examinations were performed on a 1.5 T MR scanner (Sonata, Siemens Medical Solutions). MRCA using an inversion recovery fast low angle shot sequence (Turbo-FLASH: TR 3.8 ms, TE 1.6 ms, FA 25°, band width 490 Hz/pixel, voxel size 1.8–2.3 mm3) was applied during breath hold. Image acquisition started immediately after contrast injection (MS-325, EPIX, Boston) (0.05 mmol/kg body weight) and constantly repeated over a total time period of 30 minutes. The inversion-recovery preparation pulse was

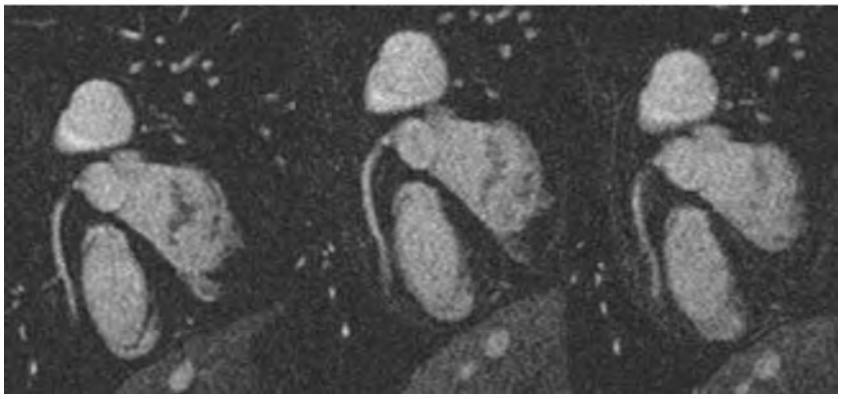

Figure 1. MRCA of the RCA 2, 9 and 20 minutes after injection of MS-325.

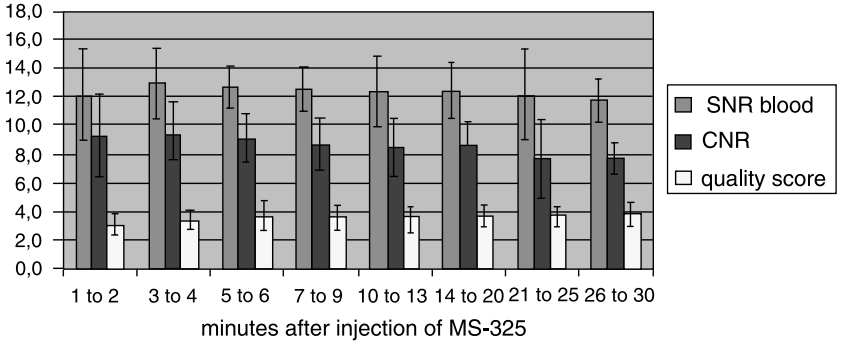

Figure 2. Bar graphs represent the time course of blod SNR, blood-to-myocardium CNR and quality score over 30 minutes.

employed to suppress myocardial signal and to maximize blood-myocardium contrast. Inversion-times for maximal blood-myocardium contrast were individually determined for each scan. Signal-to-noise ratio (SNR) and contrast-to-noise ratio (CNR) values were calculated. Image quality of the proximal and middle coronary segments was assessed by two radiologists in consensus based on a 5-point Likert scale ranging from 1 (excellent), 2 (good), 3 (moderate), 4(poor), 5 (non-diagnostic).

Results: MRCA with MS-325 was successfully completed in all volunteers. No clinically relevant adverse events were observed in our study cohort. SNR of blood showed no significant differences over 30 min after injection. However, the CNR of blood and myocardium slightly decreased over time. This may be caused by a slow diffusion of the predominantly intravascular contrast medium into the extracellular space. The mean images quality scores slightly degraded over time.

Conclusions: Image quality of MRCA could be improved by use of ultrafast imaging techniques, by suppression of myocardial signal, and by application of T1-shortening contrast media. For magnetic resonance angiography blood pool contrast media promise improved image quality due to their higher T1-relaxivities and their predominant intravascular distribution. Our studies demonstrated that high quality MRCA can be performed over a time of 30 minutes after injection of MS-325, which allows for multiple breath-hold or even navigator scans of all three mayor coronary arteries with a single injection (Figures 1 and 2).

417. Noninvasive Coronary Artery Plaque Visualization and Differentiation by Contrast Enhanced Black Blood MRI

David Maintz, MD,[1] Murat Ozgun, MD,[1] Andreas Hoffmeier, MD,[2] Walter Heindel, MD,[1] Roman Fischbach, MD,[1] René M. Botnar, PhD.[3] [1]*Department of Diagnostic Radiology, University of Muenster, Muenster, Germany,* [2]*Department of Cardiothoracic Surgery, University of Muenster, Muenster, Germany,* [3]*Cardiovascular Division, Beth Israel Deaconess Medical Center, Boston, MA, USA.*

Introduction: Noninvasive characterization of'atherosclerotic plaques using coronary MR vessel wall imaging would be a highly desirable tool for risk assessment of coronary artery disease and acute coronary syndromes.

Purpose: To evaluate contrast enhanced black blood coronary MRI for selective visualization and non-invasive differentiation of atherosclerotic coronary plaque in humans.

Methods: Eight patients with coronary artery disease (CAD) as confirmed by x-ray angiography and multi-detector CT (MDCT) were studied by T1-weighted black blood inversion recovery coronary MRI before (N-IR) and after administration of Gd-DTPA (CE-IR). Plaques were categorized as calcified, non-calcified, and mixed based on their Hounsfield number derived from MDCT.

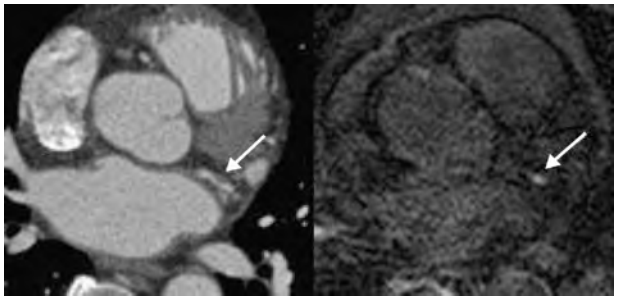

Figure 1. 56-year old patient with CAD. CT (left image) demonstrates noncalcified plaque of the circumflex coronary artery. Inversion Recovery MRI (right image) facilitates exclusive plaque visualization.

Results: With MDCT, a total of 27 plaques could be identified, 6 of whom were calcified (calcified nodules were not evaluated), 5 non-calcified and 16 mixed calcified/non-calcified. On N-IR MRI, 6/6 (100%) calcified plaques appeared dark, 3/5 (60%) non-calcified plaques were dark and the remaining 2/5 (40%) were bright. Two of 16 (13%) mixed plaques were bright and 14/16 (87%) were dark. On CE-IR MRI, all calcified plaques appeared dark, 2/5 (40%) non-calcified plaques were dark and 3/5 (60%) were bright, 10/16 (63%) mixed plaques were bright and 5/16 (31%) were dark. Of the 16 non-calcified and mixed plaques that appeared dark on N-IR MRI, 1 non-calcified and 10 mixed plaques appeared bright on CE-IR MRI (contrast uptake). There were no plaques with bright appearance on N-IR and dark appearance on CE-IR MRI.

Conclusions: In this study, we demonstrate the use of black blood CE-IR coronary MRI for the detection of selective contrast uptake in non-calcified and mixed coronary plaque in patients with CAD. The observed contrast uptake may be associated with neovascularization, inflammation, and/or endothelial dysfunction, markers for plaque vulnerability. We conclude that this method may have potential for noninvasive characterization of coronary plaque in patients with subclinical and advanced CAD (Figure 1).

418. Flow Targeted Coronary MR Angiography: Comparison of Three Different Techniques

Marcus Katoh,[1] Rene M. Botnar,[2] Arno Buecker,[1] Warren J. Manning,[2] Rolf W. GÃ□nther,[1] Matthias Stuber,[3] Elmar Spuentrup.[1] [1]*Department of Diagnostic Radiology, RWTH Aachen University Hospital, Aachen, Germany,* [2]*Department of Medicine (Cardiovascular Division), Beth Israel Deaconess Medical Center and Harvard Medical School, Aachen, MA, USA,* [3]*Department of Radiology, Division of MRI Research, Johns Hopkins University Medical School, Baltimore, MD, USA.*

Purpose: Comparison of three navigator-gated and cardiac-triggered 3D steady-stat free-precession (SSFP) sequences using varying magnetization preparation pre-pulses in order to obtain blood flow information in the coronary arteries.

Materials and Methods: Coronary MRA of the right coronary artery was performed in ten healthy volunteers (5 men, 5 women, mean age 33 years) on a 1.5 Tesla MR system (Gyroscan ACS-NT, Philips Medical Systems, Best, NL) using three 3D radial SSFP coronary MRA approaches (TR/TE 6.3/3.2 ms, FA 120, TFE factor 20, acquisition window 126 ms, FOV 360 mm^2, matrix 384 radial trajectories, spatial resolution $0.9 \times 0.9 \times 3.0$ mm^3):

Projection SSFP (ProjSSFP). Two data sets, one with and one without a 2D selective inversion (labeling) pre-pulse inverting the magnetization of the blood in the ascending aorta. During a labeling delay labeled aortic blood enters into the coronary arteries. Subtraction of the two data sets provides selective visualization of the coronary arteries.

Local Re-Inversion SSFP (LoReInSSFP). One data set, using a double-inversion pre-pulse (a non-selective inversion pulse immediately followed by a 2D selective inversion pulse; the latter re-inverts the magnetization of the blood in the ascending aorta). During an inversion delay the re-inverted aortic blood enters into the coronary arteries allowing for selective visualization of the coronary arteries, while the remaining tissue is signal suppressed.

Local Inversion Inflow SSFP (InflowSSFP). A slice-selective inversion pre-pulse positioned along the main axis of the coronary artery suppresses signal from the coronary blood and the adjacent tissue. During an inversion delay unsaturated blood from the ascending aorta enters into the inversion volume (i.e. coronary artery) allowing for visualization of the entering blood. The assets and drawbacks of each technique were evaluated. Furthermore, SNR of the coronary arteries, CNR between the coronary arteries and the epicardial fat, vessel length and vessel sharpness were analyzed.

Results: Bright-blood coronary MR angiograms providing blood flow information were successfully obtained in all volunteers. Both *ProjSSFP* (Fig. 1a) and *LoReInSSFP* (Fig. 1b) allowed for selective visualization of the coronary arteries with excellent background suppression. Scan time was doubled in *ProjSSFP* due to the two data sets. In *InflowSSFP* (Fig. 1c), only tissue included in the inversion volume was signal suppressed. *ProjSSFP* and *InflowSSFP* yielded significantly increased SNR (Proj: 26, LoReIn: 12, Inflow: 28; $p < 0.05$) and CNR (Proj: 22, LoReIn: 10, Inflow: 25; $p < 0.05$) compared to *LoReInSSFP*. Comparable vessel length was found with all sequences (Proj: 70, LoReIn: 62, Inflow: 73; n.s.) while vessel sharpness was best in *InflowSSFP* (Proj: 59, LoReIn: 54, Inflow: 68; $p < 0.05$). Constantly good image quality was achieved using *InflowSSFP* likely due to the simple planning procedure and short scanning time.

Figure 1.

Conclusion: In this study, three coronary MRA approaches with varying magnetization pre-pulses are presented providing additional blood flow information without contrast medium application. *InflowSSFP* provided

highest SNR, CNR and vessel sharpness and may prove useful as a fast tool for assessing coronary blood flow, requiring less planning skills than *ProjSSFP* and *LoReInSSFP* MRA.

419. Evaluation of Current Thoracic Aortic Stent-Graft Devices For Applicability with Use of Real-Time MRI—An In-Vitro Study

Holger Eggebrecht, Michael Zenge, Jörg Barkhausen, Raimund Erbel, Mark E. Ladd, Harald H. Quick. *Radiology, University Essen, Essen, Germany.*

Introduction: Endovascular stent-graft repair has recently emerged as a valuable, minimally-invasive alternative to surgery in the treatment of patients with diseases of the descending thoracic aorta. So far, stent-graft placement is performed under fluoroscopic/angiographic guidance, which requires the application of ionizing radiation and the administration of potentially nephrotoxic contrast material. These limitations may be overcome by magnetic resonance imaging (MRI)-based procedure guidance, as there are several advantages of MRI guidance in interventional procedures compared with fluoroscopic guidance, including superior soft-tissue contrast.

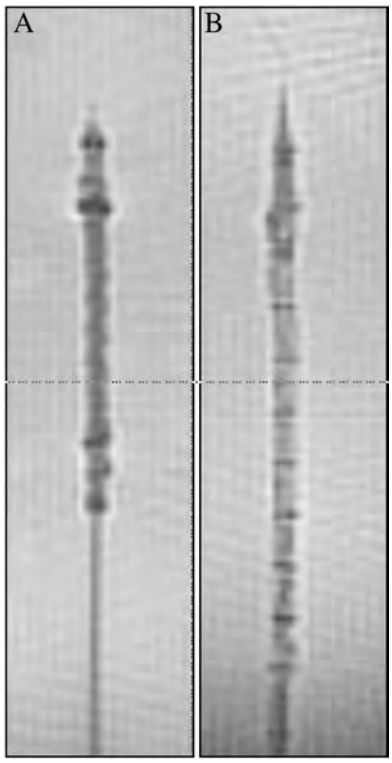

Figure 1. MRI-visualization of the delivery system with mounted stent-graft (A-GoreTAG, B-Evita).

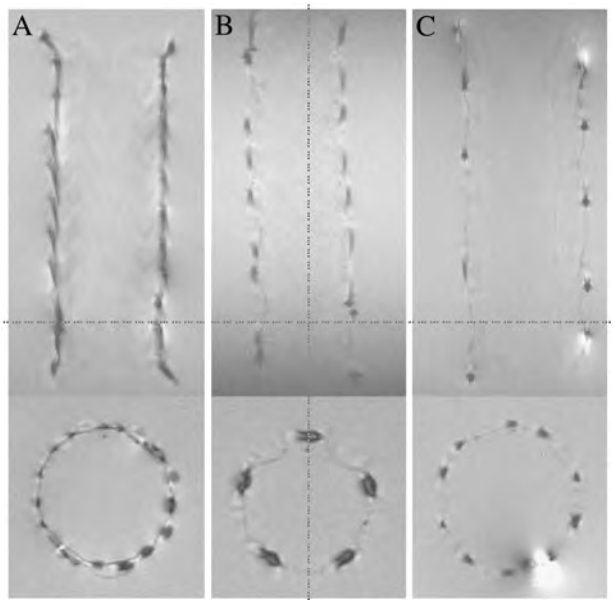

Figure 2. MRI-visualization of expanded stent-grafts (A-GoreTAG, B-Evita, C-Talent).

Purpose: To evaluate the MRI characteristics of commercially available thoracic aortic stent-graft systems.

Methods: Four commercially available stent-graft devices [Talent (Medtronic), Evita (Jotec), GoreTAG (Gore), Zenith (Cook)] used for thoracic aortic repair were examined using a 1.5-T MRI-scanner (Magnetom Sonata, Siemens Medical Systems, Erlangen, Germany). First, each stent-graft, mounted on its delivery system, was placed in the water phantom along the axis of the main magnetic field. This phantom was examined with using real-time steady-state free precession sequences (TrueFISP) with cartesian and radial k-space filling. In a second step, the expanded stent-grafts without their deployment systems were examined in a water bath containing gadolinium (1:40) using a segmented inversion-recovery TurboFLASH sequence. Image quality was visually assessed by two radiologists.

Results: Two of the 4 stent-graft delivery systems with the mounted stent-graft (GoreTAG and Evita) could be visualized by real-time MRI (Figure 1). MR imaging with radial k-space filling showed fewer artifacts than cartesian imaging. The delivery system of the Talent as well as the Zenith stent-graft contained ferromagnetic elements causing large susceptibility artifacts. Three nitinol-based stent-grafts without the delivery system could be visualized by MRI (Figure 2). Only the stainless steel-based Zenith stent-graft caused severe susceptibility artifacts, which did not allow visualization of the stent-graft lumen or its vicinity.

Conclusion: The GoreTAG and the Evita stent-graft are suitable for MRI-based procedure-guidance. The stent-grafts as well as their delivery system can be visualized using real-time MRI with only minor artifacts.

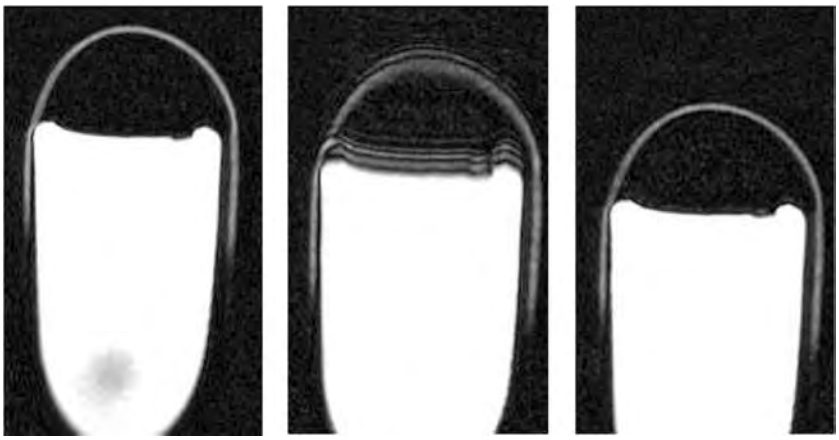

Figure 1. a-Static image; b-Image acquired at highest velocity; c-Image acquired at Tds.

420. Automated Identification of Minimal Myocardial Motion Period During a Cardiac Cycle for Coronary MRI

Ali O. Ustun,[1] Khaled Zakarya Abd-Elmoniem,[1] Christian Stehning,[2] Matthias Stuber, PhD.[3] [1]*Electrical and Computer Engineering, Johns Hopkins University, Baltimore, MD, USA,* [2]*Electrical and Computer Engineering, Univeristy of Karlsruhe, Karlsruhe, Germany,* [3]*Radiology, Johns Hopkins University, Baltimore, MD, USA.*

Introduction: For advanced motion suppression in coronary MRI, the identification of the period of minimal myocardial motion is important. Heart-rate dependent formulas and visual inspection have been used, but an objective, automated algorithm is needed for improved motion suppression.

Purpose: The development of a computer algorithm that automatically identifies rest periods in the cardiac cycle for improved motion suppression in coronary MRI.

Methods: Adjacent functional SSFP images with a high temporal resolution of 14 ms are analyzed by cross-correlations of a user-specified region of interest. Two adjacent frames with a small distance between 1) the center of gravity of their 2D correlation matrix and 2) the center of this matrix are considered as having minimal motion knowing that center of gravity and the center of the matrix are identical if there is no motion. Using this algorithm, a time dependent

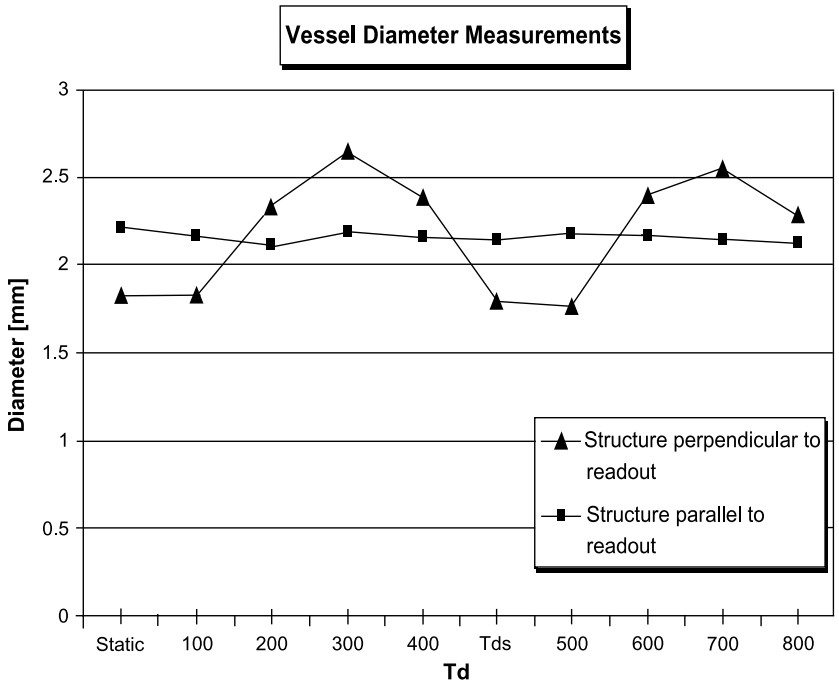

Figure 2. Vessel diameter measurements versus Td.

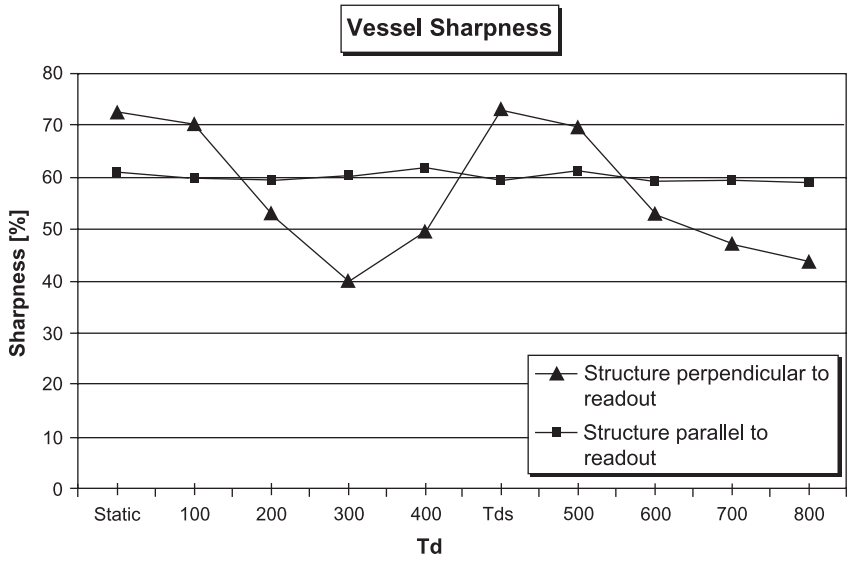

Figure 3. Vessel sharpness versus Td.

array of correlation-indexes is obtained. By generating moving integrals of this array within user-defined acquisition intervals (Ta), the interval showing the least distance to the center of the matrix is defined as the interval of minimal motion for an acquisition window of the duration Ta. The software was implemented in IDL on a commercial PC which is connected to the database of the scanner.

In order to test this software, an MR compatible, sinusoidally moving phantom with ECG output and a maximum displacement of 2.6 cm (frequency of 72 cycles/min, vmax $\sim$ 11 cm/s) was developed. A curved plastic tube (filled with oil) with an internal diameter of 1.8 mm attached to a water bottle was mounted on the moving phantom and a 2D functional SSFP scan (Δt = 14 ms, 60 frames) was obtained and further processed by the software for the automated identification of the period of minimal motion. Subsequently, the moving phantom was imaged with a conventional navigator gated and corrected 3D high-resolution segmented k-space imaging sequence (TR = 7.0 ms, TE = 2.4 ms, voxel size = 0.7 $\times$ 1.0 $\times$ 3.0 mm, 10 k-space lines per cardiac cycle, Ta = 70 ms, $\alpha = 35°$). The time delay (Td) between the phantom generated R-wave and the imaging sequence was then adjusted to 100 ms, 200 ms. . .800 ms. For comparison, one static scan without motion was acquired and another with the Td prescribed by the software (Tds).

Vessel diameter and sharpness were then analyzed using the 'Soap Bubble' software (Etienne et al, MRM 2002). Analysis was performed in two $\sim$3 cm contiguous segments of the tube perpendicular and in parallel to the readout direction.

Results: Major blurring is observed for data collection during high phantom velocities (11 cm/s) in the structure perpendicular to the readout direction (Figure 1). In these segments, this leads to a Td dependent overestimation of vessel diameter measurements (Figure 2). The values obtained from the structure in parallel to the readout direction show only minor variation. No significant difference in vessel diameter was found between the 'static' condition and data collection at Tds.

Similarly, vessel sharpness measured in the structure perpendicular to the readout direction varies as a function of Td (Figure 3). For high velocities at Td = 300 ms (10.17 cm/s) and 700 ms (10.14 cm/s), the above-described blurring leads to a compromised edge definition or sharpness. In contrast, the sharpness from the static conditions and that from Tds are identical.

Discussion and Conclusion: A computer algorithm that automatically and accurately identifies rest periods in a periodically moving object was developed. Acquisition periods prescribed by this objective tool led to image quality approaching that from static conditions. Different quantitative values found for structures in parallel and perpendicular to the readout direction may be attributed to the anisotropic spatial resolution. The utility of the tool for improved coronary MRI is currently being explored and preliminary results look very encouraging.

421. Coronary Blood Flow Visualization Using Inversion Prepared Steady-State Free-Precession (SSFP) MR Angiography

Marcus Katoh,[1] Elmar Spuentrup,[1] Matthias Stuber,[2] Arno Buecker,[1] Warren J. Manning,[3] Rolf W. GÃnther,[1] Rene M. Botnar.[3] [1]*Department of Diagnostic Radiology, RWTH Aachen University Hospital, Aachen, Germany,* [2]*Department of Radiology, Division of MRI Research, Johns Hopkins University Medical School, Baltimore, MD, USA,* [3]*Department of Medicine (Cardiovascular Division), Beth Israel Deaconess Medical Center and Harvard Medical School, Boston, MA, USA.*

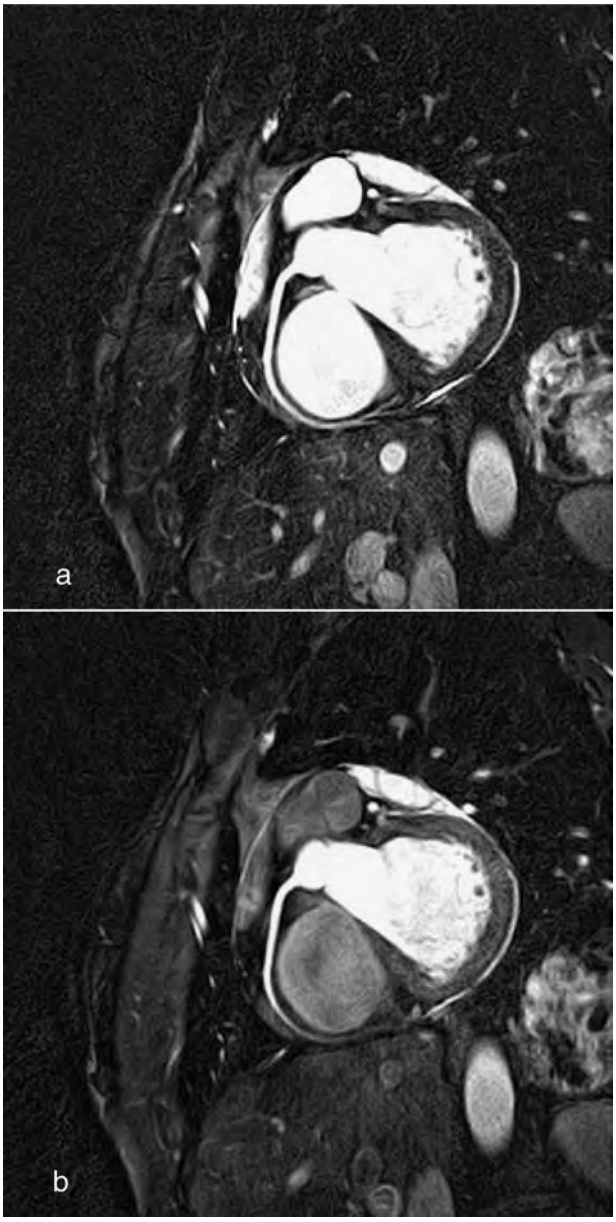

Figure 1.

Purpose: Visualization of coronary blood flow by means of a selective inversion pre-pulse in concert with bright-blood coronary MRA.

Materials and Methods: The right coronary artery (RCA) in seven healthy volunteers (6 men, 1 woman, 39 years) was investigated on a 1.5 Tesla MR system (Gyroscan ACS-NT, Philips Medical Systems, Best, NL) using a free-breathing navigator-gated and cardiac-triggered 3D SSFP sequence (TR/TE 6.3/3.2 ms, FA 120, FOV 360 mm^2, matrix 384 radial trajectories, $0.9 \times 0.9 \times 3$ mm^3). Radial k-space sampling was employed for improved motion artifact suppression. Imaging was performed twice a) with and b) without a slice-selective inversion pre-pulse, which was positioned along the main axis of the coronary artery. Using the inversion concept, coronary blood and tissues that are included in the inversion volume are signal suppressed while unsaturated blood from the ascending aorta that enters the coronary arteries during an inversion delay appears signal-enhanced. Objective image quality parameters such as SNR, CNR, maximal visible vessel length, and vessel border definition were assessed.

Results: In contrast to conventional bright-blood 3D coronary MRA, the use of a selective inversion pre-pulse provided a direct measure of coronary blood flow (Fig. 1a, b). The displayed vessel length corresponds to the distance that coronary blood travels during one RR interval. In addition, CNR between the RCA and right ventricular blood was increased (13 vs. 1; $p < 0.01$) and a tendency towards better vessel border definition was found (68 vs. 60; n.s.). Blood SNR and CNR between RCA blood and epicardial fat were comparable for both sequences. As expected, maximal visible vessel length was significantly longer using conventional SSFP imaging without the inversion pre-pulse (73 mm vs. 114 mm, $p < 0.01$).

Conclusion: The combination of a free-breathing navigator-gated and cardiac-triggered 3D SSFP sequence with a selective inversion pre-pulse allows for direct and directional visualization of inflowing coronary blood with the additional benefit of improved contrast between coronary and right ventricular blood. This approach may prove useful to differentiate between antegrade flow and collateral filling.

422. Reproducibility of Coronary Vessel Wall Dimension Measurement Obtained Using 3D Free Breathing Black Blood MRI

Milind Y. Desai, MD, Shenghan Lai, MD, PhD, Robert G. Weiss, MD, Matthias Stuber, PhD. *Johns Hopkins University, Baltimore, MD, USA.*

Background: The process of atherosclerosis generally begins in the vessel wall as outward remodeling and luminal encroachment occurs only as a later phenomenon. It is now possible to detect coronary vessel wall remodeling non-invasively, along an extended length of the coronary artery, using three dimensional (3D) free breathing black-blood magnetic resonance imaging (MRI) (*Circulation*. 2002;106:296–9). However its reproducibility for follow-up examinations in-vivo has not been investigated.

Purpose: The purpose of this study was to assess the reproducibility and the degree of variability of 3 D free breathing black blood MRI, using both manual and automatic techniques.

Methods: Right coronary arterial (RCA) wall scans in parallel to the RCA were obtained in 18 healthy adult subjects (ages 25–43 years, 6 females), with no known history of coronary artery disease, using a 3D dual-inversion navigator gated black-blood spiral imaging sequence. The dual-inversion pre-pulse was extended with a highly

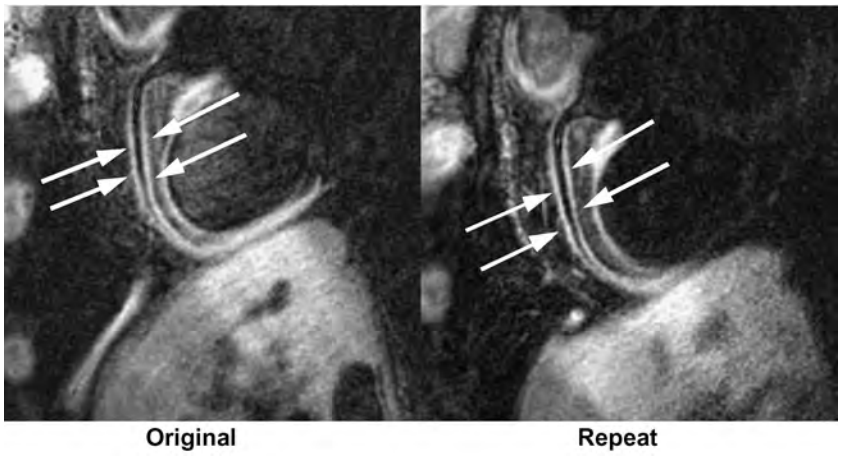

Figure 1.

spatially selective cylindrical inversion of the magnetization. The spatial resolution was $0.7 \times 0.7 \times 2$ mm and the acquisition window 50 ms. The technique was implemented on a commercial 1.5 T Philips Intera system and the scans were repeated in 9 volunteers, 1 month apart (Figure 1). The wall thickness was calculated (twice by 1 reader and once by 2nd reader) manually (average of 3 readings at different points along the vessel) as well as by using an automatic tool (*Magn Reson Med*. 2002;48:658–66), to calculate intra-observer, inter-observer and inter-scan reproducibility. Reproducibility was assessed by linear regression and intra-class correlation coefficient (ICC). Signal to noise and contrast to noise ratios (SNR and CNR) of the vessel wall were also determined.

Results: The duration for a 3D vessel wall scan was ~12 minutes. The average SNR and CNR of the vessel walls were 25 ± 12 and 17 ± 9 respectively. The average measured length of the RCA was 44.5 ± 7 mm. The average wall thickness was 1.62 ± 0.22 mm (1.65 ± 0.24 mm in males and 1.56 ± 0.15 mm in females). For the manual technique, the intra-observer inter-observer and inter-scan concordances were as follows: $r = 0.77$, $p < 0.001$, $r = 0.56$, $p < 0.05$ and $r = 0.62$, $p < 0.05$ respectively. Similarly, the ICC's for intra-observer ($r = 0.85$), inter-observer ($r = 0.32$) and inter-scan ($r = 0.83$) analyses were modest and the coefficient of variations were 5–6% (intra-observer and inter-scan) and 17% (inter-observer). For the automatic measurements, there was a significantly higher intra-observer ($r = 0.97$), inter-observer ($r = 0.94$) and inter-scan ($r = 0.90$) concordance for wall thickness (all $p < 0.001$). The ICC's for intra-observer ($r = 0.97$), inter-observer ($r = 0.92$) and inter-scan ($r = 0.86$) analyses were also excellent and the coefficients of variation were 1–2% (intra-observer) and 3-4% (inter-observer/inter-scan).

Conclusion: It is feasible to visualize long segments of RCA repeatedly with a high degree of reproducibility using free breathing 3D black blood MRI technique. Measurement of the vessel wall thickness using the automatic tecnique is superior to manual wall thickness measurement and has a very low inter-measurement variation. Thus, coronary vessel wall thickness can be assessed non-invasively in a highly reproducible manner, which could potentially have a role in screening individuals for subclinical atherosclerosis and in longitudinal therapeutic studies targeting coronary atherosclerosis.

423. Comprehensive Assessment of Coronary Artery Disease: Combination of Adenosine Stress Perfusion and MR Coronary Angiography Using an Intravascular Contrast Agent

Kai-Uwe Waltering, MD,[1] Holger Eggebrecht, MD,[2] Kai Nassenstein, MD,[1] Sandra Massing,[1] Peter Hunold, MD,[1] Jörg Barkhausen, MD.[1] [1]*Department of Diagnostic and Interventional Radiology, University Hospital Essen, Essen, Germany,* [2]*Department of Cardiology, West German Heart Center, University Hospital Essen, Essen, Germany.*

Introduction: For diagnosis of coronary artery disease (CAD), invasive coronary artery angiography (CXA) must still be considered as the standard of reference. Recently, noninvasive magnetic reconance coronary angiography (MRCA) has become possible using breath-hold ECG-gated fast gradient echo sequences with suppression of myocardial signal. To improve the performance of MRCA, intravascular MR contrast agents have been developed. Previous studies described, that intravascular contrast agents also allows for first pass myocardial perfusion imaging.

Purpose: To evaluate an intravascular contrast agent for combined first pass myocardial perfusion imaging and MR coronary angiography (MRCA).

Methods: 5 healthy volunteers (4 male, 1 female, mean age 27 ± 4) and 5 CAD (5 male, mean age 61 ± 9 years)

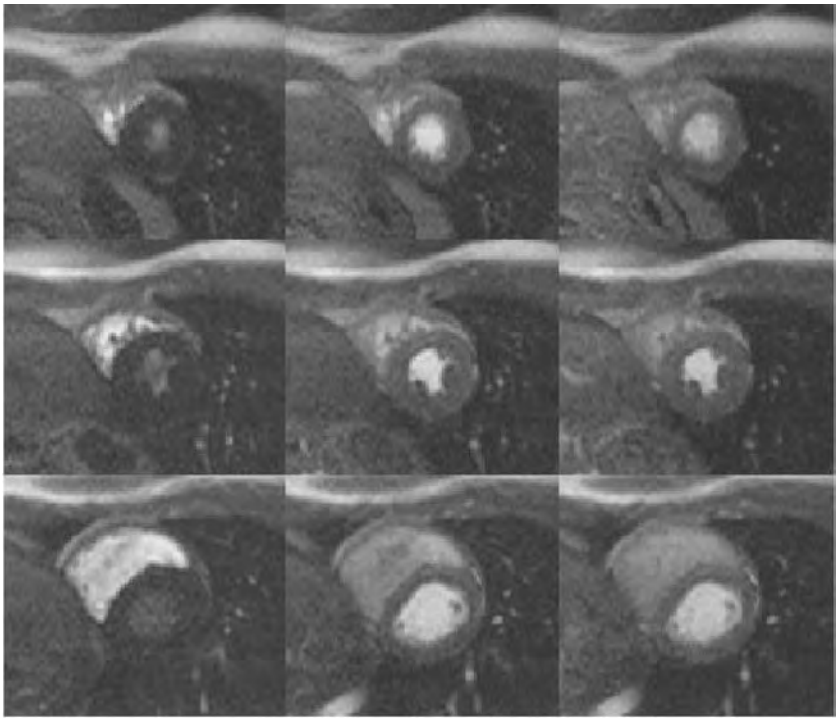

Figure 1.

patients were included in the study. Adenosine stress (0.140 mg/kg body weight) and rest first pass myocardial perfusion imaging was performed using a saturation-recovery fast gradient-echo (SR-FLASH) sequence (TR 2.4 ms, TE 1.2 ms, FA 12°) in short axis orientation. For the perfusion scans Gadomer (0.025 mmol/kg bw, Schering AG) was injected at a flow rate of 2 ml/s using a power injector. Thereafter, an additional dose of 0.1 mmol/kg bw Gadomer was applied and MRCA of the proximal and middle coronary segments was performed using a breath-hold inversion recovery fast low angle shot sequence (IR-FLASH) (TR 3.8 ms, TE 1.6 ms, FA 25°, voxel size 1.8–2.3 mm^3). Myocardial perfusion images were assessed on first-pass perfusion deficits. MRCA images were assessed on coronary artery stenosis.

Results: Stress and rest first pass perfusion and MRCA imaging was successfully completed in all subjects; Fig. 1. Neither acute nor late-phase adverse effects were observed in our study cohort. All volunteers showed homogenous enhancement of the myocardium. A subendocardial perfusion deficit in the posterior wall was detected in one of the CAD patients. MRCA allowed the visualization of the proximal and middle coronary artery segments in all subjects. In the CAD patients we found stenosis of RCA (n = 2), stenosis of LAD (n = 3) and stenosis of RCX (n = 2); Fig. 2.

Conclusions: Currently, only extracellular contrast agents are approved for cardiac MR imaging. However, using these agents about half of the compound leaks out into the interstitial space during first pass. Thus, the myocardial signal intensity depends not only on tissue blood volume and perfusion, but also on the size of the extravascular compartment and the degree of capillary permeability. Therefore, intravascular contrast agents seem to be advantageous for imaging of myocardial perfusion because myocardial signal intensity persistently reflects changes in myocardial blood volume and perfusion. Additionally, several studies have shown that intravascular contrast agents can

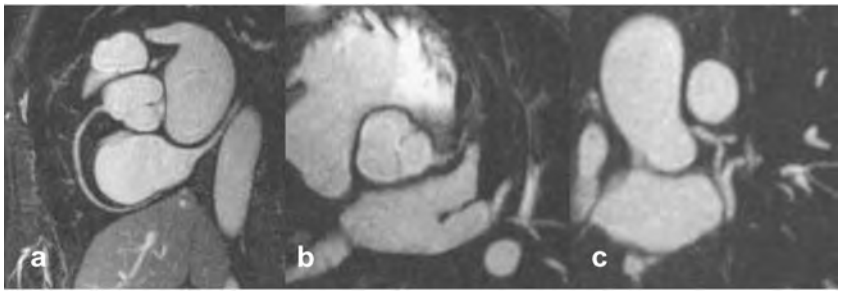

Figure 2. MRCA imaging of CAD patients. Normal RCA (b). Proximal stenosis of LAD (b) and RCX (C).

improve the image quality of MRCA and allow to perform several breath-hold scans after a single contrast injection. Our results show, that the combination of first pass myocardial perfusion imaging and MRCA using an intravascular contrast agent is feasible and mandates further clinical evaluation in a larger patient cohort with coronary artery disease.

424. Improved Spatial-Temporal Resolution MR Coronary Blood Flow Imaging at 3T

Reza Nezafat,[1] Christian Stehning,[2] Ahmed Gharib,[1] Milind Desai,[1] Robert G. Weiss,[3] Roderic Pettigrew,[1] Elliot R. McVeigh,[1] Matthias Stuber.[3] [1]*National Institute of Health, Bethesda, MD, USA,* [2]*Philips Research Laboratories, Hamburg, Germany,* [3]*Johns Hopkins Univeristy, Baltimore, MD, USA.*

In native and bypass graft coronary arteries, MR flow measurements have shown to be a successful method for the non-invasive assessment of patency (Hundley et al., 1996). Because of the small dimensions and rapid motion of the coronary arteries, a high spatial and temporal resolution is mandatory for the assessment of flow. Improved spatial resolution will reduce partial-volume effects, which supports a better estimation of the flow rate. Furthermore, an improved temporal resolution will not only minimize blurring induced by rapid myocardial motion, but will also lead to a significantly improved estimation of peak flow velocity. However, high spatial and temporal resolution imaging results in low SNR and prolonged acquisition time. In this study, we exploit the extra SNR offered by a higher magnetic field strength in combination with free-breathing navigator technology and short acquisition intervals to improve spatial and temporal resolution in coronary flow imaging.

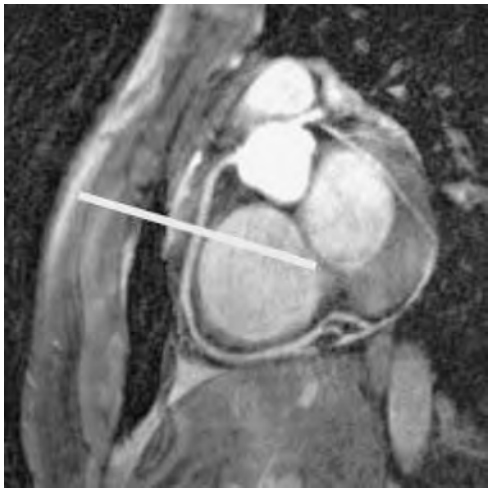

Figure 1. Localization of RCA and prescription of the phase contrast slice.

Methods: All studies were performed on 3.0 T whole body scanner (Philips Medical Systems). A six-element cardiac phased-array was used for signal reception. A slice perpendicular to the RCA was prescribed on an ECG gated, fat suppressed, 3D segmented gradient-echo image (Figure 1). Free-breathing, navigator gated coronary MR blood-flow images were acquired in 5 healthy adult subjects (TR = 5.2 ms, TE = 2.8 ms, FOV = 280 mm, Matrix = 368, V_{ENC} = 50 cm/s). A 2D-selective trailing navigator was acquired at the end of each cardiac cycle. To avoid major respiratory displacement of the coronary between the R-wave of the ECG and the trailing navigator, the trailing navigator was analyzed in relation to that of the preceding R–R interval and data were only accepted for reconstruction if the detected lung-liver interface positions fell within the same 5 mm gating window for both navigators.

Results: Figure 2 displays example magnitude and velocity map images. Note the very sharp visual delineation of the RCA on the magnitude image and high number of pixels in the phase contrast image. Due to the inflow of fresh, unsaturated magnetization into the imaging plane, the full benefits of increased polarization at 3 T are realized. An in-plane spatial resolution as low as 0.76×0.76 mm^2 (reconstructed to 0.55×0.55 mm^2) and a temporal resolution

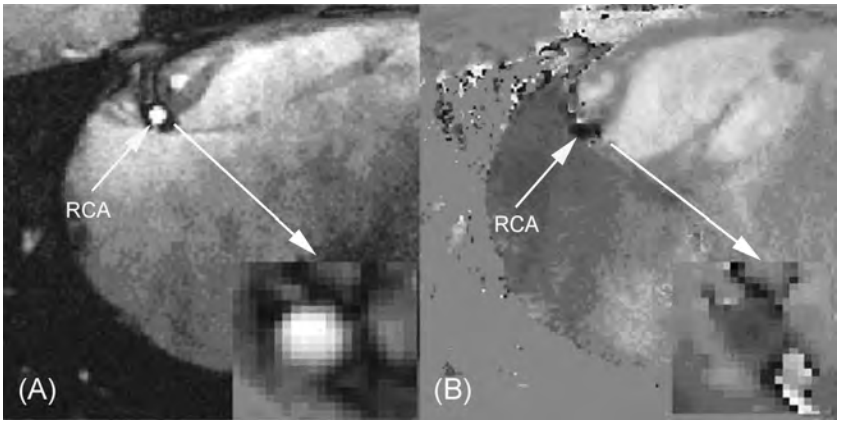

Figure 2. (A) magnitude image acquired during the phase contrast scan (B) flow map through the RCA shown at peak systole.

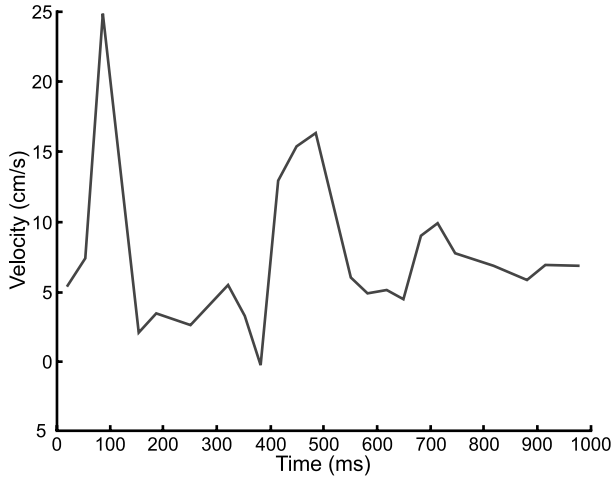

Figure 3. Through plane blood flow velocity in the RCA measured during the cardiac cycle.

as low as 15.6 ms were obtained. Figure 3 displays the expected biphasic velocity profile from the RCA of a healthy adult subject obtained with a temporal resolution of 30 ms.

Conclusions: We simultaneously exploit navigator technology and the higher SNR available at 3 T to improve the temporal and spatial resolution of coronary flow measurements. Both a high spatial (0.76×0.76 mm^2) and a temporal (15.6 ms) resolution were obtained during free-breathing and access to early systolic flow is enabled. A higher spatial resolution will significantly reduce the partial volume effects for measuring the flow-velocity map while higher temporal resolution will support an improved delineation of the vessel border and a better estimate of the peak velocity. Future studies include the validation of this method in patients with Flowire and the assessment of the coronary flow reserve.

REFERENCE

Hundley, W. G., et al. (1996). *Circulation* 93:1502–1508.

425. Optimized Suppression of Motion Artefacts for Non-Invasive Coronary Angiography: Evaluation of Coronary Motion and the Effect of Pharmacological β-Blocker Intervention

Cosima Jahnke, MD,[1] Ingo Paetsch, MD,[2] Bernhard Schnackenburg, PhD,[2] Rolf Gebker, MD,[2] Eckart Fleck, MD,[2] Eike Nagel, MD.[2] [1]*Cardiology, University of Freiburg, Freiburg, Germany,* [2]*Cardiology, German Heart Institute Berlin, Berlin, Germany.*

Background: A major determinant for the quality and accuracy of non-invasive coronary angiography (MR, MDCT) is the effective suppression of cardiac motion, optimally achieved by acquiring image data during the cardiac rest period. Thus, exact knowledge on the extent and timing of coronary arterial motion would allow to optimize image acquisition strategies. In addition, since the use of β-blockers is widely recommended for coronary artery imaging with MDCT techniques, the influence of β-blockade on coronary motion components was assessed.

Methods: 210 consecutive cardiac patients were examined by magnetic resonance imaging (Philips Intera CV 1.5 T). The rest periods of the left (LCA) and right coronary artery (RCA) were determined using a cine-scan with transversal slice orientation (SSFP, retrospective gating, 40 phases/cardiac cycle). Additionally, coronary artery rest periods were assessed in 25 patients before and after β-blockade.

Results: The rest period of the LCA was significantly longer than that of the RCA (86% of pts; 163 ± 75 vs 123 ± 60 ms; $p < 0.01$) and started earlier in the cardiac cycle (79% of pts; 521 ± 149 vs 540 ± 160 ms; $p < 0.01$). There was no correlation between the duration of the rest periods and individual heart rate (LCA: $r = -0.52$; RCA: $r = -0.38$). β-blockade significantly lowered heart rate (61 ± 7 vs 83 ± 13 bpm, $p < 0.001$) and increased duration of the coronary artery rest periods within the individual patient (LCA: 202 ± 84 vs 112 ± 45 ms; RCA: 135 ± 57 vs 83 ± 36 ms; $p < 0.001$).

Conclusions: The rest periods of the LCA and RCA showed a large variability with regard to starting point and duration, without any correlation to heart rate. The application of a β-blocker significantly prolonged rest periods of the left and right coronary artery within the individual patient. Thus, β-blockade is recommended in most patients for non-invasive coronary artery imaging with MR and MDCT.

426. Interstudy Reproducibility of Carotid Artery Wall Volume Measurement Using Semi-Automated Software

Anitha Varghese,[1] Robert D. Merrifield,[2] Lindsey A. Crowe,[1] Peter D. Gatehouse,[1] Raad H. Mohiaddin,[1] David N. Firmin,[1] Guang-Zhong Yang,[2] Dudley J. Pennell.[1] [1]*Cardiovascular Magnetic Resonance, Royal Brompton Hospital, London, UK,* [2]*Royal Society/Wolfson Medical Image Computing Laboratory, Imperial College, London, UK.*

Introduction: Cardiovascular magnetic resonance (CMR) has been validated for the assessment and monitoring of carotid artery and aortic atherosclerotic plaque burden. It permits accurate, noninvasive, serial in vivo measurements of artery wall dimensions without the need for ionizing radiation. We have previously described a three-dimensional (3D) volume-selective fast spin echo (FSE) sequence for use in carotid arterial wall imaging. The interstudy reproducibility of this 3D technique in subjects with and without evidence of carotid artery disease is similar at 4.4% and 4.6% respectively

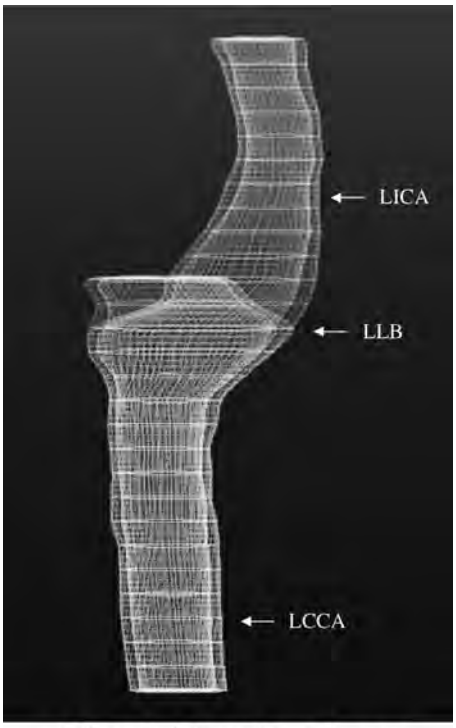

Figure 1. Example of left carotid artery model constructed from initial CMR study on subject six.

making such volumetric analysis well suited for the longitudinal study of atherosclerosis. However, dissemination of this research tool into the clinical arena is hampered by the time consuming process of manual delineation of vessel contours. Even unilateral manual contouring of carotid arterial lumen and outer vessel wall areas to obtain the total carotid artery wall volume (TWV) for one side takes an average of 88 minutes. In order to improve this process, we have recently developed a semi-automated analysis software package, Atheroma-Tools, and have assessed its interstudy reproducibility on asymptomatic controls in order to evaluate its potential to supersede manual analysis.

Purpose: Quantification of interstudy reproducibility of carotid artery wall volume measurement in asymptomatic controls using newly-developed semi-automated analysis software.

Methods: Interstudy reproducibility was evaluated in 10 asymptomatic controls. Either the right or left carotid artery was imaged alternately using a Siemens Magnetom Sonata 1.5 T scanner, a purpose-built two element phased-array surface carotid coil and a specially designed head and neck cushion. Subjects were scanned in the supine position with the carotid coil or coils in the iso-centre of the static magnetic field. Each scan took approximately 15 minutes and was performed twice with a minimum interscan time of 45 minutes. Typical sequence acquisition order and typical parameters were: true FISP (a steady state free precession technique) 5 slice pilot, 2D multi-slice time-of-flight (TOF), in-plane one slice FSE and T1-weighted 3D volume-selective FSE (matrix size = 256, 0.47 × 0.47 mm pixels; 28 slices of 2 mm thickness; field-of-view [FOV] = 120 × 24 mm approximately; time to echo [TE] = 11 ms; repetition time [TR] according to a single multiple of the subject's R–R interval; echo train length [ETL] = 11- these individual parameters were varied slightly according to individual patient requirements.). The region chosen for measurement was 56 mm centred around the carotid bifurcation. Data was collected as cross-sectional images from which TWV was calculated by subtraction of the total carotid arterial luminal volume from the total outer carotid arterial volume. Analysis was performed by a single observer (AV) using Atheroma-Tools (plug-in of CMRtools, Cardiovascular Imaging Solutions, London, UK) with the time taken from start of data processing to recording of results also documented.

Results: The mean TWV for scans 1 and 2 was 1.16 cm^3 and 1.15 cm^3 and were not significantly different from each other (mean difference 0.016, $P = 0.3$). The standard deviation of the differences between the measurements was 0.049 cm^3 yielding a coefficient of variation of 4.3%. The average time taken for unilateral TWV quantification was 33 minutes (range 21 to 53; Figure 1).

Conclusions: CMR volumetric analysis of TWV using newly-developed semi-automated analysis software is as reproducible as manual contouring, but considerably faster.

427. Identification and Reduction of Residual Signal from Slow Flowing Blood in 3D Volume Selective Turbo Spin Echo Arterial Wall Imaging Using a Velocity Sensitive Phase Reconstruction Method

Lindsey Crowe, PhD,[1] Raad Mohiaddin,[2] Anitha Varghese,[2] Guang-Zhong Yang,[3] David Firmin.[1] [1]*Imperial College/ Royal Brompton Hospital, London, UK,* [2]*Royal Brompton Hospital, London, UK,* [3]*Imperial College, London, UK.*

Aim: Reduction of residual blood signal in 3D volume-selective TSE artery wall imaging using velocity sensitivity and phase reconstruction in post-processing.

Introduction: Vessel wall imaging of the carotid artery is usually 2D for time and blood suppression reasons (Fayad and Fuster, 2001; Toussaint et al., 1996; Yarnykh and Yuan, 2003; Yuan et al., 2001). Slow recirculating flow affects the efficiency of double inversion blood suppression. We present a method for reducing residual blood signal in 3D TSE (Crowe et al., 2003) and identifying the true vessel wall and luminal encroachment due to atherosclerosis. Data is shown for both phantom validation and in-vivo studies.

Methods: Parameters: Siemens Magnetom 1.5 T scanner, FOV 120 × 24 mm, matrix 256 × 52, 28 × 2 mm slices

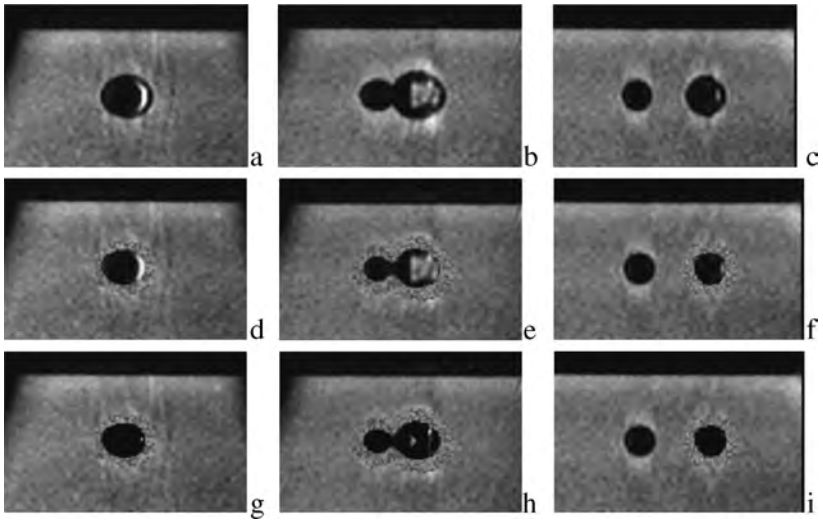

Figure 1. Correction of three slices below, at and above the bifurcation. a, b, c are magnitude images; d, e, f have simulated wall; g, h, i corrected.

centred around the bifurcation, ETL 11, TI 600 ms, TE 11 ms and cardiac gating. A velocity encoding bipolar gradient pulse was added to the sequence with magnitude and phase image reconstruction. Assuming most flow has a component along the vessel axis and the bipolar gradient is added without affecting the sequence timing. The gradient amplitude is maximised for a venc of around 36 cm/s. Lumen:wall contrast was measured from standard and velocity-sensitive sequences over slices with residual signal. MATLAB was used to threshold the phase images to identify and remove blood signal from affected magnitude images by multiplication. Phantom validation used pulsatile blood-mimicking fluid, realistic carotid artery geometry, tissue-mimicking gel (Shelley Medical Imaging Technologies). A carotid pulse waveform (peak 40 ml/s) and ECG gating were simulated (RR 828 ms). The lumen delineation validates the removal of blood signal. A simulated wall was added before post-

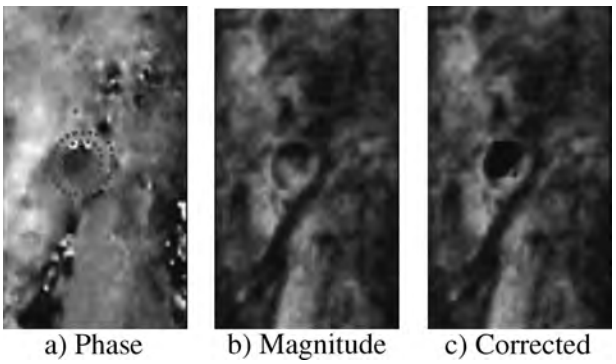

Figure 3. ICA of diseased artery.

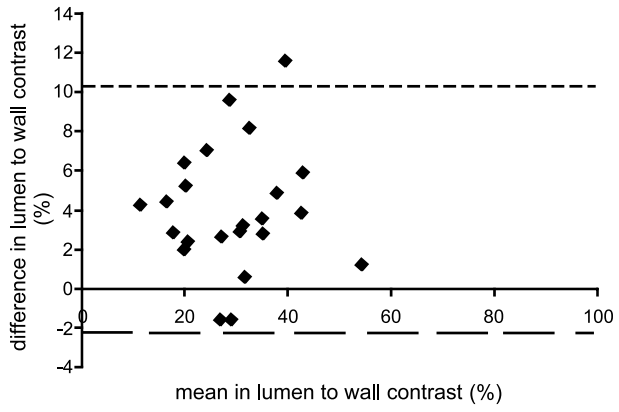

Figure 2. Bland-Altman of lumen: wall contrast between standard and velocity sensitive sequences.

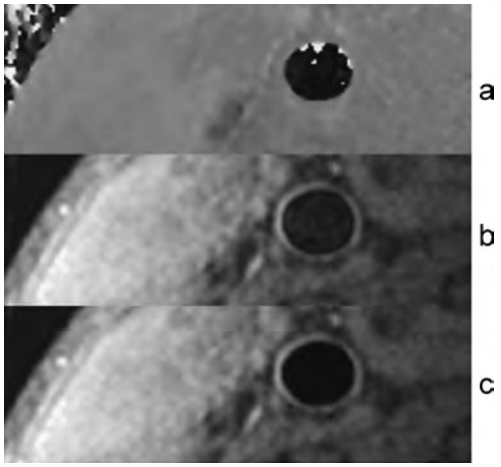

Figure 4. CCA of healthy subject.

Figure 5. Healthy carotid bifurcation. a) Phase, b) Magnitude, c) Corrected.

processing. We scanned 6 healthy subjects (23–47 years, mean 35) and 17 patients (48–76 years, mean 63) with known carotid disease. All gave informed consent.

Results: There was a significant difference between lumen signal intensity for the standard and velocity sensitive sequences. In the phantom a reduction of 10% was found ($p < 0.01$) for the 'lumen/tissue' contrast. In-vivo values were 32% compared to 28% ($p < 0.01$).

Bland-Altman analysis of in-vivo data is in Figure 1. The velocity sensitivity introduced may produce velocity gradients within pixels causing signal cancellation. As the extent of the artifact varies between subjects, there is a wide range of signal intensity changes. The signal intensity of the muscle tissue in the image does not show significant difference ($p = 0.4$). Figure 2 shows phantom images of residual signal removal with the simulated wall.

Figure 3 shows removal of residual blood signal in a diseased ICA. Even in the CCA, heart rate regularity and incorrect inversion time can give poor blood suppression. Figure 4a–c illustrates an improvement in lumen clarity without significant changes at the lumen/wall interface. In the example in Figure 5, some recirculating blood has zero resultant velocity in the slice direction.

Discussion: There are limits to the effectiveness of this method when velocity is zero. In between circulating currents there will be a boundary region of stationary blood. This method assists the observer in identifying blood signal and assessment of disease more accurately.

Conclusion: Addition of a velocity sensitive pulse to 3D volume selective TSE imaging with magnitude and phase reconstruction and post processing can be used to identify and reduce residual signal from slow moving blood to improve image clarity and assist conclusions about vessel disease structure.

ACKNOWLEDGMENTS

British Heart Foundation, HEFCE and CORDA for funding.

REFERENCES

Crowe, Gatehouse, Yang, Mohiaddin, Varghese, Charrier, Keegan, Firmin (2003). *J. Magn. Reson. Imaging* 17(5):572–580.
Fayad, Fuster. (2001). *Circ. Res.* 89(4):305–316.
Toussaint, LaMuraglia, Southern, Fuster, Kantor. (1996). *Circulation* 94(5):932–938.
Yarnykh, F., Yuan, F. (2003). *J. Magn. Reson. Imaging* 17(4):478–483.
Yuan, Mitsumori, Beach, Maravilla. (2001). *Radiology* 221:285–299.

428. Improvement of 3D Volume Selective Turbo Spin Echo Imaging for Carotid Artery Wall Imaging With Navigator Detection of Swallowing

Lindsey Crowe,[1] Jennifer Keegan,[2] Peter Gatehouse,[2] Raad Mohiaddhin,[2] Anitha Varghese,[2] Karen Symmonds,[2] Timothy Cannell,[2] Guang-Zhong Yang,[3] David Firmin.[1] [1]*CMR Unit, Royal Brompton Hospital/Imperial College, London, UK,* [2]*CMR Unit, Royal Brompton Hospital, London, UK,* [3]*Royal Society/Wolfson MIC Laboratory, Imperial College, London, UK.*

Aim: Improvement of 3D volume selective TSE carotid artery wall imaging by the addition of navigators to reduce artefacts caused by swallowing.

Introduction: Atherosclerosis and arterial wall imaging is increasingly common in a clinical setting (Fayad and Fuster, 2001; Toussaint et al., 1996; Yuan et al., 2001). 3D volume selective TSE (Crowe et al., 2003) scans of carotid artery may be degraded by swallowing during the scan. Motion of vessels or tissue, changes in blood flow patterns or an increase in heart rate can occur. Similar effects have been observed previously (Serfaty et al., 2003). During a 3D acquisition a single, badly timed swallow may affect the whole slab image quality. Detection of this motion is needed to improve 3D scans.

Methods: Parameters: Siemens Magnetom 1.5 T scanner, FOV 120 × 24 mm, matrix 256 × 52, 28 × 2 mm slices centred around the bifurcation, ETL 11, inversion time 600 ms, TE 11 ms and cardiac gating. 3D volume selective TSE scans of carotid artery were acquired in 6 healthy volunteers. A cross-pair navigator on back of the tongue was used to detect swallowing. The navigator was acquired in all scans, for monitoring or with an accept/reject algorithm (±2 mm acceptance window). Two swallowing patterns were tested; a swallow midway through the scan (worst case single swallow) and repeated swallowing, as often as physically possible. This was around every 10–20 seconds during a 2 minute scan. Signal intensity in the lumen was quantified and images ranked by 4 observers in terms of the clarity of the

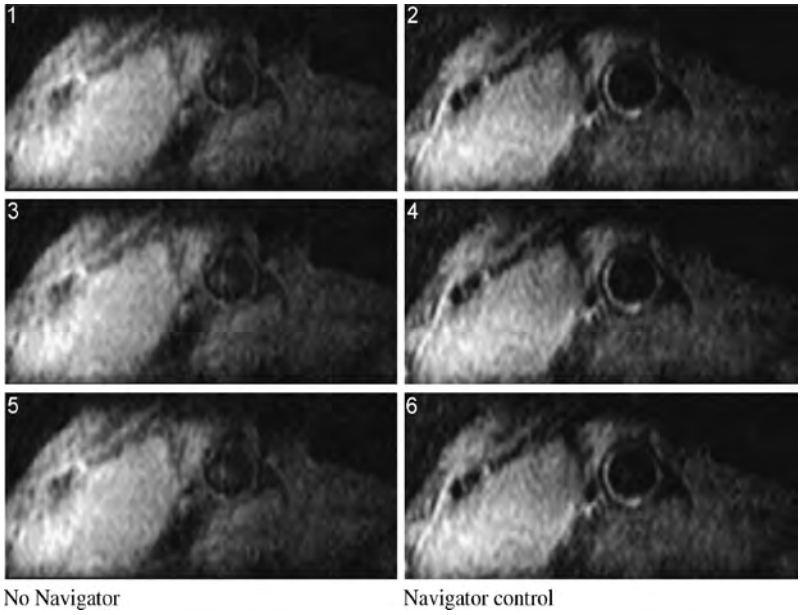

Figure 1. Comparison of image quality in the common carotid.

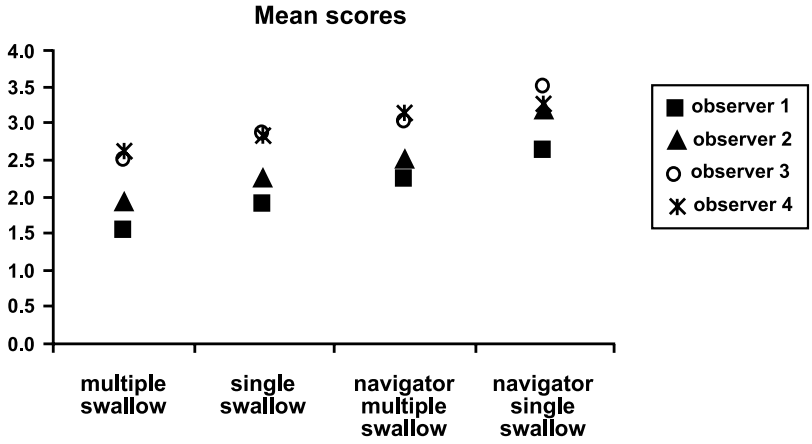

Figure 2. Mean score for each type of image over all subjects.

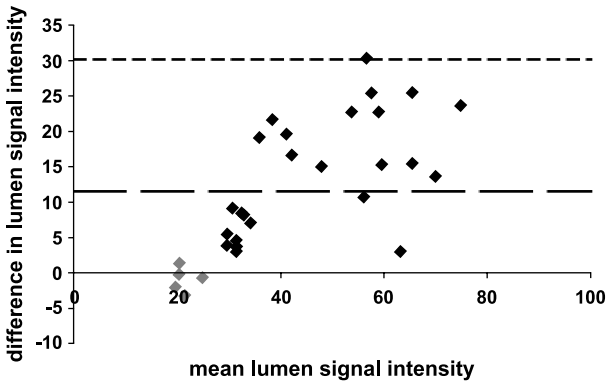

Figure 3. Quantitative analysis of dark blood efficiency via residual lumen signal intensity.

vessel wall. Eleven slices in the common carotid and start of the bifurcation were graded on a scale of 0–5.

Results and Discussion: There is higher signal in the lumen and increased blurring on scans without navigator control. Differences are likely either to be an effect of a decrease in blood suppression efficiency due to heart rate changes, or due to increased motional blurring of tissue into the lumen. One exception, where no significant difference was observed, had poorer SNR. The blurring in the k_z and k_y directions causes a reduction in image quality throughout the volume. Figures 1–3 show a comparison of three slices, quantitative analysis of lumen signal and mean score.

Difference in mean score between navigator and non-navigator images was on average > 0.6 ($p < 0.01$ for all observers). All but one navigator image scored higher than the

corresponding non-navigator scans. The one exception is likely to result from a poor choice of navigator window, with lines wrongly accepted during the swallowing motion. Central swallow scans scored higher than repeated swallow. Heart rate increased on swallowing and lasted one or two cardiac cycles after the navigator returned to accept position. This is likely to have an effect on blood suppression, repeated swallowing having more effect. A further improvement is to use additional arrhythmia rejection to reject the additional short cycles that follow the swallow or a more intelligent algorithm that calculates and adjusts the inversion time during the scan.

Conclusions: Clarity of wall delineation and apparent efficiency of blood suppression are reduced by swallowing during acquisition. The image quality can be improved using a navigator accept/reject method. The worst case acceptance rate was > 70%, therefore it is possible to use this technique as a 'safety net' without affecting the image acquisition, or increasing scan time, significantly. This helps significantly in scans of a few minutes where a single movement can affect image quality.

ACKNOWLEDGMENTS

British Heart Foundation, HEFCE and CORDA for funding.

REFERENCES

Crowe, Gatehouse, Yang, Mohiaddin, Varghese, Charrier, Keegan, Firmin. (2003). *J. Magn. Reson. Imaging* 17(5):572–580.
Fayad, Fuster. (2001 Aug 17). *Circ. Res.* 89(4):305–316.
Serfaty, Herigault, Yuan, Douek. (Sept 2003). *XV MR Angio Club*. Dublin.
Toussaint, LaMuraglia, Southern, Fuster, Kantor. (1996). *Circulation* 94(5):932–938.
Yuan, Mitsumori, Beach, Maravilla. (2001). *Radiology* 221:285–299.

429. 160-Micron Resolution Black-blood Carotid MRI at 3T Using Inner Volume FSE

Belinda S. Y. Li, PhD,[1] Vu M. Mai, PhD,[2] Eugene E. Dunkle, RT,[3] Wei Li, MD,[2] Susan Mathew, MS,[4] LeRoy R. Blawat, BS,[5] John E. Lorbiecki,[5] Bernice E. Hoppel, PhD,[5] Eddy B. Boskamp, PhD,[5] Robert R. Edelman, MD.[2] [1]*Applied Science Laboratory Central, GE Healthcare, Evanston, IL, USA,* [2]*Department of Radiology, Evanston Hospital and Northwestern University Feinberg School of Medicine, Evanston, IL, USA,* [3]*Department of Radiology, Evanston Northwestern Healthcare, Evanston, IL, USA,* [4]*Texas A&M University, College Station, TX, USA,* [5]*Applied Science Laboratory, GE Healthcare, Waukesha, WI, USA.*

Introduction: High-resolution black-blood carotid artery MR imaging has great potential for visualizing and characterizing atherosclerotic plaques. However, due to aliasing artifacts in MRI, the field-of-view (FOV) along the phase-encoding direction must, in general, be larger than the total anatomy size in that direction. This introduces an inherent inefficiency in spatial resolution and scan time, particularly when high-resolution imaging is only required for either the left carotid artery or the right carotid artery, not for both sides. The use of the inner volume (IV) technique (Feinberg et al., 1985; Li et al., 2003) with double-inversion fast-spin-echo (DIR-FSE), together with the use of a high-field, 3 T, MRI system for signal-to-noise ratio (SNR) advantages, presents a scheme to perform ultra high-resolution black-blood FSE carotid artery MRI.

Purpose: To demonstrate the ability to achieve down to 0.16×0.16 mm^2 in-plane spatial resolution, with 2 mm slice thickness, in 2.5 to 4.8 minutes at 3 T, with inner volume black-blood carotid imaging.

Methods: Six healthy subjects (3 M, 3 F, age 19–41 yr.) underwent this Institutional Review Board approved study, after signing an informed consent. All studies were performed on a 3 T whole body TwinSpeed MR scanner (GE Healthcare, Waukesha WI, USA), with a maximum gradient strength of 40 mT/m and a maximum gradient slew rate of 150 T/m/s. A custom-made 6-element carotid phased-array coil was used. With IV sequences, wrap-around artifacts are not a concern, and therefore the FOV can be reduced to "zoom" onto the anatomy/pathology of interest. In our studies, a FOV of 8 cm × 4 cm was used, centered on either the left carotid artery or the right carotid artery, with a matrix size of 512 × 256, resulting in an in-plane resolution of 0.16×0.16 mm^2. The slice thickness was 2 mm, the receiver bandwidth was ± 62.5 kHz, the

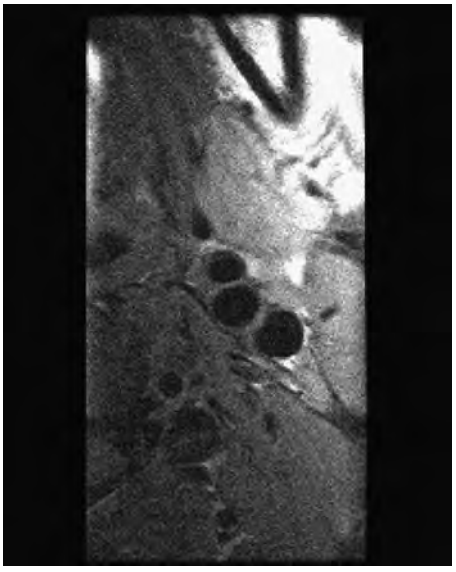

Figure 1. Inner volume black-blood image of the left carotid artery on one volunteer, with 160-micron in-plane resolution, 2 mm slice thickness, and 8 cm × 4 cm FOV. Scan time = 3.5 min.

echo train length was 16, and cardiac gating was used, with an interval of 2 heartbeats between slices (i.e., TR = 2R–R). Effective TE was 10 ms, and 8 averages were acquired. DIR pulses were used at an appropriate delay time before the excitation pulse in order to produce black-blood images. Depending on the heart rate, the total scan time per slice ranged from 2.5 to 4.8 min. For data analysis, since the FOV was too small to include any background region, it was, therefore, not possible to measure the standard deviation of the background noise to calculate SNR and contrast-to-noise ratio.

Results: Fig. 1 shows an example of an IV-DIR-FSE black-blood carotid artery image. Fig. 2 shows, on the same volunteer and the same imaging slice as Fig. 1, a DIR-FSE image achieved in the same total scan time without using IV- with a FOV of 12 cm × 12 cm, wrap-around artifacts can be seen.

Conclusions: We have demonstrated the feasibility of acquiring ultra high-resolution (160-micron) black-blood images of the carotid artery using IV-DIR-FSE at 3 T, within a reasonable scan time. Improvement in SNR, by optimizing sequence, protocol and coil-design, will help further reduce the scan time and/or increase the spatial resolution. The use of a non-gated version of IV-DIR-FSE will also be explored, which can significantly reduce scan time as well. This technique has great potential in characterizing vascular stenosis and atherosclerotic plaques.

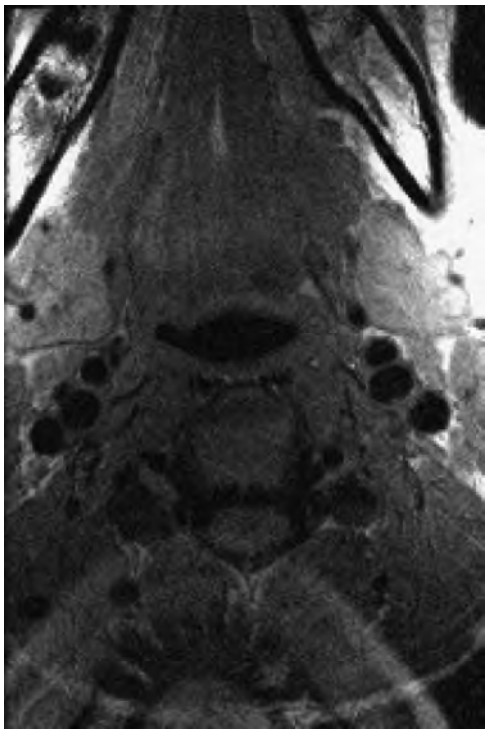

Figure 2. A DIR-FSE image acquired without using IV, on the same volunteer and the same imaging slice as Fig. 99, with FOV = 12 cm × 12 cm, matrix size = 512 × 512, 2 mm slice thickness, 4 averages, and the same scan time of 3.5 min. Wrap-around artifacts can be seen.

REFERENCES

Feinberg, D. A., et al. (1985). *Radiology* 156:743–747.
Li, B. S. Y., et al. (2003). *ISMRM*:2598. Abstracts.

430. Localization of Gadofluorine in Atherosclerotic Plaques of Apolipoprotein E Knockout Mice

Juan Gilberto Aguinaldo, MD,[1] Marc Sirol, MD,[1] Venkatesh Mani, PhD,[1] Juan Carlos Frias, PhD,[1] Vitalii Itskovich, PhD,[1] John Fallon, MD, PhD,[2] Hanns-Joachim Weinmann, PhD,[3] Bernd Misselwitz, PhD,[3] Zahi Fayad, PhD.[1] [1]*Imaging Science Laboratories, Mount Sinai School of Medicine, New York, NY, USA,* [2]*Mount Sinai School of Medicine, New York, NY, USA,* [3]*Schering AG, Berlin, Germany.*

Molecular targeting using magnetic resonance (MR) contrast agents has the potential to assess the morphological and functional activity of atherosclerotic plaque components. Gadofluorine M (Schering AG), is a gadolinium complex with a perfluorinated chain that forms micelles in aqueous solution, and provides plaque enhancement. Our objective was to localize Gadofluorine M in Apolipoprotein E knock-out (ApoE KO) mice plaques using MR and fluorescence microscopy.

Methods: Fifteen-month-old ApoE KO ($n = 12$) and wild type (WT) ($n = 6$) mice underwent in vivo imaging of the abdominal aorta using a 9.4 T MR system. Pre-and post-contrast enhanced (CE) T1 W MR was performed at 30 minutes to 72 hrs. Carbocyanin labeled Gadofluorine M (100 μmol/kg) was injected via tail vein. Frozen sections of aorta were stained with fluorescently labeled antibodies for macrophages, smooth muscle cells, lymphocytes and tenascin (large extracellular matrix [ECM] glycoprotein shown to be expressed in plaques) and imaged by confocal microscopy.

Results: In the KO mouse group, there was heterogeneous enhancement with an increase in contrast-to-noise ratio (CNR) for wall/lumen and wall/muscle in the post-CE vs. pre-CE images (paired t-test, $p < 0.05$). There was no increase in CNR for wall/lumen and wall/muscle in WT aorta. Confocal microscopy showed the Gadofluorine M colocalized with tenascin in the ECM of plaques, with no localization in plaque cells.

Conclusions: Gadofluorine M showed MR contrast enhancement in plaques of KO mice with specific uptake in the ECM. CE MR with Gadofluorine M may delineate plaque burden in vivo, and help understand the role of ECM components in the pathogenesis of atherosclerosis.

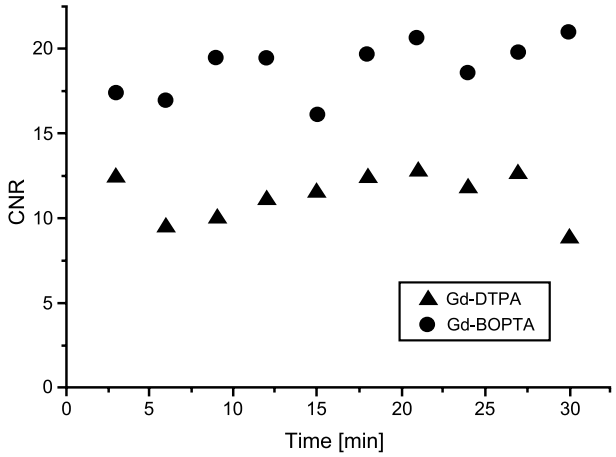

Figure 1. CNR for Gd-DTPA and Gd-BOPTA enhanced FLASH-sequences up to 30 min after contrast injection.

431. Coronary Magnetic Resonance Angiography—Comparisons Between Gd-DTPA and Gd-BOPTA Enhanced FLASH Sequence and Non-Contrast Enhanced SSFP Sequence

Thomas Schlosser, MD, Christoph U. Herborn, MD, Florian Vogt, MD, Peter Hunold, MD, Joerg Barkhausen, MD. *Radiology, University Hospital Essen, Essen, Germany.*

Introduction: Several studies have demonstrated that intravenous administration of contrast agents improves the intravascular signal of coronary arteries. However, this effect is described as short-lived for extracellular contrast agents and therefore these compounds seem to be not well suited for MR coronary angiography (MRCA) requiring scan times of several minutes. To overcome these limitations intravascular contrast agents have been introduced, but these compounds have not been approved for clinical use yet. However, Gd-BOPTA, an approved extracellular contrast agent with protein binding might be an attractive alternative to the intravascular research compounds.

Purpose: The aim of this study was to compare non-contrast enhanced steady state free precession (SSFP) sequences with contrast enhanced MRCA using two different extracellular contrast agents.

Methods: 8 healthy volunteers were included into the study. All examinations were performed on a 1.5 T MR scanner (Magnetom Sonata, Siemens, Erlangen, Germany) using a breath-hold segmented 3D SSFP sequence (TR 3.9 ms, TE 1.7 ms, FA 65°) for non-contrast enhanced MRCA. Contrast-enhanced MRCA was performed twice on two different occasions using either Gd-DTPA (Magnevist, Schering AG, Berlin, Germany) or Gd-BOPTA (Multihance, Bracco S.p.A., Milan, Italy) in randomised order. Three, 6, 9, 12, 15, 18, 21, 24, 27, and 30 min following injection of contrast (0.2 mmol per kilogram of body weight; injection rate: 2 ml/sec; 20 ml saline-flush: 2 ml/sec) MRCA was performed using a breath-hold segmented 3D inversion recovery gradient echo sequence with fat suppression (IR-FLASH; TR 4.1 ms, TE 1.7 ms, FA = 15°). The inversion time was set to minimize the signal intensity of the myocardium resulting in an optimized contrast between the coronary arteries and the surrounding tissues. SNR and CNR were measured for both contrast agents at different time points after injection as well as for the non-contrast enhanced SSFP images. For the assessment of T1-values a steady state free precession sequence with incrementally increased inversion times was acquired during a single breath-hold (TI-Scout; TR 2.4 ms; TE: 1.0 ms; FA: 50°; temporal resolution 15 ms). T1-values of the myocardium and the LV cavity were obtained using the following equation: $T1 = TI(min)/\ln 2$, where TI(min) is the inversion time of the image with the minimum signal intensity of the tissue.

Results: MRCA could successfully be performed in all volunteers using both sequences. Mean SNR values and the contrast between the coronaries and the myocardium were significantly higher for Gd-BOPTA compared to the Gd-DTPA images (SNR: 24.4 ± 1.1 for Gd-BOPTA vs 16.6 ± 1.6 for Gd-DTPA, $p < 0.05$; CNR: 18.8 ± 1.6 for Gd-BOPTA vs. 11.3 ± 1.4 for Gd-DTPA, $p < 0.05$; Figure 1). Compared to the SSFP sequences SNR (28.7 ± 6.9) was not statistically different for Gd-BOPTA images ($p = 0.07$) whereas Gd-DTPA showed lower SNR values ($p < 0.05$) (Figure 2). However, Gd-BOPTA showed an increased CNR compared to SSFP images (CNR 14.3 ± 6.4, $p < 0.05$) whereas Gd-DTPA did not ($p = 0.17$). T1 values in the LV cavity were not statistically significantly different for both agents 1 min after contrast administration ($p > 0.05$), they were statistically significantly lower for Gd-BOPTA ($p < 0.05$) at 7, 13, 19 and 25 min after injection (Figure 3).

Conclusions: Coronary magnetic resonance angiography is feasible using Gd-DTPA and Gd-BOPTA enhanced

Figure 2. LAD using a SSFP sequence (left), IR-FLASH with Gd-DTPA (middle) and IR-FLASH with Gd-BOPTA (right).

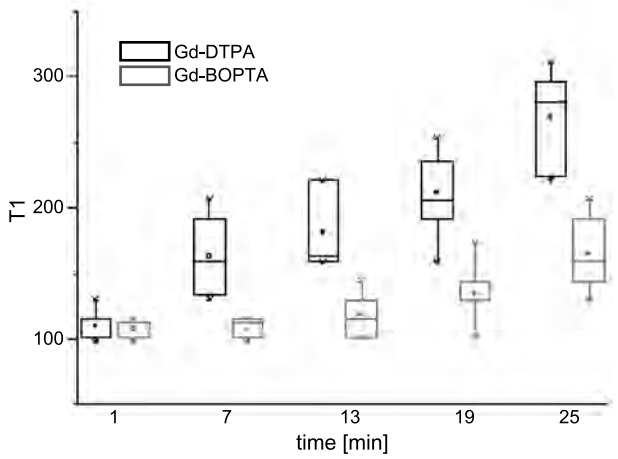

Figure 3. Mean T1-values in the LV cavity after GD-DTPA and Gd-BOPTA, respectively, at different time points.

inversion recovery gradient echo sequences and non-contrast SSFP sequence. Due to the higher relaxivity and the mild protein binding Gd-BOPTA proved to be superior to Gd-DTPA for contrast enhanced MRCA. Compared to non-contrast enhanced SSFP sequences inversion recovery gradient echo sequences combined with double dose of Gd-BOPTA significantly improved the contrast between the coronary arteries and the myocardium.

432. Comparison of Inversion Recovery Steady-State Free Precision and Inversion Recovery Fast Low Angle Shot Sequences For Contrast Enhanced Magnetic Resonance Coronary Angiography

Kai Nassenstein, Kai Uwe Waltering, Sandra Massing, Thomas Schlosser, Peter Hunold, Joerg Barkhausen. *Department of Diagnostic and Interventional Radiology, University Hospital Essen, Essen, Germany.*

Introduction: High contrast between the lumen of the coronary arteries and the surrounding myocardium is a prerequisite for high quality magnetic resonance coronary angiography (MRCA). For Cine-MR sequences it has been shown that steady state free precession (SSFP) techniques provide higher signal and contrast to noise ratios compared to gradient echo (FLASH) sequences. Recently, 3D inversion recovery SSFP sequences have been introduced for contrast enhanced MRCA. Purpose of our study was to compare the signal-and contrast-to-noise ratio as well as the image quality of breath-hold 3D inversion recovery SSFP and FLASH sequences in volunteers using an intravascular contrast agent.

Materials and Method: The study was approved by the institutional review board, and informed consent was obtained from all study participants prior to enrollment to the study. 24 healthy volunteers (10 female, 14 male, mean age 29.8 ± 6.1 years) were included into this study. All examinations were performed on a 1.5 T MR scanner (Sonata, Siemens Medical Solutions). All subjects received a single dose of 0.05 mmol/kg MS-325 (Epix, Boston, USA). Thereafter, MRCA was performed using 3D inversion recovery steady-state free precision (IR-SSFP: TR 3.8 ms, TE 1.6 ms, FA 65°, band width 540 Hz/pixel, voxel size 1,8−2,3 mm^3) and 3D inversion recovery fast low angle shot (IR-FLASH: TR 3.8 ms, TE 1.6 ms, FA 25°, band width 490 Hz/pixel, voxel size 1,8−2,3 mm^3) sequences. For all scans the inversion time was set to null the signal intensity of the myocardium. All examinations were performed in deep inspiration and breath-hold. 3D data sets of the right coronary artery (RCA), the left anterior descending coronary artery (LAD) and the left circumflex coronary artery (CIRC) were obtained. For all MR exams, signal-to-noise ratio (SNR) as well as contrast-to-noise ratio (CNR) measurements (blood versus myocardium) were performed. Image quality of the proximal and middle coronary segments was assessed by two radiologists in consensus based on a 5-point Likert scale ranging from 1 (excellent), 2 (good), 3 (moderate), 4(poor), 5 (non-diagnostic).

Results: The mean acquisition time was comparable for both sequences (39.8 ± 5.3 s for SSFP vs. 38.2 ± 4.7 s for FLASH). The calculated mean signal-to-noise ratio of blood (6.2 ± 1.2 vs. 5.2 ± 1.1; $p < 0.05$) and the contrast-to-noise ratio (4.7 ± 1.1 vs. 3.6 ± 1.1; $p < 0.05$) showed significant higher values for IR-SSFP sequences. The mean images quality scores were significantly higher for SSFP (3,62) compared to FLASH (2,86) sequences ($p < 0.05$).

Discussion: Although hard-and software developments have dramatically improved image quality of MRCA in the last three years, limited signal to noise and contrast to noise ratios are still an issue. Several studies have shown that intravascular contrast agents can help to overcome these limitations. However, the search for a perfect MRCA sequence is not over yet. Recently, 3D inversion recovery steady state free precision sequences have been introduced for MRCA. Our results show a considerable overall improvement of image quality and CNR for IR-SSFP compared to IR-FLASH sequences in breath-hold MRCA after injection of an intravascular contrast agent (Fig. 1).

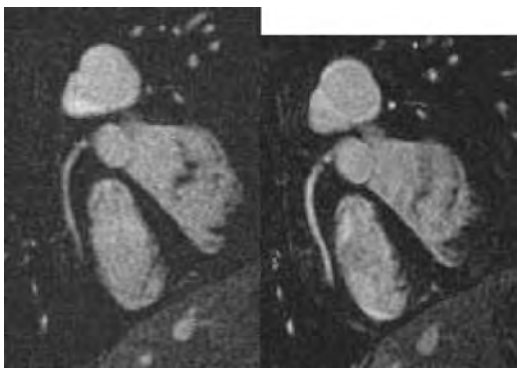

Figure 1. Improved image quality and blood-to-myocardium contrast for IR-FSSP (right image, 3D-slot) compared to 3D-FLASH (left image, 3D-slot).

433. Model-Based UNFOLD for Dynamic Contrast-Enhanced MRI of the Atherosclerotic Carotid Artery

William Kerwin, Chun Yuan, PhD. *Radiology, University of Washington, Seattle, WA, USA.*

Introduction: Parametric maps of contrast agent uptake-plasma volume (v_p) and transfer constant (K^{trans})-from dynamic contrast-enhanced (DCE) MRI provide insight into the inflammatory status of advanced carotid atherosclerotic plaques (Kerwin et al., 2003, 2004). To evaluate early lesions with DCE-MRI, higher temporal and spatial resolution is needed. Improved resolution in related applications has been accomplished using reduced k-space sampling, for example, Keyhole acquisition (Van Vaals et al., 1993), but these techniques blur signal from the vessel lumen into the adjacent wall making them unsuitable for vessel wall imaging. Reduced k-space sampling using the UNFOLD technique (Madore et al., 1999), on the other hand, is less susceptible to such blurring.

Purpose: To develop a high resolution DCE-MRI technique based on UNFOLD that is suitable for vessel wall imaging.

Method: The new method presented here uses an alternative reconstruction approach unique to DCE-MRI. Standard UNFOLD is a technique to remove wrap-around artifacts by temporal filtering, provided that the artifacts can be separated in the temporal frequency domain (Tsao, 2002). Here, the temporal filters are replaced by kinetic modeling of contrast agent dynamics. Both the true image and the wrapped image are assumed to obey a two-compartment model of contrast agent uptake. This assumption coupled with the UNFOLD acquisition scheme leads to a simple, over-determined system of equations describing the image sequence. After solving this system of equations, parametric versions of the wrap-around artifacts are subtracted from the images, thereby eliminating the artifacts.

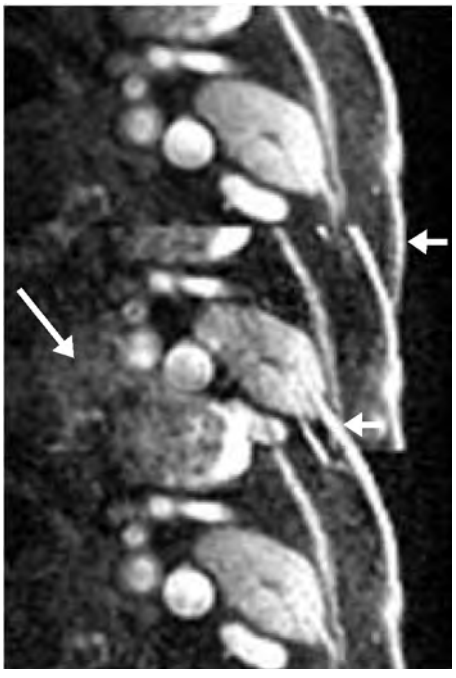

Figure 1.

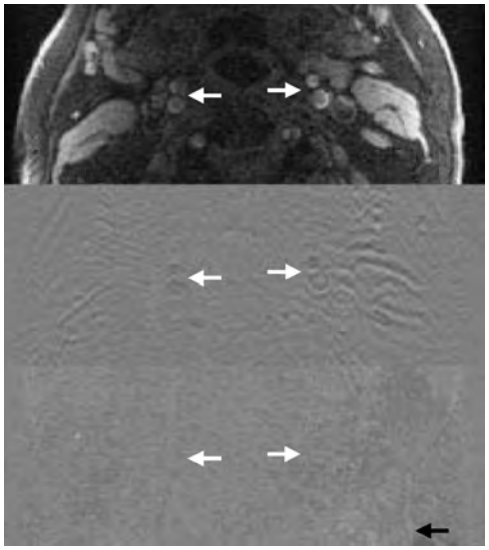

Figure 2.

Validation of the kinetic-model-based (mb) UNFOLD technique was performed using 9 DCE-MRI sequences of cervical carotid arteries. Images were obtained with a 2D spoiled gradient echo sequence on a 1.5 T MRI scanner with TR = 100 ms, TE = 3.5 ms, fli*p* = 60°, thickness = 3 mm, field-of-view = 16 × 12 cm, and matrix = 256 × 144. Twelve time points (15 second intervals) were acquired with a bolus of 0.1 mmol/kg of a Gadolinium-based contrast agent arriving in the fourth image. The fully sampled k-space data from each set was then down-sampled to simulate two-and three-fold undersampled images and Keyhole acquisition. The reconstruction quality using mb-UNFOLD was compared to Keyhole. Additionally, v_p and K^{trans} were determined for the carotid wall using three-fold mb-UNFOLD and compared to the results from the fully sampled images.

Results: Figure 1 shows examples of images obtained from three-fold down-sampled k-space before and after applying mb-UNFOLD. The mb-UNFOLD result (bottom) exhibits good agreement with the true image (top) without artifacts as in the original down-sampled image (middle, arrows). Figure 2 shows the original image (top) subtracted from the Keyhole image (middle) revealing blur near the artery (arrows). The blurring is absent from the mb-UNFOLD result (bottom) although some residual wrap-around is apparent (black arrow). In quantitative comparisons, v_p and K^{trans} computed from mb-UNFOLD images correlated strongly with results from fully sampled images (r = 0.75 and 0.79, respectively). The discrepancies can be attributed to the loss of SNR as a result of downsampling, which is mitigated by the increased sampling density and/or larger TR.

Conclusion: The mb-UNFOLD technique permits new flexibility in DCE-MRI through improved spatial resolution, temporal resolution, or SNR (by increasing TR). Compared to Keyhole, mb-UNFOLD does not blur the lumen into the adjacent wall. Compared to standard UNFOLD, mb-UNFOLD does not require temporal filters, which can be complicated to implement for such non-periodic sequences. More significantly, if the kinetic model accurately describes contrast kinetics, mb-UNFOLD exactly reconstructs the images even if an overlap in temporal frequency occurs.

REFERENCES

Kerwin, et al. (2003). *Circulation* 107:851–856.
Kerwin, et al. (2004). *JACC* 43:534A.
Madore, et al. (1999). *MRM* 42:813–828.
Tsao (2002). *MRM* 47:202–207.
van Vaals, et al. (1993). *JMRI'* 3:671–675.

434. Utilization of Newer Highly Spatially Selective Cylindrical Dual Inversion Prepulse Leads to Significantly Improved SNR and CNR in 3D Free Breathing Black Blood Coronary Vessel Wall Imaging

Milind Y. Desai,[1] Christoph Barmet,[2] Matthias Stuber, PhD.[1]
[1]*Johns Hopkins University, Baltimore, MD, USA,* [2]*Institute for Biomedical Engineering, University and ETH, Zurich, Switzerland.*

Background: It is feasible to assess in-vivo outward coronary arterial remodeling using magnetic resonance imaging (MRI). Botnar et al have imaged the remodeling in the right coronary artery (RCA) wall using three dimensional (3D), free-breathing black-blood coronary MRI and a 2D selective local inversion prepulse (*Circulation* 2002; 106:296–9). However, the 2D selective local inversion prepulse suffered from a relatively low spatial selectivity (Figure 1A) thereby compromising signal to noise and contrast to noise ratio (SNR and CNR). In order to overcome that limitation, we have refined the 3D spiral coronary vessel wall imaging sequence through the design and implementation of a highly spatially selective cylindrical 2D local inversion pre-pulse (Figure 1B) (*Stuber M et al, SCMR, 2004*).

Purpose: The purpose of this study was to determine if the use of the new and highly spatially selective 2D local inversion pre-pulse improves the SNR/CNR of the 3D free breathing black blood coronary vessel wall scan as compared to the older pulse.

Methods: RCA's of 7 healthy adult subjects (ages 27–35 years, 1 female) were imaged on a commercial 1.5 T Phillips MR scanner (Best, NL) using a 3D free-breathing navigator gated local inversion black blood spiral imaging sequence. We obtained 2 RCA wall scans in each volunteer in the same setting: one with the older (Figure 1C) 2D local dual inversion prepulse (pulse duration 6 ms) and one with the newer (Figure 1D) highly spatially selective local inversion prepulse (pulse duration 8.2 ms). The inner and outer walls of the RCA were analyzed semi-automatically, using

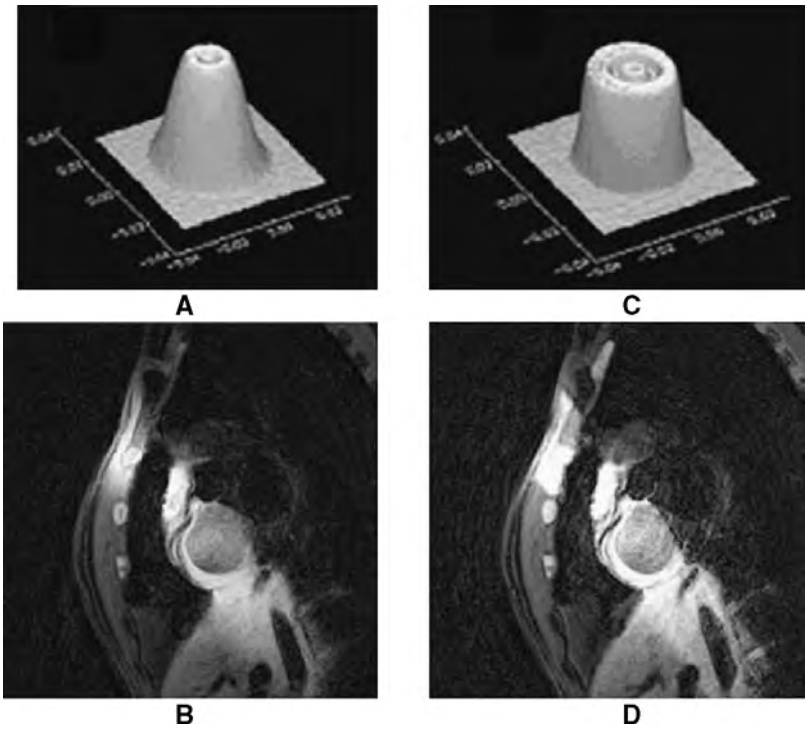

Figure 1.

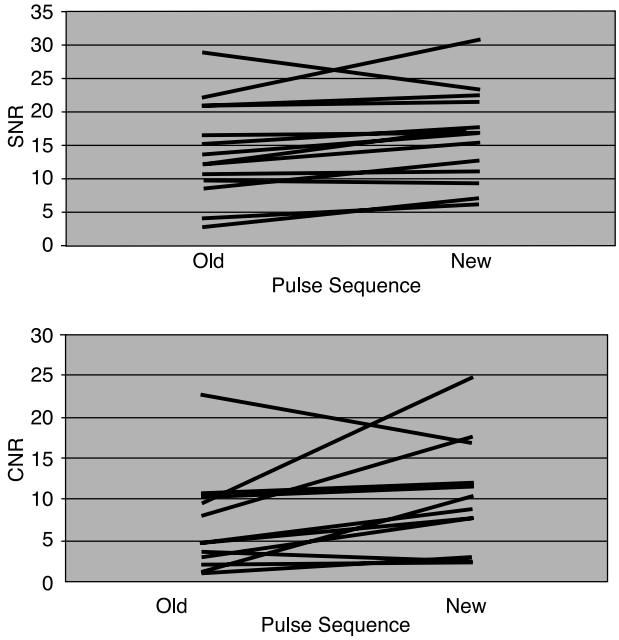

Figure 2.

the soap-bubble tool (*Magn Reson Med*. 2002; 48:658–66) and average wall thickness from both data sets was measured. Mean SNR and CNR were also calculated using the following formulae: SNR = (Signal $\text{Intensity}_{\text{wall}}$)/standard deviation $_{\text{background}}$ and CNR = (Signal $\text{Intensity}_{\text{wall-}}$ Signal Intensity $_{\text{lumen}}$)/Standard Deviation $_{\text{background}}$. The authors were blinded to the pulse sequence at the time of analysis.

Results: The average scan duration per 3D vessel wall scan was ∼ 12 minutes. The average imaged length of the RCA was 44 ± 7 mm. The mean thickness of the RCA wall measured by the new vs. old pulse sequence was not significantly different (1.67 ± 0.25 mm vs. 1.60 ± 0.23 mm, p = ns). The mean SNR obtained using the newer pulse sequence was significantly improved (by about 15%) as compared to the old pulse sequence (16 ± 7 vs. 14 ± 7, $p < 0.02$). The CNR demonstrated a greater improvement (66%) with the newer pulse sequence as compared to the older pulse sequence (10 ± 6 vs. 6 ± 6, $p < 0.02$). The changes in SNR and CNR in individual subjects are demonstrated in Figure 2A and B.

Discussion: Utilization of the newer highly spatially selective 2D local inversion pre-pulse for 3D free breathing black blood coronary vessel wall MRI results in significantly improved SNR and CNR, as compared to the older pulse. The main reason is that the older pulse had a low spatial selectivity leading to varying excitation angles within the nominal diameter of the cylindrical radiofrequency pulse. Hence, the optimal inversion of magnetization of the protons could only be obtained along the center of the beam, generating vessel wall images with sub-optimal SNR. as the course of a typical coronary artery is tortuous as opposed to a straight line. Further, a higher spatial selectivity also avoids re-inversion of the blood-pool in the ascending aorta and in the left ventricle that flows into the coronary arteries. Therefore, in-flow of signal-nulled blood-pool magnetization is facilitated leading to the observed improvement in CNR.

435. Coronary Magnetic Resonance Angiography Using Parallel Acquisition Techniques and Intravascular Contrast Media

Kai-Uwe Waltering, MD, Kai Nassenstein, MD, Sandra Massing, Thomas Schlosser, MD, Peter Hunold, MD, Jörg Barkhausen, MD. *Department of Diagnostic and Interventional Radiology, University Hospital Essen, Essen, Germany.*

Introduction: For diagnosis of CAD, invasive coronary artery angiography must still be considered as the standard of reference. Recently, magnetic resonance angiography of the coronary arteries (MRCA) has become feasible due to further developments of ultrafast imaging sequences. Additionally, blood pool MR contrast agents have been introduced, which have improved the performance of MRCA. However, limited spatial resolution and limited coverage are still a mayor problem of breath-hold MRCA.

Purpose: The purpose of our study was to investigate the use of a parallel acquisition technique (PAT) for contrast enhanced MRCA to increase the overall coverage.

Methods: 12 healthy volunteers (6 male, 6 female, mean age 30 ± 5 years, range 22–40) were included in this study. All examinations were performed on a 1.5 T MR scanner (Magnetom Sonata, Siemens). MRCA was performed using an inversion recovery prepared fast low angle shot (IR-FLASH) sequence (TR/TE 3.8/1.6 ms, bandwidth 490 Hz/pixel, matrix 320) after i.v. administration of a Gadolinium-based intravascular contrast media (SH L 643A, Schering) with a dose of 0.150 mmol per kilogram of body weight. The inversion time (TI) was individually adjusted to minimize the signal of the myocardium und to increase the contrast between blood and myocardium. Scans were performed without and with PAT in a single breath-hold. The use of GRAPPA with a PAT-faktor of 2 and 37 reference lines allows increasing the coverage i.e. more slices per slab in the

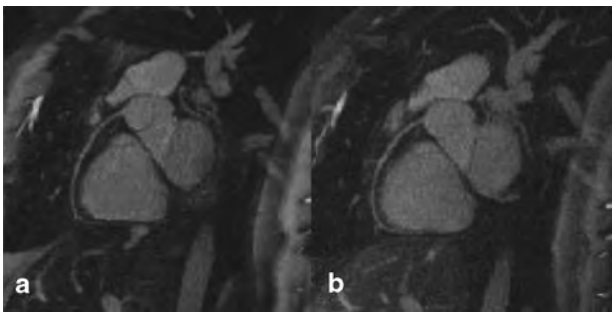

Figure 1. MRCA without (a) and with PAT (b) allows visualization of the right coronary artery.

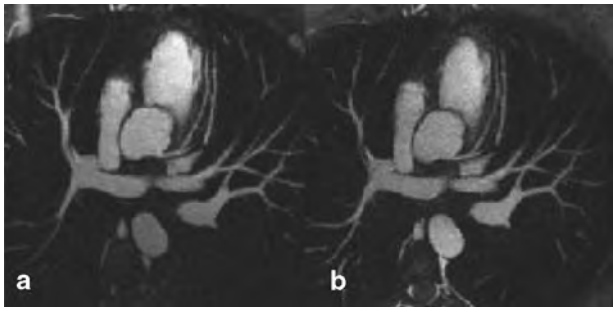

Figure 2. MRCA of the LAD without (a) and with PAT (b).

same acquisition time. The SNR loss due to PAT is absorbed by the higher signal value of the thicker 3D slab. For quantitative comparison of the different acquisition techniques, signal-to-noise-ratio (SNR) and contrast-to-noise-ratio (CNR) values were calculated based on signal intensity (SI) measurements in regions-of-interest (ROI) with the assumption of uniformly distributed noise within PAT images. Image quality was assessed based on a 5-point Likert scale ranging from 1 = excellent, 2 = good, 3 = equivocal, 4 = poor to 5 = non-diagnostic.

Results: The mean image quality score for all volunteers was higher for FLASH imaging without PAT (2.9 ± 0.8) compared to MRCA with parallel imaging (3.5 ± 0.9). Signal intensity measurements showed higher SNR for FLASH imaging without PAT (blood pool: 15.7 ± 2.8 versus 13.0 ± 3.6), while the CNR calculation showed no significant differences (12.2 ± 2.6 versus 10.4 ± 3.3).

Conclusions: Recently, intravascular contrast agents have been introduced for MRCA which provide important advantages compared to standard extracellular compounds. Due to long plasma half-life time several breath-hold scans can be performed after a single injection and additionally these new agents are characterized by higher T1-relaxivities resulting in improved SNR and CNR values. However, the limited spatial coverage of breath-hold MRCA sequences is still an issue. Our results show, that GRAPPA with a PAT-factor of 2 allows increasing spatial coverage without increasing the acquisition time. The SNR loss due to PAT is partly absorbed by the higher signal value of the thicker 3D slab. Although, overall image quality and SNR values were slightly reduced, delineation of the proximal and middle coronary segments was possible (Figs. 1 and 2). Therefore, after administration of an intravascular contrast agent MRCA with PAT can be applied to improve coverage in breath-hold MRCA.

436. Reduction of Eddy Currents Induced Image Artifacts in Coronary MRA Using SSFP Sequence

Xiaoming Bi,[1] Jaeseok Park,[1] Vibhas Deshpande,[2] Debiao Li.[1] [1]*Department of Radiology and Biomedical Engineering, Northwestern University, Chicago, IL, USA,* [2]*Siemens Medical Solutions, Erlangen, Germany.*

Introduction: Segmented SSFP (steady-state free precession) sequence has been demonstrated to yield higher signal-to-noise ratio (SNR) and contrast-to-noise ratio (CNR) than

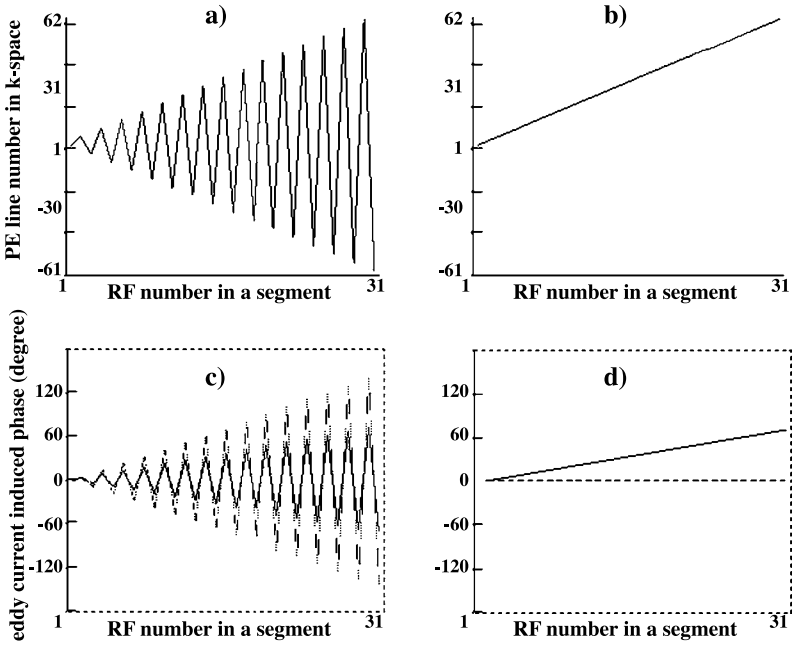

Figure 1. Order of k-space coverage in one segment with ACE (a) and LCE scheme (b). Alternating gradient in ACE induces oscillating eddy currents while LCE scheme induces constant eddy current. Eddy currents induced phase in each TR (dahed line) and cumulative phase (solid line) in one segment are illustrated in (c) and (d).

conventional gradient-echo sequence in coronary MRA (Deshpande et al, 2001). However, SSFP is sensitive to off-resonance frequencies resulting from local field inhomogeneities. Eddy current induced by gradient switching is one source of such field imperfections. The k-space trajectory of a conventional ECG gated, segmented SSFP sequence in phase-encoding (PE) direction moves from central to outer lines in both positive and negative directions in each segment (Fig. 1a). The sign as well as magnitude of the PE gradient alternates from excitation to excitation, inducing oscillating eddy currents. This results in discontinuities of phase (Fig. 1c) and ghosting in images. Such artifacts can be alleviated by reducing large change of gradient in PE direction (Scheffler et al, 2003).

Purpose: The purpose of this study was to develop a linear-centric-encoding (LCE) PE order SSFP sequence to reduce eddy currents induced image artifacts in coronary MRA. In-vivo studies were performed to evaluate the efficacy of such LCE scheme over conventional alternating-centric-encoding (ACE) PE scheme.

Methods: Fourteen healthy volunteers were scanned at 1.5 T (Sonata, $n = 6$) and 3.0 T (Trio, $n = 8$) Siemens whole-body scanners. Both scanners are capable of operating at a maximum gradient strength of 40 mT/m and a slew rate of 200 mT/m/ms. A twelve-element cardiac phased array coil was used at 1.5 T for signal reception. At 3.0 T, an 8-channel cardiac phased array coil was used. A segmented 3D, cardiac gated, breath-hold, SSFP sequence was used for coronary artery imaging. The whole k-space of each slice was covered in four heartbeats with 31–35 lines acquired in each heartbeat. Figure 1 illustrated the order of k-space coverage in one segment of ACE (a) and LCE (b) schemes. The k-space trajectory in LCE scheme traveled unidirectionally toward one side of k-space in each segment. The upper k-space of each slice was collected in the first two segments and the lower half was covered in the next two segments. Coronary artery images were acquired from each subject using ACE and LCE schemes, respectively. Imaging parameters included: TR/TE = 3.2/1.3 msec, flip angle = 62°–70°, readout bandwidth = 980 Hz/pixel, matrix size = (122–140) × 384, (1.2–1.7) × (0.9–1.0) in-plane resolution. Slab thickness = 18 mm, number of partitions = 6 (12 after sinc-interpolation). Total imaging time for acquiring one slab was 24 cardiac cycles. Synthesizer frequency was adjusted when necessary (Deshpande et al, 2003) to reduce obvious off-resonance artifacts in ACE scheme. Same adjustments were applied to LCE acquisition. Image quality was blindly evaluated by a radiologist on a scale of 1 (poor) to 4 (excellent). The results were presented as mean ± standard deviation. Comparison between two different data acquisition schemes was performed using a paired t-test.

Results: Figure 2 shows coronary images from 1.5 T (a, b) and 3.0 T (c, d) using ACE and LCE schemes. Image artifacts are substantially reduced in LCE images (b, d) as compared to those acquired with ACE scheme (a, c). Image quality is significantly improved at both field strengths using LCE order (1.5 T: ACE/LCE = 2.2 ± 0.8/3.0 ± 0.6, $p = 0.02$; 3.0T: ACE/LCE = 2.1 ± 1.1/3.0 ± 0.8, $p = 0.01$).

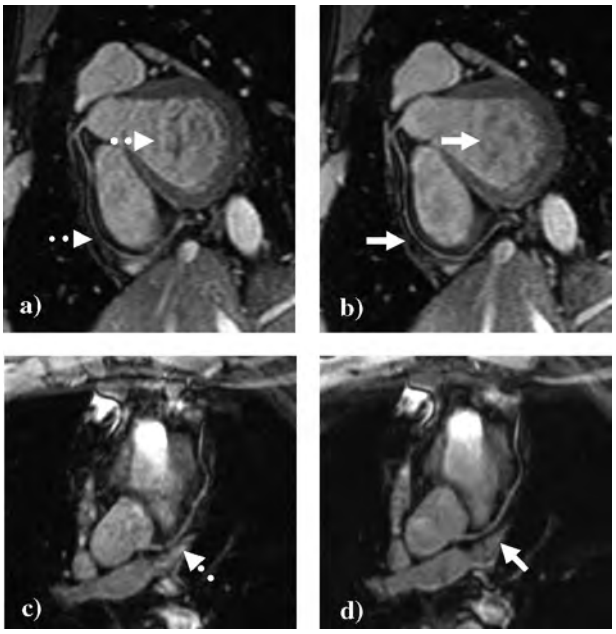

Figure 2. Apparent image artifacts in ACE (a, c) are markedly reduced in LCE images (b, d) as indicated by arrows. Images are acquired at 1.5 T (a, b) and 3.0 T (c, d), respectively.

Conclusions: Changing PE order in data acquisition markedly reduced eddy currents induced image artifacts and improved image quality in coronary MRA using SSFP sequence.

REFERENCES

Deshpande, V. S., et al. (2001). *Magn. Reson. Med.* 46(3):494–502.
Deshpande, V. S., et al. (2003). *Magn. Reson. Med.* 49(5):803–809.
Scheffler, K., et al. (2003). *Proc. Int. Soc. Magn. Reson.* 294.

437. Reproducibility of Free-Breathing Magnetic Resonance Coronary Angiography

Gerald F. Greil, MD,[1] Milind Y. Desai, MD,[2] Michael Fenchel, MD,[3] Stephan Miller, MD,[3] Ludger Sieverding, MD,[1] Matthias Stuber, PhD.[2] [1]*Department of Pediatric Cardiology, University of Tuebingen, Tuebingen, Germany,* [2]*Johns Hopkins University, Baltimore, MD, USA,* [3]*Department of Radiology, University of Tuebingen, Tuebingen, Germany.*

Background: Magnetic resonance coronary angiography (MRCA) is a promising technique that has been successfully utilized for visualizing coronary arteries without radiation or contrast agents (*N Engl J Med. 2001 Dec 27; 345(26):1863–9*). However its reproducibility for follow-up examinations in-vivo has not been investigated.

Purpose: The purpose of this study was to assess the reproducibility of free-breathing steady-state free precession (SSFP) MRA in right and left coronary arteries (RCA and LCA).

Methods: Twenty two healthy volunteers (mean age 32 ± 7 years, 12 males) without known coronary artery disease were imaged at 2 centers (Tuebingen, Germany and Baltimore, USA) using navigator-gated and corrected 3D SSFP MRCA with a T2 preparation pulse for endogenous contrast enhancement (TR 6.15, TE 3.08, FA 110°, slice thickness 1.5 mm, FOV 27 × 27 cm, 20 slices) on a commercial whole body 1.5 T System (Philips Medical Systems, Best, NL). RCA was imaged in 21 volunteers (Figure 1) and LCA (Figure 2, LAD = Left anterior descending and LCX = left circumflex) in 14 volunteers. Repeat images of RCA and LCA were obtained using identical imaging parameters, approximately 1–2 months apart. True visible vessel length (cm) and contrast to noise ratios (CNR) were measured for original and follow up studies. The average luminal diameter over the first 4 cm of the vessel was also measured (twice by 1st reader and once by 2nd reader) by using a semi-automatic (“Soapbubble”) tool (*Magn Reson Med*. 2002; 48:658–66), to calculate intra-observer, inter-observer and inter-scan reproducibility. Reproducibility was assessed by linear regression and intra-class correlation coefficient (ICC) methods.

Results: The approximate time of imaging for each vessel was 3 minutes. The mean length of the RCA (12.5 ± 2 vs. 12.4 ± 2 cm) and LCA (8 ± 2 vs. 8 ± 1 cm) imaged for original and repeat scans were not significantly different (both $p > 0.90$). Mean CNR was similar between original and repeat scans for RCA (39 ± 10 vs. 35 ± 13, $p = 0.28$) and LCA (25 ± 8 vs. 24 ± 11, $p = 0.98$). The mean length and mean CNR of imaged RCA was significantly higher than that of the LCA (both $p < 0.001$). For RCA luminal diameter, there was a highly significant intra-observer (r = 0.99), inter-observer (r = 0.98) and interscan (r = 0.84) correlation (all $p < 0.001$). Similarly, excellent ICC’s were calculated for intra-observer, inter-observer and interscan measurements of RCA diameter (r = 0.98, 0.98 and 0.86, respectively). For the LCA luminal diameter, there was a highly significant (although not as high as RCA) intra-observer (r = 0.90), inter-observer (r = 0.90) and interscan (r = 0.81) correlation (all $p < 0.001$). The ICC’s for intra-observer and inter-observer measurements of LCA diameter were less than that of RCA (r = 0.89 and 0.89, respectively). The ICC for inter-scan measurement of LCA diameter was significantly reduced when compared to the RCA (r = 0.63).

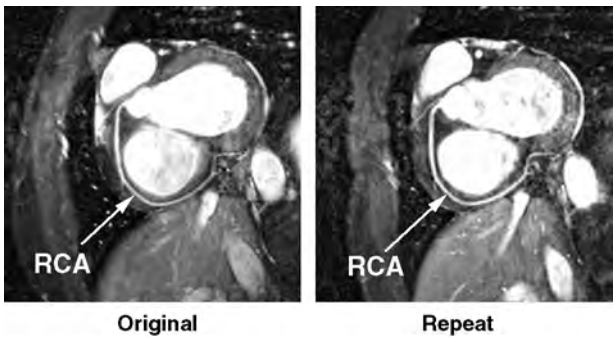

Figure 1.

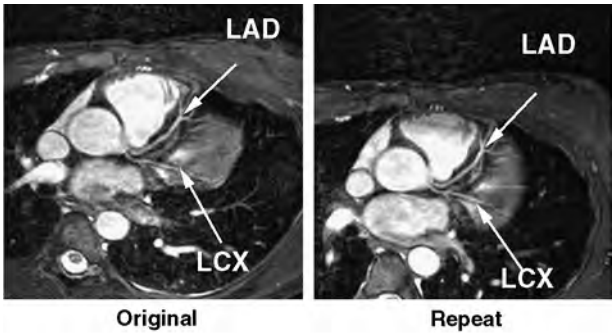

Figure 2.

Conclusion: Free breathing SSFP MRCA is a rapid, non-invasive technique which can repeatedly visualize long segments of the vessel, with high reproducibility, particularly in the RCA. Imaging of the LCA is technically more challenging than the RCA (as demonstrated by smaller length imaged, poorer CNR and weaker reproducibility). Among other things, this could be due to increased distance from the surface coils. Also, in order to maintain and improve the interscan reproducibility for follow up studies, very careful planning of follow-up scans is necessary. MRCA could potentially have a role in following of progression of coronary artery disease and in longitudinal therapeutic studies involving coronary arteries.

438. MR Coronary Vessel Wall Imaging Using Radial and Spiral K-Space Sampling

Marcus Katoh,[1] Elmar Spuentrup,[1] Arno Buecker,[1] Warren J. Manning,[2] Rolf W. GÃ□nther,[1] Rene M. Botnar.[2] [1]*Department of Diagnostic Radiology, RWTH Aachen University Hospital, Aachen, Germany,* [2]*Department of Medicine (Cardiovascular Division), Beth Israel Deaconess Medical Center and Harvard Medical School, Boston, MA, USA.*

Purpose: Two high-resolution navigator-gated and cardiac-triggered 3D gradient-echo sequences using radial and spiral k-space sampling were compared for the visualization of the coronary artery vessel wall.

Materials and Methods: Right coronary artery vessel walls of eight healthy subjects (6 men, 2 women; mean age: 37 years) were imaged on a 1.5 Tesla MR system (Gyroscan

ACS-NT, Philips Medical Systems, Best, NL) using a double-inversion prepared black-blood gradient-echo sequence (radial: TR/TE 8.0/2.0 ms, FA 30, 13 profiles/cardiac cycle; spiral: TR/TE 30.0/2.0 ms, FA 45/90, spiral interleaves 42, 2 profiles/cardiac cycle) with identical spatial resolution ($0.6 \times 0.6 \times 2.0$ mm^3). For data analysis, two investigators blinded to sequence parameters subjectively assessed image quality in terms of artifacts and vessel wall visualization. In addition, SNR, CNR and vessel wall definition were objectively assessed.

Results: Radial k-space sampling (Fig. 1a) demonstrated fewer motion artifacts and led to improved visualization of the coronary vessel wall compared to spiral imaging (Fig. 1b). In addition, significantly better vessel wall definition was found with radial imaging (62 vs. 56, $p < 0.05$). In contrast, a tendency towards increased SNR and CNR were found using spiral k-space sampling (n.s.).

Conclusion: Radial k-space sampling in free-breathing navigator-gated and cardiac-triggered MRI of the coronary vessel wall resulted in fewer motion artifacts and improved vessel wall definition compared to spiral k-space sampling.

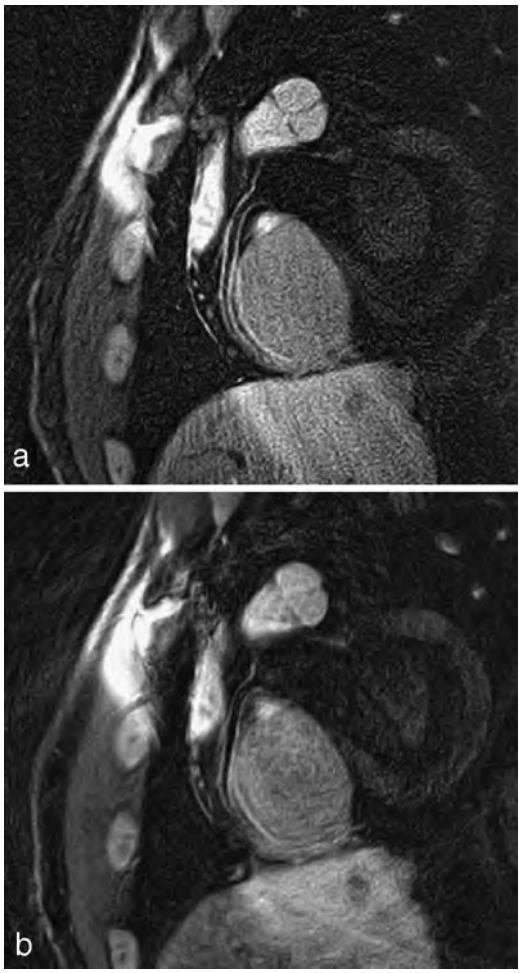

Figure 1.

439. In Vivo Carotid Plaque Tissue Segmentation Using Probability Maps and Multiple Active Contour Competition

Fei Liu, Dongxiang Xu, Chun Yuan, William Kerwin. *Radiology, University of Washington, Seattle, WA, USA.*

Introduction: MRI is a promising tool for analysis of plaque vulnerability, through quantitative assessment of carotid plaque composition (Yuan et al., 2004). Although manual segmentation methods based on multi-contrast weighted MR images accurately assess plaque composition, automatic segmentation methods are more efficient and provide more reproducible results. However, automated methods capable of segmenting ex vivo plaque specimens have not yet been translated into reliable in vivo methods. One difficulty is due to the complex tissue intensity distribution.

Purpose: We propose an efficient, consistent, and flexible framework for automatic plaque composition segmentation in vivo based on multi-contrast weighted MR images. The segmentation results of 4 types of tissue- calcification, necrotic core, loose matrix and others (predominately dense fibrous tissue)- are quantitatively compared with the corresponding histology segmentation results.

Methods: Thirteen patients scheduled for carotid endarterectomy (CEA) were imaged on a 1.5 T MR scanner to obtain images with T1 (TR = 800, TE = 11), T2 (TR = 3150, TE = 66), PD (TR = 2770, TE = 9.3) and contrast-enhanced (CE) T1 (TR = 800, TE = 11) weightings. These images were registered, and the lumen and outer wall contours were drawn manually before applying our algorithm.

The first step is to establish a baseline intensity. The plaque and vicinity region is compensated by a coil correction algorithm and normalized to a consistent intensity range. Then, using an active region algorithm (Paragios et al., 2000) each MR image is pre-segmented into bright, medium and dark intensity regions. All pixels are then divided by the average of the medium intensity region to produce a normalized image. Next, a probability map for each tissue is generated based on rules established for manual review. Using histologically confirmed regions, typical intensity values for each type of tissue were measured from each relevant weighting. The probability that a pixel is calcification, necrotic core or loose matrix is determined by its minimum distance to the representative intensity values. The probability of others is $Pr_{others} = 1 - (Pr_{calc} + Pr_{necr} + Pr_{loose})$. Based on the generated probability map for each tissue, the active region method is again used to seek each tissue with one active contour. Each contour moves under a smoothness constraint to maximize the total probability for the corresponding tissue within it. For validation, the surgical specimens from CEA were sectioned and stained and measurements of plaque composition were extracted from MRI-matched sections.

Results: Typical examples of the relevant steps are illustrated in Figure 1. Results comparing MR and histological

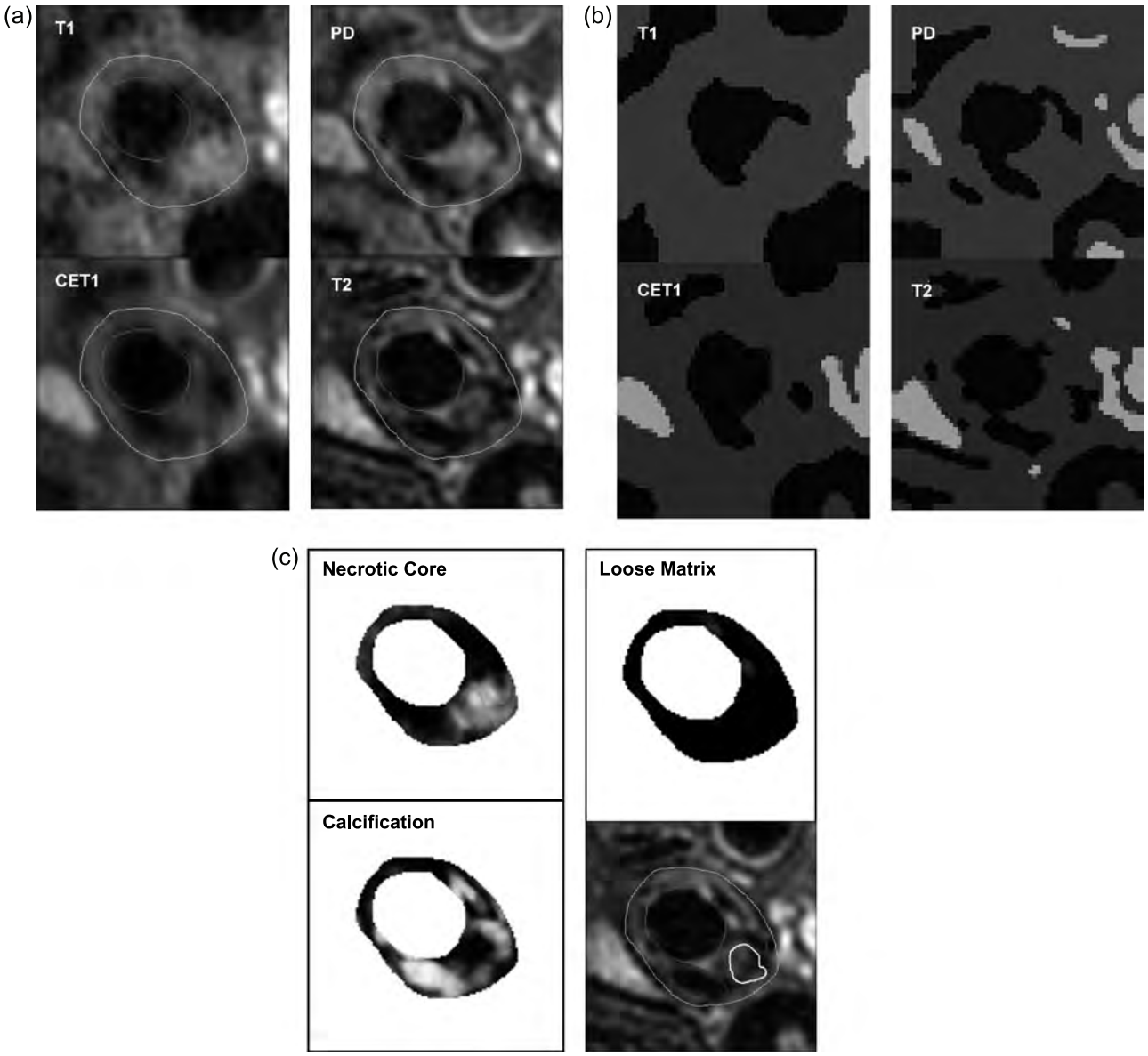

Figure 1. (a) MR images (b) pre-segmentation (c) probability map and final segmentation (1 necrotic core and 3 calcifications are displayed in a T2 image).

segmentation are presented in Table 1. The first row shows the correlation of the total area for each tissue using automatic MR segmentation and the second row for manual MR segmentation.

Table 1. Correlation between MR and histology segmentation

	Calcification	Necrotic core	Loose matrix	Others
Automatic	R = 0.940	R = 0.593	R = 0.745	R = 0.545
Manual	R = 0.922	R = 0.524	R = 0.632	R = 0.654

Conclusion: These results demonstrate that reliable, automated, in vivo segmentation of carotid plaque components is possible and quantitatively comparable to manual results. This technique could thus be used to reduce manual labor and bias in the assessment of plaque vulnerability or the time course of plaque evolution. The success of the technique is likely due to the pre-segmentation providing consistent intensity normalization across individuals and the probability map being generated without any assumptions on the pattern of tissue intensity distribution. Because the algorithm incorporates rules arising from manual review, it also provides a flexible way for radiology experts to incorporate further experience in the analysis of multi-contrast weighted MR plaque images.

REFERENCES

Paragios, N., et al. (2000). *ECCV*:224–240.
Yuan, C., et al. (2004). *JMRI* 19:710–719.

440. Black-Blood Imaging Using Stimulated Echo Aquisition Mode

Matthias Stuber, PhD,[1] Li Pan,[1] Nael Osman, PhD,[1] David A. Steinman, PhD,[2] Bruce Wasserman, MD.[1] [1]*Radiology, Johns Hopkins University, Baltimore, MD, USA,* [2]*Robarts Research Institute, London, ON, Canada.*

Introduction: Dual-inversion recovery (IR) black-blood magnetic resonance imaging (MRI) was introduced by Bob Edelman in 1991 and is a very powerful tool for the visualization of the vessel wall with and without exogenous contrast enhancement. To obtain an efficient signal-nulling of the blood-pool, the inversion time TI between the dual-inversion pre-pulse and the imaging part of the sequence has to be adjusted very carefully. Simultaneously, slow flowing blood or blood that re-enters the imaged slice because of turbulence sometimes lead to image artifacts that may easily be misinterpreted as focal thickening of the vessel wall. This adversely affects the measurement and identification of plaque especially near the bifurcation in the carotid arteries.

Purpose: To develop a black-blood MRI sequence without the need of a dual-inversion pre-pulse.

Methods: It has been demonstrated that stimulated echo imaging (STEAM) leads to a substantial signal attenuation in the ventricular cavities (Fischer et al, 1995) in cardiac imaging. This has been attributed to turbulence, and to the relative distribution of blood-flow velocities in the chambers of the heart. While one specific modulation and demodulation frequency is a prerequisite for successful STEAM imaging, flow and motion induce not only a frequency shift but also a substantial broadening of the spectrum in the frequency domain. Therefore, during STEAM demodulation (= imaging) with the same gradient that is used for STEAM preparation, a coherent signal can no longer be obtained and subsequent loss of signal occurs. While this is a shortcoming for many cardiovascular applications, this effect could be used for black-blood contrast generation for atherosclerosis imaging. For these reasons, a fast spin-echo sequence was extended for STEAM imaging as shown in Figure 1. A STEAM preparation pulse (STEAM modulation) preceded a fast spin-echo sequence in which the STEAM demodulation gradient was added to the refocusing gradient of the slice selection. The technique was implemented on a commercial Philips Gyroscan Intera system. ECG triggered STEAM fast spin-echo images (TE = 24 ms, ETL = 24, Inter Echo spacing = 5 ms, 256 matrix, 17 cm FOV, 3 mm slice thickness, TR = 2RR, fat saturation) and conventional dual-IR (TI = 660 ms, other parameters identical) fast spin-echo images of the carotid artery were acquired.

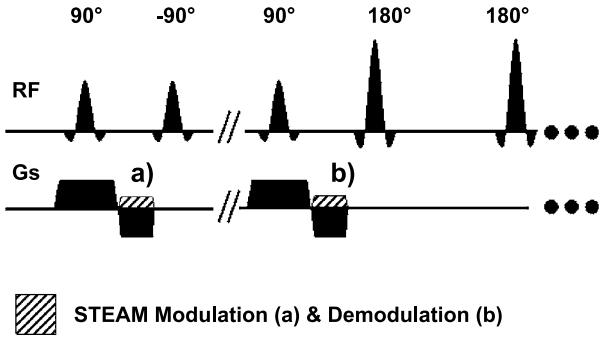

Figure 1. STEAM fast spin-echo black-blood imaging sequence without the need for a dual-inversion pre-pulse. a = STEAM modulation gradient & b = STEAM demodulation gradient.

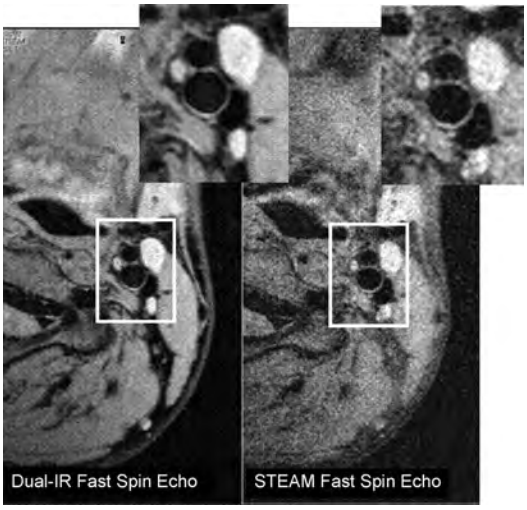

Figure 2. Dual-IR fast spin-echo (left) and STEAM fast spin-echo (right) black-blood images.

Results: In Figure 2 (left), a conventional dual-IR fast spin-echo image is displayed. A high contrast between the carotid arterial wall and the lumen is observed. The corresponding STEAM fast spin-echo image is shown in Figure 2 (right). Even though no dual-IR pre-pulse for black-blood generation was applied, the blood-pool in the carotid artery appears entirely signal-suppressed while the arterial vessel wall is displayed signal-enhanced. The visual signal-to-noise ratio in the STEAM fast spin-echo image is reduced.

Discussion and Conclusions: A black-blood MRI sequence without the need of a dual-inversion pre-pulse was developed, implemented, and successfully applied in the carotid artery. STEAM fast spin-echo imaging avoids the adjustment of an inversion-time for signal-nulling while slow flowing blood or blood that re-enters the slice is expected to be signal attenuated as well. Nevertheless, a 50% signal-loss has to be considered when using stimulated echo imaging. However, this could be compensated by using a higher magnetic field strength or by extending the technique with a 3D signal

read-out. Especially for 3D imaging, a more effective signal-nulling is expected for STEAM fast spin-echo imaging in comparison to conventional dual-IR fast spin echo imaging.

REFERENCE

Fischer, et al. (1995). *MRM.*

441. Whole-Heart Coronary MRI Using Undersampled Radial Acquisition

Dana C. Peters,[1] Rene M. Botnar,[1] Pratik Rohatgi,[2] Susan B. Yeon,[1] Kraig V. Kissinger,[1] Warren J. Manning.[1] [1]*Cardiology, Beth Israel Deaconess Medical Center, Boston, MA, USA,* [2]*Biomedical Engineering Department, University of Michigan- Ann Arbor, Ann Arbor, MI, USA.*

Introduction: Promising coronary MRI results have been obtained using a whole-heart scan, which requires a combination of longer scan times, lower in-plane spatial and temporal resolution, compared with a targeted coronary scan, but displays both the left and right coronary systems in a single acquisition. Such protocols are ideal for image acceleration techniques, e.g. parallel imaging, since slice coverage can be increased while maintaining spatial resolution and scan time, and therefore unchanged theoretical SNR, except for SNR penalties due to the acceleration method itself. We hypothesize that undersampled radial will also provide for whole-heart imaging, since the undersampling will allow increased slice coverage, at unchanged scan time. The tradeoff of numbers of projections for slice coverage will be limited by the appearance of artifacts.

Methods: Five healthy adult subjects (1 male, age 27 ± 12 yrs) were scanned on a 1.5 T Gyroscan ACS-NT (Philips Medical Systems, Best, NL) using previously described protocols. The radial acquisition was a 3D (projections in x–y plane, partitions in z) radial SSFP, preceded by T2prep, fat saturation, and navigator gating/tracking (6 mm acceptance window) preparation phases. The data was acquired with the following scan parameters: axial slices, TR/TE/θ = 4.2 ms/2.5 ms/90°, FOV = 360 mm, 320 readout points × 112 Np, slices = 96, 1.5 mm thick, zero-filled to 0.75 mm, scan time ∼ 10 to 12 minutes at 50% navigator efficiency. For acquisition, 5 acquisition order. The Cartesian acquisition was similar except for the use of SENSE factor 2 in the phase-encoding (anterior-posterior) direction, and view order centric in y and z, TR/TE/θ = 3.7 ms/2.0 ms/90°, FOV = 280 mm, 256 readout points × 204 Ny (102 with SENSE), scan time is 8–10 minutes at 50% navigator efficiency. The images and the individual left main, left anterior descending, left circumflex, and right coronary arterial trees (excluding diagonals) were evaluated, using the subjective score of two experienced readers (1.0 = uninterpretable 2.0 = good 3.0 = very good 4.0 = excellent) and the objective measure of total length (“soapbubble” tool).

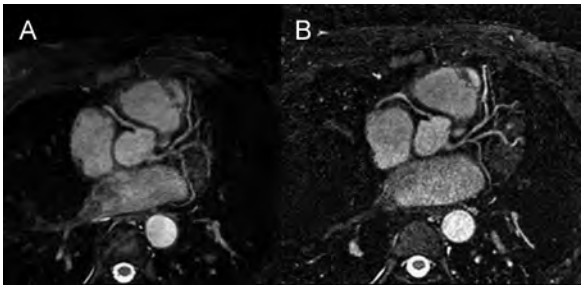

Figure 1. Comparison of whole-heart coronary MIPS using (A) Cartesian-SENSE, and (B) undersampled radial.

Table 1.

Segment	Undersampled radial	Cartesian-SENSE	Significance
Left Main visual	2.2 ± 0.4	2.5 ± 0.5	0.096
LAD visual	2.4 ± 0.6	2.6 ± 0.7	0.168
LAD length (mm)	50.8 ± 9.5	55.1 ± 10.6	0.345
LCx visual	2.1 ± 0.6	2.2 ± 0.7	0.591
LCx length (mm)	31.3 ± 6.4	39.0 ± 8.1	0.057
RCA visual	2.9 ± 0.6	3.1 ± 0.8	0.052
RCA length (mm)	99.4 ± 21.6	97.7 ± 24.8	0.964

Results: Figure 1 shows a comparison of the radial and Cartesian image quality, displaying a MIP which contains the left system, and a portion of the right system (part intentionally not displayed). Table 1 compares results for Cartesian and radial whole heart methods. No significant differences ($p < 0.05$) were found, though there was a trend for a greater LCx length visualization using the Cartesian-SENSE approach.

Conclusions: Our investigation demonstrates that undersampled radial may be a suitable acceleration method for whole heart coronary MRI. The trend towards better image quality with Cartesian, which might be significant with greater numbers of subjects, is likely to be related to the worse fat-saturation achieved with the radial technique, rather than the acceleration method.

REFERENCES

Etienne, A., et al. (2002). *Magn. Reson. Med.* 48(4):658–666.
Huber, M. E., et al. (2004). *Magn. Reson. Med.* 52(2):221–227.
Leiner, T., Botnar, R. M. (2004). *SCMR*:291.
Spuentrup, E., et al. (2004). *Radiology* 231(2):581–586.
Stuber, M., et al. (1999). *JACC* 34(2):524–531.
Weber, O. M., et al. (2003). *Magn. Reson. Med.* 50(6):1223–1228.

442. Whole Heart MRI Using 3D Spiral/Radial Sampling Trajectories

Paul Gurney, Brian Hargreaves, Dwight Nishimura. *Electrical Engineering, Stanford University, Stanford, CA, USA.*

Introduction: Whole-heart MRI has been shown to be effective in obtaining diagnostic-quality images of the coronary arteries using cartesian 3DFT acquisitions (Weber et al., 2003). Using alternative 3D trajectories, such as "Cones" or "Spiral/PR" (Irarrazabal et al., 1995), for whole-heart imaging can provide many advantages over the 3DFT method.

Purpose: Radial trajectories provide many benefits including isotropic resolution and FOV, insensitivity to flow and motion and the ability to trade off scan time against the structured noise-like artifacts resulting from undersampling. These benefits apply particularly well to the coronary arteries, which are almost always in motion and whose tortuous geometry calls for isotropic resolution and large FOVs. The purpose of this work is to use true 3D radial sampling trajectories for whole-heart SSFP MR imaging.

Methods: True 3D radial k-space trajectories include the "Cones" trajectory (shown in Figure 1) and the "Spiral/PR" trajectory (shown in Figure 2). While the "Spiral/PR" trajectory requires approximately 20% more interleaves, it has better flow properties and is easier to implement. These trajectories begin in the center of k-space and move outwards. As a result, the low-frequency components of the image are oversampled so motion leads to local blurring instead of global artifacts. Furthermore, since no prewinder is required, the scanner acquires usable data for a longer period of time per TR, resulting in higher SNR efficiency than 3DFT acquisitions. A key design parameter is the length of the readout. Longer readouts result in a reduction in total required scan time (because there can be more twist in the spiral leading to fewer required interleaves) and also better SNR efficiency. Unfortunately, the SSFP dark-band artifact and off-resonance limit the maximum TR (and therefore the maximum readout length). A TR of about 6 ms was chosen as a reasonable trade-off.

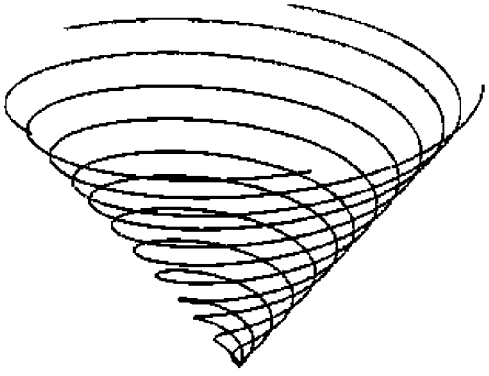

Figure 1. "Cones" trajectory. All of k-space can be covered by varying the pitch of the cone.

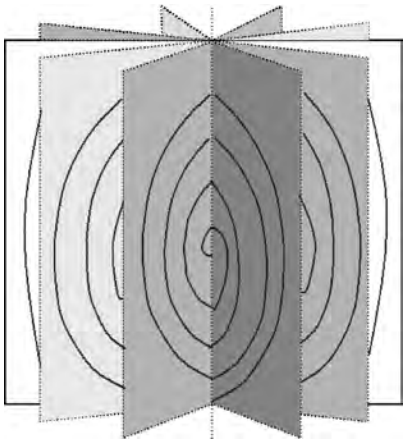

Figure 2. "Spiral-PR" trajectory. All of k-space is covered by rotating the spiral around the z axis.

Results: These 3D trajectories were implemented on a GE Signa LX 1.5 T scanner in an SSFP sequence using a TR of 6 ms. Figure 3 shows a reformatted image from the 3D dataset obtained using the "Cones" trajectory with a resolution of 1.25 mm and FOV of 30 cm in about 15 minutes of free-breathing, cardiac gated acquisitions (aquisition window of about 200 ms) with a single 5″ surface coil. Rudimentary retrospective respiratory gating was performed in which approximately 30% of the acquired interleaves were thrown away. The remaining motion results in mild blurring instead of distracting motion artifacts.

Conclusions: True 3D radial trajectories provide increased resilience to motion and better SNR efficiency than cartesian aquisitions and are ideally suited to the application of whole-heart MR imaging for coronary angiography.

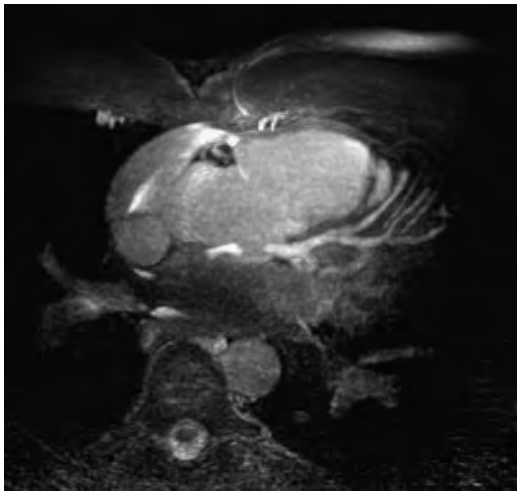

Figure 3. A thin-slab double-oblique MIP view from the 3D whole heart dataset obtained using the Cones trajectory.

REFERENCES

Irarrazabal, P., et al. (1995). Fast three dimensional magnetic resonance imaging. *MRM* 33(5):656–662.

Weber, O. M., et al. (2003). Whole-heart steady-state free precession coronary artery magnetic resonance angiography. *MRM* 50(6):1223–1228.

443. Optimizing Imaging Strategies For Non-Invasive Coronary Angiography Based on a Large Database of Invasive Coronary Angiograms

Sebastian Kelle, MD, Jürgen Hug, MD, Uwe Köhler, PhD, Eckart Fleck, MD, Eike Nagel, MD. *Internal Medicine/ Cardiology, German Heart Institute Berlin, Berlin, Germany.*

Introduction: Current non-invasive imaging techniques as MRI or CT have one of their limitations in a low spatial resolution in comparison to invasive angiography and therefore allow only a partial coverage of the coronary artery tree.

Purpose: Aim of the current report was to extract information from invasive coronary angiograms to quantify the potential intrinsic error of non-invasive coronary angiography due to partial coverage.

Methods: Coronary angiograms of 14.473 patients, examined at our institution from November 1997 until October 2003, were reviewed. The location and severity of stenoses and the balloon or stent-size of percutaneous coronary interventions (PCIs) were extracted.

Results: Out of a total of 92.333 stenoses, 69.564 stenoses (75.3%) were significant with a $\geq$ 50% diameter reduction. Of these stenoses, 30.9% were located in major and minor side branches, contributing to only 16.5% of the PCIs. Only 5% of the patients with invasive diagnostic for suspected coronary artery disease had their most proximal significant stenosis in a distal segment, or in a minor side branch. More than 90% of interventions were performed in coronary arteries of 2.5 mm or more in diameter.

Conclusions: Coronary artery stenoses were found and PCIs performed in all coronary segments. Therefore non-invasive coronary imaging of only proximal and medial segments and major side branches is an inadequate strategy for complete diagnosis and to guide therapeutic decisions. However, the current available non-invasive techniques allow to detect significant stenoses in 95% of the patients with suspected CAD to decide on further invasive diagnostic and therapy.

444. CoroViz: Visualization of 3D Whole-Heart Coronary Artery MRA Data

Stefan Tuchschmid, MS,[1] Alastair J. Martin, PhD,[2] Peter Boesiger, PhD,[3] Oliver M. Weber, PhD.[1] [1]*Department of Radiology, University of California, San Francisco, San Francisco, CA, USA,* [2]*Philips Medical Systems, Best, The Netherlands,* [3]*Swiss Federal Insitute of Technology, Institute for Biomedical Engineering, Zurich, Switzerland.*

Introduction: Whole-heart coronary MRA has been demonstrated to allow the imaging of the entire coronary tree in a single volume (Weber et al., 2003). With this method, long segments of all major vessels can be visualized with high quality and good discrimination from the background. However, a tool for comprehensive display of the 3D data sets has been lacking. The previously described SoapBubble tool (Etienne et al., 2002) is intended for targeted volume data, relies on in-plane vessels, and generates two-dimensional output images. Alternatively, a volume rendering approach has recently been reported to be useful in coronary MRA display (Ichikawa et al., 2004). However, the images may involve the risk of either artificially creating or obliterating stenoses. Approaches closer to the source data may be preferable.

Purpose: To develop a comprehensive tool for 2D and 3D visualization and quantification of whole-heart coronary MRA data sets.

Methods: The CoroViz software package was implemented under IDL6.1 (RSI; Boulder, CO) on a commercial WindowsXP PC with a 3.0 GHz Pentium4 processor. The advanced visualization modules are based on knowledge of the vessel centerline. Semi-automatic tracking based on at least one user defined point on the coronary tree was implemented, combining a vessel enhancement filter (Frangi et al., 1998) with a basic wave-front propagation algorithm. After definition of the vessel centerline, a number of visualization modes are available. One mode ('GlobeViz') utilizes a maximum intensity projection (MIP) onto a deformed sphere defined by the coronary vessels. The user can freely choose the thickness of the MIP-volume. An alternative mode ('VolumeViz') creates a masked MIP volume rendering. The mask consists of a tube with user-defined diameter along the vessels. In all views, an interactive user interface allows zooming, panning and rotation of the data space, manual correction of the found centerline, as well as display of all visualization modules. Besides the display of axial, coronal and sagittal viewports, the current vessel cross-section is shown, allowing the identification of vessel branching and stenoses. Additional modules include a local region-growing segmentation tool as well as planar and curved reformats. Quantification tools include interactive vessel length measurement and indication of maximum, minimum and average diameter along the vessel.

Results: Eight datasets were successfully processed. The time required to automatically track the vessel centerline and generate the different visualization was < 2 minutes for all datasets; a manual refinement and alignment of the vessel axis for optimal results added between 1 and 10 minutes to the preparation time.

Figure 1A shows a globe visualization of all the coronary vessels. The deformed sphere can be interactively rotated, zoomed, panned, and windowed. Figure 1B presents the segmented coronaries, together with the globe visualization (set to a 40% transparency value), allowing simultaneous perception of the coronaries and the shape of the deformed surface. Figure 1C and 1D show the left circumflex coronary artery. A three-dimensional curved reformat (MIP slice

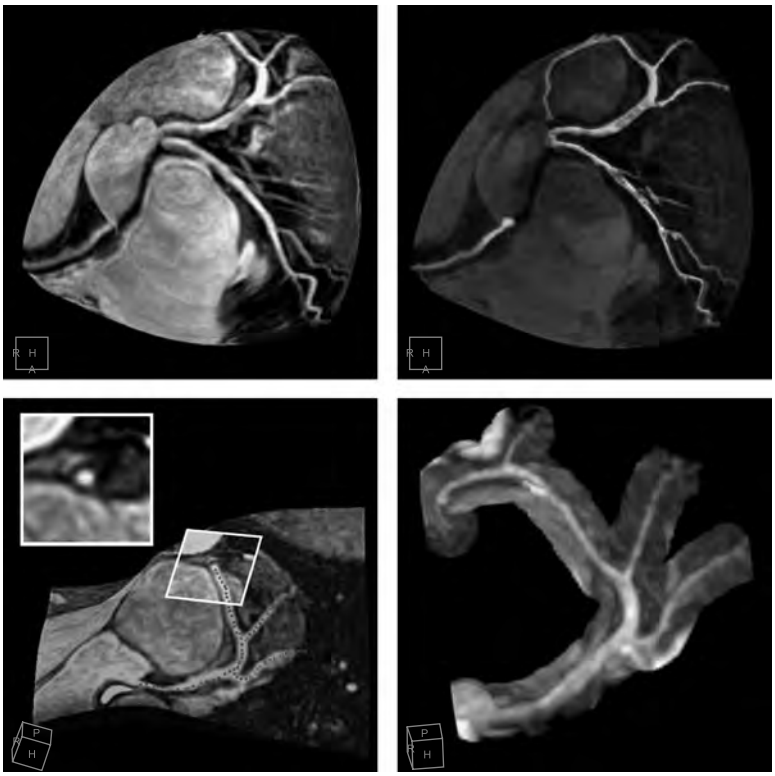

Figure 1.

thickness 1.5 mm) and the vessel centerline found by the tracking algorithm are displayed in Figure 1C. The masked volume rendering module restricts the MIP to a tubular structure around the vessel center line, allowing an accurate local assessment of the vessel structure (Figure 1D).

Conclusions: A comprehensive tool for processing and display of whole-heart data sets was developed. Globe visualization and masked MIP volume rendering allow the three-dimensional assessment of the coronary arteries with only marginal concealment from signals originating outside the vessel. The use for clinical routine image post-processing and modalities other than coronary MRA remain to be investigated.

REFERENCES

Etienne, A., et al. (2002). *MRM* 48:658.
Frangi, A., et al. (1998). *LNCS* 1496:130.
Ichikawa, Y., et al. (2004). *Proc. ISMRM Kyoto* 704.
Weber, O. M., et al. (2003). *MRM* 50:1223.

445. Rapid and Complete Coronary Arterial Tree Visualization with Magnetic Resonance Imaging

Cosima Jahnke, MD,[1] Ingo Paetsch, MD,[2] Kay Nehrke, PhD,[3] Bernhard Schnackenburg, PhD,[2] Rolf Gebker, MD,[2] Eckart Fleck, MD,[2] Eike Nagel, MD.[2] [1]*Cardiology, University of Freiburg, Freiburg, Germany,* [2]*Cardiology, German Heart Institute Berlin, Berlin, Germany,* [3]*Philips Research Laboratories, Hamburg, Germany.*

Purpose: A major limitation of magnetic resonance coronary angiography (MRCA) is the limited coverage of the coronary arteries. We present and evaluate an accelerated, single-scan MRCA approach with complete coverage of the whole coronary arterial tree.

Methods: 52 consecutive patients with suspected coronary artery disease underwent free-breathing, navigator-gated MRCA using a single 3D-volume with transversal slice orientation and nearly isotropic spatial resolution (1.2 × 1.2 × 1.4 mm) with coverage of the whole heart (SSFP, TR/TE/flip angle: 5.3 ms/2.6 ms/90°; Philips Intera CV 1.5 T). Acquisition duration per heart beat was individually adapted to

the cardiac rest period. Respiratory motion was corrected with a patient-specific affine prospective navigator technique (two navigator beams: cranio-caudal position on the dome of the right hemidiaphragm and anterior-posterior position on the right chest wall; gating window 10 mm). Stenosis detection was verified against invasive x-ray angiography (32 patients) using a 16 segment model.

Results: Effective scan duration was 18 ± 6 min (navigator efficiency: 68 ± 14%). In all examinations the main epicardial vessels (LAD, LCX and RCA) including their distal segments and major side branches (number of visible side branches: LAD, 2.0 ± 0.9; LCX, 1.5 ± 0.6; RCA, 2.3 ± 0.9) were reliably visualized. 83% of all coronary segments were evaluable; sensitivity, specificity and diagnostic accuracy were 78%, 91% and 89%.

Conclusions: The combination of an imaging sequence with an intrinsically high contrast (SSFP) and a sophisticated navigator technique (affine transformation) resulted in high quality, high resolution imaging of the whole coronary arterial tree within a short examination duration. Robustness and diagnostic accuracy may allow for a routine application in the near future.

446. Detection of Perioperative Myocardial Necrosis After Surgical Revascularization Using Contrast-Enhanced MRI

Olga Bondarenko, MD, Aernout M. Beek, MD, Mark B. M. Hofman, PhD, Harald P. Kûhl, MD, PhD, Robin Nijveldt, MD, Albert C. van Rossum, MD, PhD. *Cardiology, VU University Medical Center, Amsterdam, The Netherlands.*

Background: Delayed contrast-enhanced (DCE) MRI may be more sensitive than enzymatic or electrocardiographic criteria in detecting perioperative myocardial necrosis in patients undergoing coronary artery bypass grafting (CABG).

Methods: 24 patients with chronic ischemic left ventricular dysfunction underwent cine MRI for assessment of left ventricular function and DCE MRI for assessment of total myocardial scar mass (TSM) 1 month before and 3 months after surgical revascularization.

Results: Mean TSM increased from 16 ± 12 g at baseline to 18 ± 14 g at follow-up (p = 0,005). Postoperative changes in ejection fraction were inversely related to changes in mean TSM (r = 0.47, p = 0.007). No patient developed new Q-waves after revascularization. 12 patients showed an increase in TSM at follow-up. Only 3 of these had biochemical evidence of myocardial infarction (CK-MB elevation > 2 times ULN). The increase in TSM was larger in patients with enzymatic evidence of infarction: 8.0 ± 3.6 g vs. 3.4 ± 2.5 g (p = 0.03).

Conclusions: Perioperative myocardial micro-infarctions frequently occur in patients undergoing surgical revascularization. DCE MRI is more sensitive than CK-MB and ECG in detecting CABG-related myocardial necrosis.

447. Rapid Magnetic Resonance Infarct Imaging by Single-Shot Inversion Recovery TrueFISP Compared to Segmented Inversion Recovery TurboFLASH

Daniel C. Lee, MD,[1] Paula Tejedor, MD,[1] Edwin Wu, MD,[1] Yiu-Cho Chung, PhD,[2] Thomas A. Holly, MD,[1] James Carr, MD,[1] Francis J. Klocke, MD,[1] Robert O. Bonow, MD.[1] [1]*Feinberg Cardiovascular Research Institute, Northwestern University Medical School, Chicago, IL, USA,* [2]*Siemens Medical Systems, Chicago, IL, USA.*

Background: Contrast-enhanced MRI identifies infarcted myocardium and can predict wall motion recovery following revascularization. The inversion-recovery, segmented turboflash (FLASH) sequence accurately identifies the size of infarction and produces the greatest difference in signal intensity between infarcted and viable myocardium. Single-shot inversion recovery trueFISP (FISP) is a newer sequence that acquires an image in one heartbeat, enabling faster imaging without the sensitivity to arrhythmia or breath-hold requirement of the FLASH technique. To evaluate its diagnostic accuracy we compared FISP to conventional FLASH in the evaluation of patients with acute and chronic myocardial infarction.

Methods: During the same imaging session, FLASH and FISP images were acquired at identical short axis positions in 49 patient studies more than 5–10 minutes following IV gadolinium contrast injection (0.1–0.2 mmol/kg). Typical voxel size was 2.0 × 1.6 × 5 mm for FLASH and 3.1 × 1.6 × 8 mm for FISP. For both sequences, the inversion time was selected to null normal myocardium (FLASH TI 280–350 ms, FISP TI 330–400 ms). All 98 image sets were then blinded and randomized for analysis. Infarct size was measured in grams by a blinded reader. Four blinded readers scored the images for the visual extent of hyperenhancement (HE) on a 5-point scale (0 = no HE, 1 = 1–25% HE, 2 = 26–50% HE, 3 = 51–74% HE, 4 = 76–100% HE) using a standard 17-segment model. Mean signal intensity within the infarct and in remote normal myocardium was measured in FLASH and FISP images.

Results: Using FLASH, each slice of a 6–8 slice short-axis stack was acquired during a separate 8–10 second breath-hold. Conversely, each FISP image was acquired in a single heartbeat during free breathing. Measured infarct size by the two techniques demonstrated good correlation ($y = 0.82x + 2.6$, $r^2 = 0.82$) as did total visual infarct score ($y = 0.92x + 1$, $r^2 = 0.85$). FISP tended to underestimate infarct size compared to FLASH. The ratio of infarct signal intensity to the signal intensity in normal myocardium was significantly higher in FLASH images than in FISP images (FLASH mean 7.1 ± 2.8 SD, FISP mean 4.4 ± 1.9 SD, $p < 0.001$). In four cases, subendocardial infarcts visually appreciated on FLASH were missed by FISP because of poorer infarct signal intensity on the FISP images.

Conclusions: Contrast-enhanced MRI using FISP can rapidly assess the entire LV for myocardial infarction. The improved speed, insensitivity to arrhythmias, and the ability to image during free breathing may expand the clinical applicability of MR infarct imaging. Measured and visual size of infarction by FISP correlates well with FLASH. However, infarct size is somewhat underestimated by FISP and lower resolution along with weaker infarct signal intensity may cause small subendocardial infarcts to be missed. Therefore, FLASH remains the preferred infarct imaging technique when patient conditions allow.

448. Delayed Contrast-Enhanced Cardiovascular Magnetic Resonance Imaging of Myocardial Infarction at 3.0 Tesla in Humans—Preliminary Experience

Christian Schlundt,[1] Johannes von Erffa,[1] Robert Krähner,[1] Michaela Schmidt,[2] Werner G. Daniel,[1] Matthias Regenfus[1]
[1]*Medical Clinic II, FAU Erlangen-Nürnberg, Erlangen, Germany,* [2]*Siemens Medical Solutions, Erlangen, Germany.*

Introduction: Contrast-enhanced cardiovascular magnetic resonance (CMR) using a segmented inversion-recovery turbo FLASH technique for visualization of myocardial infarction (MI) has been presented recently. 3.0 T systems which have recently been approved for clinical use are expected to supply improved signal-to-noise ratio (SNR).

Purpose: We evaluated the feasability of DE-CMR data acquisition at 3.0 Tesla in humans.

Methods: 14 consecutive patients who had suffered clinically proven MI (elevation of myocardium-specific creatine iseoenzyme more than twice the upper limit) were examined on a 3.0 T scanner (TRIO, Siemens, Erlangen, Germany). DE-CMR in long-and short-axis orientation of the heart was acquired 10 min after intravenous injection of 0.15 mmol/kg Gd-DTPA (MAGNEVIST, Schering, Berlin, Germany) using an inversion recovery Turbo FLASH sequence (TE 4.3 ms, TR 8,3 ms, flip angle 30°, inversion time 220–360 ms). For each of the patient studies, a single short-axis image showing both the largest high-signal lintensity region and normal regions of myocardium was selected. The mean signal intensity of the myocardial regions with elevated signal intensity and that of a remote normal myocardium, as well as the SD of noise in a rectangular region outside the patient body, was measured. The percent signal intensity elevation in the infarcted myocardium was calculated by the following equation: percent elevation = 100 × (mean signal intensity of high-signal-intensity region- mean signal intensity of normal region)/(mean signal intensity of normal region). Image contrast-to-noise ratios (CNR) were calculated by the following equation: (mean signal intensity of high-signal-intensity region- mean signal intensity of normal region)/(1.5 × SD of noise).

Results: Data in all 14 patients were acquired without any side effects reported by patients. ECG artifacts related to scanning did occur in 2 patients, but did not interfere with data acquisiton. DE-CMR images showed evidence of myocardial infarction in all of the 14 patients by exhibiting areas of elevated signal intensity. The mean percent signal intensity elevation in the infarcted myocardium was 1107 ± 87%, the mean CNR 36.0 ± 7.3.

Conclusions: DE-CMR imaging of MI using a segmented inversion-recovery turbo FLASH technique on a 3.0 T system is feasible and produces stable results concerning image quality and visualization of MI. Quantitative image parameters as the percent signal intensity elevation in the infarcted myocardium and the CNR showed even better values than reported for use of the same sequence on a dedicated cardiac 1.5 T scanner.

449. Semi-Automatic Determination of Infarct Size in Patients with Chronic Ischemic Heart Disease: Comparison with Manually Assessed Infarct Size

Harald P. Kühl, MD,[1] Markus Katoh, MD,[2] Elisabeth Schade,[1] Maren Tomars, MD,[1] Gabriele Krombach, MD,[2] Arno Buecker, MD.[2] [1]*Medical Clinic I, University Hosptial, Aachen, Germany,* [2]*Department of Radiology, University Hosptial, Aachen, Germany.*

Introduction: Contrast-enhanced magnetic resonance imaging (ce-CMR) is an emerging modality for the assessment of myocardial viability. Although visual interpretation of ce-CMR imaging is straight-forward, a comprehensive quantitative analysis has been hampered by laborious manual tracing. Owing to the sharp contrast between contrast-enhanced (infracted) and non-enhanced (viable) tissue, ce-CMR may allow for a facilitated semi-automatic quantification of infracted tissue by means of a threshold technique.

Purpose: The aim of the study was to compare a commercial available, semi-automatic infarct quantification tool with manual tracing for the determination of total infarct mass in patients with chronic ischemic cardiomyopathy.

Methods: Forty patients (64 ± 12 years) with ischemic cardiomyopathy and clinical indication for viability testing underwent cine and contrast-enhanced CMR on a 1.5 Tesla

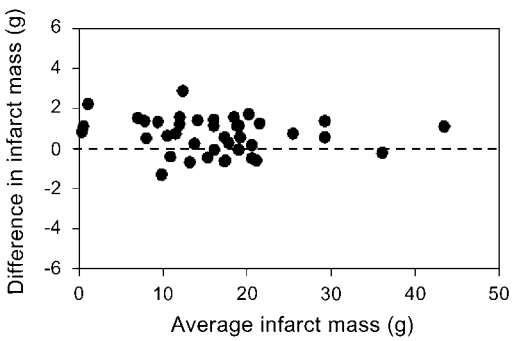

Figure 1.

scanner (Intera, Philips, Best, The Netherlands). Cine CMR was performed using a SSFP sequence (TR 3.6 ms, TE 1.8 ms, FA 20°). For delayed enhancement imaging a 2D inversion-recovery sequence (TR 2 heart beats, TE 5.2 ms, FA 25°, TI 250 to 300 ms, resolution 1,4 × 1,8 × 8 mm^3) was applied 15 minutes after i.v. administration of 0.2 mmol/kg gadolinium-DTPA. The TI was adjusted individually to null the signal of the non-infarcted myocardium. Double oblique short-axis slices covering the entire LV were acquired. Infarct size was determined semi-automatically using a threshold tool (MASS, Medis, Leiden, The Netherlands). With this method a threshold value of relative signal intensities (SI) of pixels encompassed within the manually drawn endocardial and epicardial contours is selected. Pixels demonstrating SI values above the chosen threshold are considered to represent scar. These pixels are automatically segmented and quantified to yield infarct mass. The optimal threshold is selected individually by visual inspection after optimizing window settings and is kept constant for each patient. Data analysis using the threshold method and manual tracing was performed by the same observer with a time delay of at least one week between the two examinations. Moreover, analysis was performed in random order with the investigator blinded to the patient data.

Results: Mean ejection fraction of the population was 31 ± 11% and mean LV mass averaged 126 ± 28 g (range 71–214 g). Mean infarct mass was 16.6 ± 8.6 g (range 0.8-44.1 g) with the threshold method and 15.9 ± 8.7 g (range 0–43 g) with manual tracing. When expressed as percentage of LV mass percent infarct mass averaged 13.7 ± 7.1% (range 1–33%) for the threshold method and 13.2 ± 7.3% (range 0–31.9%) with manual tracing. An excellent correlation was observed between the semi-automatically defined and the manually assessed infarct size (r = 0.995, $p < 0.001$). There was a clinically insignificant overestimation of infarct size by the threshold method compared with manual tracing (mean bias 0.7 ± 0.9 g or 0.5 ± 0.8%; $p < 0.001$, Figure 1). Inter- and intraobserver variability assessed for 15 patients was low for the semi-automatic method (6% and 3% resp.) as well as for the manual method (8 and 5% resp.).

Conclusions: Determination of infarct size by a semi-automatic threshold method agrees closely with results obtained by manual tracing. These results suggest that semi-automatic analysis of contrast-enhanced CMR images may allow for a rapid and observer independent quantification of infarct size.

450. Infarct Transmurality and Adjacent Segmental Function as Determinants of Wall Thickening in Revascularised Chronic Ischaemic Heart Disease

Martin Ugander, MD, Peter Cain, MBBS, PhD, Annick Perron, BSc, Håkan Arheden, MD PhD. *Clinical Physiology, Lund University Hospital, Lund, Sweden.*

Introduction: There are many factors which influence regional left ventricular wall thickening (WT) in ischaemic heart disease (IHD).

Purpose: We used magnetic resonance imaging (MRI) to explore, in patients with chronic IHD, how regional WT is affected by both infarct transmurality (IT) and the function of adjacent segments. We also compared these findings with a group of healthy volunteers (controls).

Methods: Twenty patients (20 men, mean age 63, range 45–80 years) were imaged with cine MRI for function and delayed enhancement MRI for infarction six months after revascularisation. Twenty age and sex matched controls

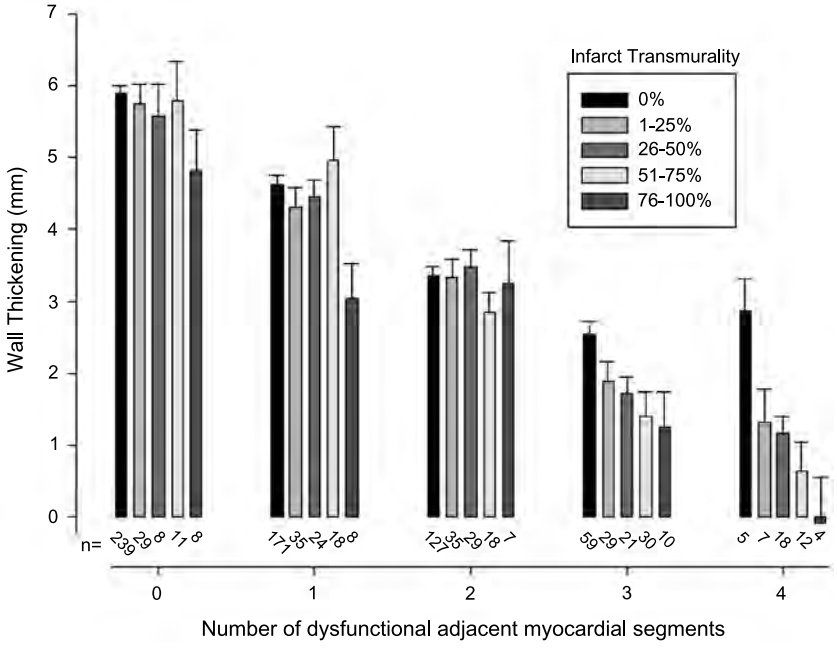

underwent cine MRI. WT and IT were inversely related ($R2 = 0.11$, $p < 0.001$).

Results: WT of non-infarcted segments in patients was lower than corresponding segments in controls (5.14 vs. 4.64 mm, $p < 0.001$). WT in patients decreased with an increasing number of dysfunctional adjacent segments ($p < 0.001$) and increasing IT ($p < 0.001$). WT was more strongly influenced by the number of dysfunctional adjacent segments ($t = -22.93$, $p < 0.001$) than by IT ($t = -4.50$, $p < 0.001$).

Conclusions: The number of dysfunctional adjacent segments is a more important determinant than IT on regional WT.

451. Delayed Gadolinium-enhanced MR Viability: Hypo-vs Hyper-Enhancement Imaging

James William Goldfarb, PhD, Nathaniel Reicheck, MD. *Research and Education, St Francis Hospital, Roslyn, NY, USA.*

Introduction: Several studies have shown that MR imaging after the administration of gadolinium contrast material can be used to accurately distinguish between reversible and irreversible myocardial ischemic injury using delayed T1 sensitive imaging. Irreversibly injured regions of the myocardium have a slightly higher concentration of intravenously injected gadolinium contrast agents when compared to normal myocardium. Typically, inversion recovery (IR) gradient-echo pulse sequences are used to identify regions of injured myocardium. Inversion recovery times are individually adjusted to null the signal from viable myocardium resulting in hyper-enhancement of necrotic tissue. Difficulties still exist in identifying distinct regions of heart (LV bloodpool, viable myocardium and necrotic tissue) based on post-contrast signal intensities using hyper-enhancement. Often the LV bloodpool has a similar signal intensity to that of necrotic tissue. Due to poor contrast, infarct volumes are measured by segmentation based on endocardial border estimates and require extensive user interaction.

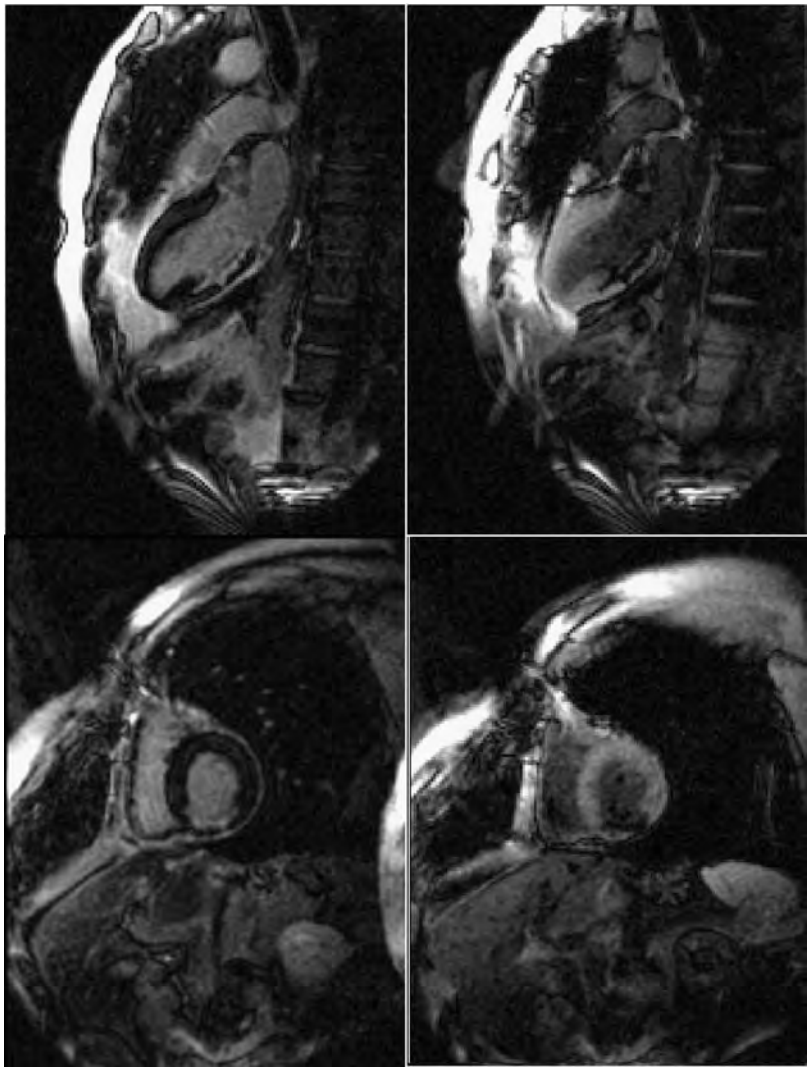

Figure 1.

We investigated the selection of an inversion time set to null the signal from necrotic tissue, which results in hypo-enhancement of the necrotic tissue when compared with viable tissue.

Purpose: To compare image contrast between hypo-and hyper-enhancement delayed gadolinium imaging for optimal infarct detection.

Methods: Ten subjects (mean 65; range 43–84 years) with known myocardial infarctions (mean infarct age: 9; range 2–21 years) underwent MR imaging on a 1.5 T clinical scanner (Siemens Magnetom Sonata, Erlangen, Germany). A 2D cardiac-gated inversion recovery multiple TI TrueFISP sequence was used. Sequence parameters were: (TR = 2.5 ms, TE = 1.25 ms, FA = 50 degrees, BW = 965 Hz/pixel, voxel size = 2.5 × 1.8 × 8.0 mm3, 15 k-space lines per cardiac cycle and 19 segments per cardiac cycle yielding 19 images with increasing inversion times of 39 ms). Images were acquired 30 minutes after contrast agent administration. ROI analysis was performed on the images and signal intensities of the infarct, viable myocardium and bloodpool were measured. T1 values of these regions were calculated. From plots of the signal intensities, two images were selected. The first having the lowest signal intensity of viable myocardium (hyper-enhancement) and the second having the lowest signal intensity of the infarct (hypo-enhancement). Image contrast values for three regions were calculated and compared using a paired student's t-test with Analyse-It (Analyse-It Software, Ltd., Leeds, England).

Results: Average T1 values (msec) of viable myocardium, infarct and blood were 339 ± 28, 261 ± 24 and 413 ± 34, respectively. Example images of hyper-(left) and hypo-enhancement (right) from the same subject are shown in Figure 1. Contrast measurements showed a significant difference between hypo-and hyper-enhancement images for Contrast(Blood/Infarct) and Contrast(Blood/ViableMyo), but not Contrast(ViableMyo/Infarct).

	Hypo-enhancement	Hyper-enhancement	
Contrast (Blood/Infarct)	2.20 ± 0.45	0.29 ± 0.09	$p = 0.0014$
Contrast (ViableMyo/Infarct)	2.37 ± 0.35	3.10 ± 0.49	$p = 0.15$
Contrast (Blood/ViableMyo)	−0.02 ± 0.11	2.08 ± 0.28	$p < 0.0001$

Conclusions: Images with TIs set to null infarcted tissue have significantly better contrast between necrotic tissue and the LV bloodpool. Contrast was equivalent between viable myocardium and necrotic tissue when compared with images optimized to null signal from viable myocardium. Increased contrast may lead to improved infarct detection accuracy and automated infarct volume measurements.

452. Myocardial Viability Assessed by Delayed-Enhanced CMR and Recovery of Function After Surgical Revascularization

Sandra Pujadas, Francesc Carreras, MD, Susagna Prat, MD, Ruben Leta, MD, Guillem Pons-Llado, MD. *Cardiology, Hospital Sant Pau, Barcelona, Spain.*

Introduction: A unique feature of cardiovascular magnetic resonance (CMR) is that it allows, by means of the delayed contrast-enhancement (DCE) technique, an in vivo detection of myocardial scar due to necrosis. Therefore, it has been proposed as a useful technique in the differential diagnosis between irreversible and viable myocardium in patients with ischemic heart disease.

Purpose: To study the diagnostic value of the presence and extension of myocardial viability, as assessed by DCE CMR studies, in predicting recovery of function late after coronary artery bypass surgery (CABS) in patients with chronic coronary artery disease.

Methods: Twenty-five consecutive patients scheduled for elective CABS were studied by CMR (Philips Intera 1.5 T) before and between 4 and 6 months after the revascularization procedure. In all patients a complete functional cine study and DCE images were obtained by CMR. Left ventricular ejection fraction (LVEF) was calculated for each study and presence and extension of DCE was visually assessed as transmural (> 50%) vs non-transmural (< 50%).

Results: 3 patients were excluded (2 perioperative deaths and 1 patient lost to follow-up). In the remaining 22 patients, 374 segments were analysed. *Before CABS*, 138 segments (37%) showed abnormal contractility, either akynesia (58), or hypokynesia (80). Of 58 akynetic segments, 27 (47%) showed transmural DCE, 13 (22%) non-transmural and 17 (29%) did not show any DCE. Of the 80 hypokinetic segments pre-CABS, transmural DCE was shown in 2 (3%), non-transmural DCE was observed in 21 (26%), and DCE was absent in 57 (71%). *After CABS*, 62 of the 138 (45%) segments with abnormal contractility showed improvement in function. Improvement was observed in both akynetic (28 of 58, 48%) and hypokynetic (34 of 80, 43%) segments. In relation with the presence and distribution of DCE, improved function was present in none (0%) of those 29 segments with transmural DCE, in 22 of 34 (65%) segments with non-transmural DCE, and in 40 of 74 (54%) of those without DCE. On the other hand, contractility actually worsened after CABS in 57 segments, 48 of them (84%) corresponding to 6 patients with perioperative infarction demonstrated by DCE at the post-CABS CMR study, not present before CABS.

Conclusions: The pattern of regional myocardial contractile function does not reliably discriminates between viable and irreversibly damaged tissue. DCE CMR studies, however, are of great help in this sense, as the presence of transmural DCE specifically identifies non-viable myocardial segments that do not recover after CABS surgery, while absence or non-transmural extension of DCE indicates potential for recovery of function in most cases. In those viable segments with lack of improvement or worsening of function after CABS, a perioperative infarction must be ruled out.

453. Prediction of β-Blocker Therapy Effect in Ischemic Cardiomyopathy: Assessment of LVEF Using Dobutamine Stress MRI

Theodorus A. M. Kaandorp,[1] Hildo J. Lamb, MD,[1] Jeroen Bax, MD,[2] Eric Boersma, PhD,[3] Eric Viergever, MD,[2] Ernst E. van der Wall, MD,[2] Albert de Roos, MD.[1] [1]*Radiology, Leiden University Medical Center, Leiden, The Netherlands,* [2]*Cardiology, Leiden University Medical Center, Leiden, The Netherlands,* [3]*Cardiology, Erasmus MC, Rotterdam, The Netherlands.*

Introduction: Left ventricular ejection fraction (LVEF) does not improve in all patients with ischemic cardiomyopathy in response to β-blocker therapy. Therefore, an investigation to predict the likelihood of a response is desirable.

Purpose: To evaluate the feasibility for prediction of β-blocker therapy effect on global LVEF, by measurement of global LVEF during low-dose dobutamine MRI, before therapy, in patients with severe ischemic cardiomyopathy.

Methods: In 20 patients with chronic coronary artery disease, MRI was performed at rest and during low-dose dobutamine stress before starting carvedilol therapy and at follow up to assess global LVEF. Additionally, a NYHA classification was assessed by the patient's cardiologist before and after β-blocker therapy.

Results: Global LVEF at follow up may be predicted by using the formula: β-blocker induced LVEF improvement = $0.66 \times (LVEF_{stress} - LVEF_{rest}) + 0.34$ ($R^2 = 0.67$, $p < 0.01$). An induced improvement in LVEF $\geq$ 7% may predict a positive response $\geq$ 5% at follow-up. This improvement was consistent with the NYHA classification before and after β-blocker therapy.

Conclusion: Therapy effect of carvedilol may be predicted at baseline by using the formula: β-blocker induced LVEF improvement = $0.66 \times (LVEF_{stress} - LVEF_{rest}) + 0.34$ ($R^2 = 0.67$, $p < 0.01$). MRI may be helpful to select patients who benefit from β-blocker therapy.

454. Assessment of Myocardial Viability Using Contrast Enhanced MRI—Comparison of Gd-DTPA, Gd-BOPTA and Gadobutrol

Thomas Schlosser, MD, Peter Hunold, MD, Kai-Uwe Waltering, MD, Kai Nassenstein, MD, Christoph U. Herborn, MD, Joerg Barkhausen, MD. *Radiology, University Hospital Essen, Essen, Germany.*

Introduction: Several studies demonstrated that contrast-enhanced magnetic resonance imaging (MRI) allows differentiation between reversible and irreversible ischemic injury. Much effort has been spent to find both optimum dose and time point for data acquisition after contrast injection. However, the effect of different contrast agents on contrast to noise ratios and the course of T1 values over time in damaged and normal myocardium have not been assessed yet.

Purpose: To compare two 0.5 molar MR contrast agents, Gadobenate Dimeglumine (Gd-BOPTA) and Gadopentate Dimeglumine (Gd-DTPA) and one 1.0 molar MR contrast agents, Gadobutrol, for the assessment of myocardial viability in patients with chronic myocardial infarction (MI).

Methods: 30 consecutive patients with a history of MI were examined using a 1.5 T scanner. Following the acquisition of cine MRI images to assess myocardial function, contrast enhanced MR imaging was performed after injection of 0.2 mmol/kg of contrast. The patients were examined using either Gd-DTPA (Magnevist, Schering AG, Berlin, Germany; $n = 10$), Gd-BOPTA (Multihance, Bracco S.p.A., Milan, Italy; $n = 10$) or Gadobutrol (Gadovist, Schering AG, Berlin, Germany; $n = 10$) in randomised order. T_1 values of non-infarcted myocardium, infarcted myocardium and left ventricular cavity (LVC) were estimated based on steady state free precession images with incrementally increased inversion times acquired during a single breath-hold. This sequence was performed 1, 3, 5, 10 and 20 minutes after contrast injection. T1-values were obtained using the following equation: $T1 = TI_{(min)}/\ln 2$, where $TI_{(min)}$ is the inversion time of the image with the minimum signal intensity of the tissue. 15 min after injection of the contrast agent late enhancement MR imaging was performed using a segmented inversion-recovery gradient-echo sequence (TR: 8 msec; TE: 4,3 msec; flip angle: 25°). Signal intensities and contrast-to-noise-ratios were measured in the non-infarcted myocardium, the infarcted myocardium and the LVC.

Results: Analysis of T1 values at all time points after contrast injection showed significantly ($p < 0.05$) lower values for Gd-BOPTA and Gadobutrol data sets in the infarcted and non-infarcted myocardium compared to Gd-DTPA. The T1 values in the LVC were not significantly different 1 min after contrast administration, however 3, 5, 10 and 20 min following injection they were significantly ($p < 0.05$) lower for Gd-BOPTA and Gadobutrol compared to Gd-DTPA (Table 1). 15 minutes after injection highest signal intensities in the infarcted myocardium were obtained in the Gadobutrol group (69.2 ± 11.3) followed by Gd-BOPTA (58.6 ± 10.9) and Gd-DTPA (45.2 ± 13.3), whereas in the LVC highest signal intensities were found in the Gd-BOPTA (69.8 ± 18.5) data sets (Gadobutrol: 60.1 ± 13.8; Gd-DTPA: 41.4 ± 9.0). $CNR_{infarct-noninfarct}$ was significantly higher in the Gd-BOPTA (48.6 ± 14.2) and Gadobutrol (51.5 ± 15.3) data sets compared to Gd-DTPA (34.5 ± 15.4), whereas $CNR_{infarct-LVC}$ was significantly higher in Gd-DTPA and Gadobutrol enhanced images (5.2 ± 8.5 and 8.3 ± 6.2) compared to Gd-BOPTA (− 10.9 ± 17.9).

Conclusions: The three contrast agents show different T1 times of normal myocardium, infarcted tissue and the LV cavity and have a significant influence on image contrast. 15 minutes after contrast injection CNR between infarcted und normal myocardium was higher in the Gd-BOPTA and Gadobutrol data sets compared to Gd-DTPA. However,

Table 1. Comparison of T1-values in the infarcted myocardium and the non-infarcted myocardium and the LVC for Gd-DTPA, Gd-BOPTA and Godobutrol 1, 3, 5, 10 and 20 min after contrast injection

		1 min	3 min	5 min	10 min	20 min
Myo_{inf}	Gd-DTPA	176±38	181±28	207±30	217±22	249±18
	Gd-BOPTA	109±7	138±22	134±21	165±18	178±29
	Gadobutrol	109±11	120±19	129±17	159±25	138±31
$Myo_{non-inf}$	Gd-DTPA	204±30	243±46	269±58	300±47	344±64
	Gd-BOPTA	154±14	196±35	205±42	228±34	267±36
	Gadobutrol	173±22	177±27	195±37	227±37	283±34
LVC	Gd-DTPA	109±12	162±30	181±28	211±31	268±37
	Gd-BOPTA	107±7	107±8	118±18	134±20	164±27
	Gadobutrol	109±9	115±15	137±11	180±24	222±31

Gd-DTPA and Gadobutrol permitted better differentiation between the infarcted myocardium and the LV cavity because 15 minutes after injection of Gd-BOPTA the LV cavity was still isointense or slightly hyperintense compared to the infarcted tissue due to a weak reversible binding to albumin.

455. Quantification of Myocardial Scar in Delayed Enhancement MR Images

Thomas P. ODonnell, PhD,[1] Engin Dikici, BS,[2] Randolph Setser, ScD,[3] Richard D. White, MD.[3] [1]*Imaging and Visualization, Siemens Corporate Research, Princeton, NJ, USA,* [2]*Computer and Information Science, University of Pennsylvania, Philadelphia, PA, USA,* [3]*Department of Radiology, Cleveland Clinic Foundation, Cleveland, OH, USA.*

Introduction: The extent of non-viable tissue in the left ventricle (LV) is a direct indicator of patient survival. Moreover, tissues that are non-viable will not benefit from coronary revascularization. Delayed Enhancement (DE) magnetic resonance (MR) imaging can accurately depict the extent of non-viable tissue in the LV. However, analysis of DEMR images is typically qualitative, despite the excellent spatial resolution and image contrast inherent to the technique. In this paper, we propose a two-stage, quantitative method for determining the extent of non-viable myocardium in DEMR images.

Methods: The method involves two separate stages: segmentation of the LV and classification of myocardial tissue. For segmentation, a registration-based technique is used. First, a Cine image matching the DE image in anatomic location and trigger time is selected. Next, the LV is segmented in this Cine image using the fully automatic technique by Jolly (Jolly et al., 2001); contours can also be manually adjusted, if needed. Cine segmentation results are then propagated to the corresponding DEMR image, and adjusted automatically using the technique proposed in (Chefd'Hotel et al., 2001) and subsequent affine registrations. Following LV segmentation in the DEMR image, classification of the myocardial pixels is performed using a Support Vector Machine (SVM), a supervised machine learning technique in which the computer is taught to recognize a phenomenon given a series of examples. In this case, the SVM is trained to recognize non-viable tissue in the LV using ground truth provided by experts at the Cleveland Clinic. To train and validate the SVM, images from 45 patients with known chronic ischemic heart disease were analyzed. All patients underwent DEMR and cine TrueFISP imaging using standard acquisition protocols on a clinical 1.5 T scanner (Sonata, Siemens Medical Solutions, Erlangen, Germany). For each image type, short-axis images were acquired at the LV base, middle and apex. Patients were divided into training (31 patients) and testing (14 patients) groups. For the training group, myocardial borders were manually drawn and the non-viable pixels identified by an expert using manual thresholding software (Argus prototype, Siemens). For the testing group, segmentation and classification were performed automatically, as described

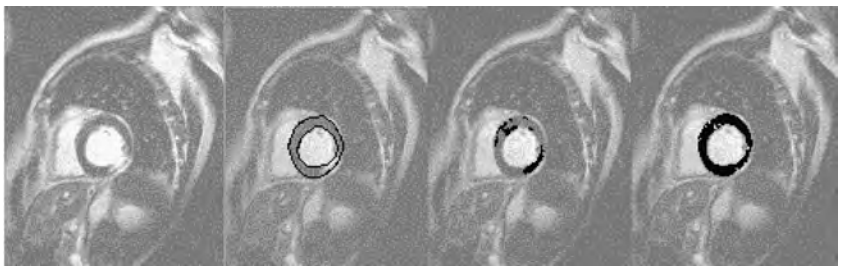

Figure 1. Left to Right: A DEMR image. Our automatic segmentation. Our classification of non-viable tissues (black indicated non-viability). Agreement with the expert (black pixels indicate agreement; white pixels indicate disagreement).

above, and validated against manually thresholded images; results were compared on a pixel-by-pixel basis.

Results: An example segmentation/classification is shown in Figure 1. The error in automatic segmentation was 1.5 ± 0.4 pixels (mean ± standard deviation) over the test group's 42 images (14 patients, 3 levels). The SVM accurately classified 88% ± 6% of pixels, with 81% sensitivity and 92% specificity. ROC analysis yielded a curve covering an area of 96.2%.

Conclusions: DEMR images can be accurately segmented using cine images as a template, despite the poor contrast between blood pool and non-viable myocardium. Furthermore, an SVM can be used to locate non-viable pixels accurately and reliably. We believe this technique shows great promise as a tool for characterizing the extent of non-viable tissue in DEMR images.

REFERENCES

Chefd'Hotel, C., Hermosillo, G., Faugeras, O. (2001). *A Variational Approach to Multi-Modal Image Matching*. IEEE Workshop on Variational and Level Set Methods (VLSM'01): July 13–13.

Jolly, M.-P., Duta, N., Funka-Lea, G. (2001). *Segmentation of the Left Ventricle in Cardiac MR Images*, Vancouver, Canada: Proc. ICCV.

456. Delayed Enhancement Imaging: Standardized Segmental Assessment of Myocardial Viability in Patients with ST-Elevation Myocardial Infarction

Daniel R. Messroghli, MD,[1] Khaled Alfakih, MD,[1] Kevin Walters, PhD,[2] Patrick Sparrow, MSc,[1] Gavin Bainbridge,[1] John P. Ridgway, PhD,[3] Mohan U. Sivananthan, MD.[1]
[1]*Cardiac MRI Unit, Leeds General Infirmary, Leeds, UK,* [2]*Division of Genomic Medicine, University of Sheffield, Sheffield, UK,* [3]*Department of Medical Physics, Leeds General Infirmary, Leeds, UK.*

Introduction: Delayed enhancement (DE) magnetic resonance imaging has emerged as a robust and simple tool for the assessment of myocardial viability. State-of-the-art reporting is based on a 17-segment model of the left ventricle (LV). A selective 3-slice short-axis (SA) positioning approach ("systolic 3-of-5") has recently been proposed for functional imaging of the LV, which facilitates segmental assessment by visualizing standardized basal, mid-cavity, and apical slices.

Purpose: To investigate if the "systolic 3-of-5" slice positioning approach, combined with long-axis (LA) views, can be useful for the assessment of DE.

Methods: 27 patients (22 male, 58 ± 12 years) with acute (n = 11) and chronic (n = 16) ST-elevation myocardial infarction (STEMI) underwent contrast-enhanced MRI (Gd-DTPA, 0.15 mmol/kg body weight) including non-selective multi-slice SA, selective 3-slice SA, and single-plane LA DE imaging using an inversion recovery-prepared gradient echo pulse sequence on a 1.5 T MR system (TR 4.7 ms, TE 1.9 ms, TI 250- 300 ms). Viability was assessed visually by two

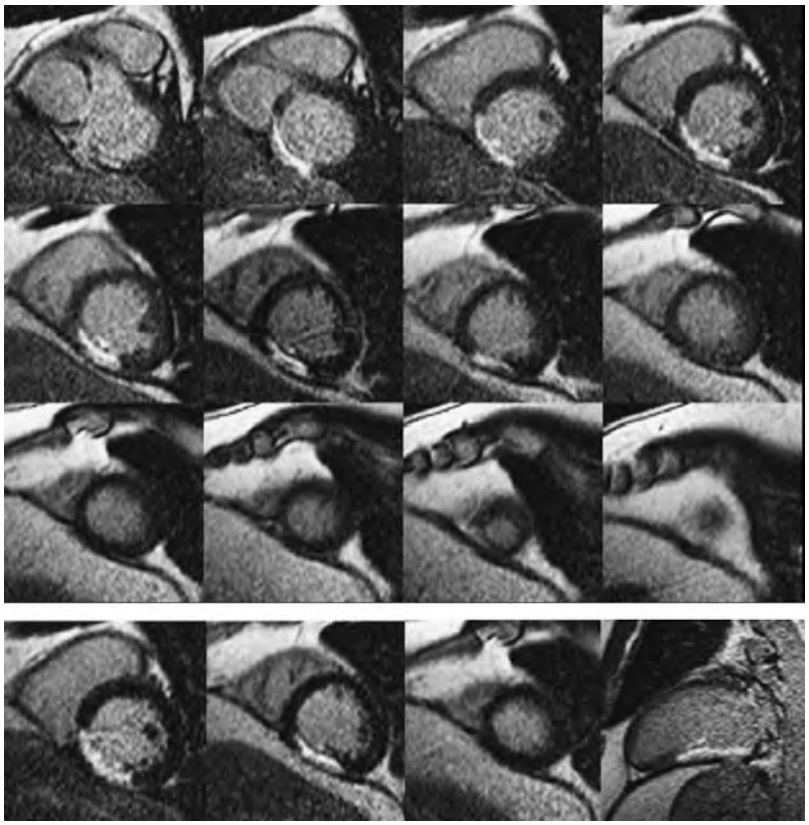

Figure 1.